Reduced exposure time as a method of minimising the impact of vibration on Electronic Speckle Pattern Interferometry

Prepared by: **David J Reid Rowland**
MSc (Mech Eng) student
Department of Mechanical Engineering
University of Cape Town

Prepared for: **Department of Mechanical Engineering**
University of Cape Town

Date: 17th September 2002

Thesis prepared in partial fulfilment of the requirements of the degree of MSc. (Mechanical Engineering)

Declaration

I, David James Reid Rowland declare that this dissertation contains only my own work, except where reference is made with the acknowledgement to contributions from others. I also declare that this material has not been submitted for any purpose or examination to any other department or university.

Signed this 20th day of September 2002

Signed by candidate

David James Reid Rowland

Acknowledgements

I would like to extend my heartfelt thanks to the following people, without who I could not have completed this project.

- My supervisors, Mr. D. Findeis and Prof. J. Gryzagoridis, who provided all the necessary introduction and support for the various aspects of my project.

- Mr J. Mayer of the Department of Mechanical Engineering and Mr C. Wosniak and Mr S. Shrire of the Department of Electrical Engineering, who assisted extensively with electrical and electronic components and design.

- My family for their support and encouragement.

- The workshop staff for their willingness to assist in many aspects of this and other projects

- The National Research Foundation and the Department of Mechanical Engineering for their financial support, without which this project would not have been possible.

- The admin and support staff in the department.

Terms of Reference

The author was given this project by Prof. J. Gryzagoridis and Mr D. Findeis of the Department of Mechanical Engineering at the University of Cape Town as a partial requirement for the degree of MSc (Mech Eng) in February 2000. The main objective of the thesis was to investigate the effects of vibration on Electronic Speckle Pattern Interferometry or ESPI, and the influence of a reduced exposure time with a view to eliminating or reducing these effects. This work forms part of a project to prototype a portable ESPI system that was under development by Mr Findeis and Prof. Gryzagoridis of the Department.

This thesis investigated:

- The effects of vibration on the successful performance of ESPI. This vibration included environmental vibration as well as simulated vibration using a loudspeaker and compressor.
- Methods that are currently used to overcome these effects. These include pulsed lasers and vibration-isolation tables.
- Alternative methods to overcome these effects that would be suited to a portable low cost ESPI system.
- A suitable method of pulsing a continuos wave (CW) laser and the use of the camera's built-in shutter with the aim of enabling ESPI inspection to be performed in hostile environments. The methods investigated included "pulsing" the laser with the use of physical obstructions such as slotted discs as well as optical shuttering devices such as a Liquid crystal shutter and a Lithium Niobate shutter.
- The success and reliability of these methods for the application intended.

Synopsis

Electronic Speckle Pattern Interferometry or ESPI is a non-destructive optical technique that enables the user to measure very small changes in displacement of an object's surface, usually as a result of an applied stress. The ESPI equipment consists of a laser, a variety of optical components, a CCD camera, a framegrabber and a computer. The equipment is used to capture two images of the object under investigation; a reference image of the object in its natural state and another after the object's surface has displaced. (For example as a result of stressing.) The computer digitally compares these two images with one another, and if there has been any surface displacement change between the two images, a zebra-like fringe pattern is produced and displayed on the computer monitor. This fringe pattern is essentially a 'contour map' of the object's surface displacement profile, and each fringe line represents a displacement of the surface by an amount equal to half the wavelength of the light that is, used relative to another fringe line. (0.316μm for Helium-Neon laser).

The technique can be used for the detection of flaws, the location of areas of high stress or loading and for vibration analysis amongst others. In the example of flaw detection, flaws are indicated by an irregular or rapid change in the density or direction of the fringe pattern. Areas of high stress or loading are characterised by a zone of dense fringe lines amongst areas of low fringe density. In the case of vibration analysis, nodal and anti-nodal regions are highlighted using a technique known as Time Average ESPI.

Extraneous vibration has an adverse effect on ESPI investigation if it is performed in conditions where no precautions have been taken to eliminate it. This vibration is

transferred to the object, and causes minuscule whole-body movement of the object relative to the camera. This motion masks the surface displacements that result from the actual stress applied, and frequently destroys the ESPI fringe pattern obtained. The vibration may arise from a variety of sources, such as machinery or vehicles operating in the vicinity of an ESPI inspection, airborne vibration, or from general low level vibration from the surroundings. The motion may occur either during the capturing of the individual images by the camera (typically lasting 20ms) or between the grabbing of the reference image and subsequent image, and makes ESPI inspection difficult or impossible. Pulsed lasers and vibration-isolation tables can be used as solutions to this problem, but each have their own drawbacks. Pulsed laser systems are generally much larger physically and more costly, and vibration isolation tables are usually laboratory bound.

This thesis investigated a method of making ESPI resistant to vibration by using the same principle as a pulsed laser system. Continuos Wave (CW) lasers were pulsed using an assortment of techniques in order to provide exposure times of considerably shorter duration than the normal duration. By capturing the image over a fraction of the usual 20ms, the object's motion would effectively be frozen, and would consequently eliminate the effects of vibration that occurred during the image capture itself. It would, however, do nothing to counter the effects of vibration that occurred between the capture of the first reference image and subsequent images.

Initially the laser was pulsed by placing it behind a rotating disc with slots in it. The disc was rotated at a speed that equated to 3000 pulses per minute, or 50 pulses per second. This was with the purpose of co-ordinating the laser pulse with the camera's field imaging

rate. By adjusting the point on the disc's radius that the laser shone through, it was possible to vary the laser pulse duration easily, while maintaining the same pulse frequency. This was repeated with two different discs and motors. The first disc was larger and able to provide pulses as low as 0.4ms. The second disc was much smaller than the first. It was driven by a stepper motor and able to pulse the laser to 1ms with a greater degree of accuracy and control.

A Liquid Crystal (LC) shutter was then used to pulse the laser. This is effectively a window that is normally clear, but when a voltage is applied across it, it darkens and allows little or no light to pass though it. A Lithium Niobate (LN) shutter was also used to pulse the laser, and operates on the same principle as the LC shutter. The crystal required very high voltages (approximately 1400V) in order to operate, but was able to pulse the laser to less than 0.1ms

The CCD camera that was used to capture the ESPI images has an adjustable built-in shutter facility with shutter periods of 20ms, 8.33ms, 4ms, 2ms, 1ms, 0.5ms, 0.25ms and 0.1ms, which was also investigated. This meant that the CCD would capture the image over the defined shutter period within the 20ms field period, and sit idle for the rest.

A helicopter tail rotor blade with two deliberately induced flaws on its surface was used as a specimen for ESPI inspection. A hair dryer was used to create thermal stresses in the rotor blade, which allowed a fringe pattern to be generated.

ESPI examination of the blade was initially performed on the table in order to investigate the effect of a reduced exposure time. Care was taken to ensure that the ESPI layout was

the same for all the different pulsing methods and arrangements that were investigated. Consequently, the intensity and definition of the EPSI images would be comparable when different shuttering methods were investigated.

From this investigation, the LC shutter and stepper motor and disc were abandoned after testing indicated that they were not suitable. The stepper disc could only pulse as short as 1.1ms, and was too large physically to be of use in the final ESPI system. The large disc was used instead because although it was also too large for a compact system, it had a shorter pulse period, and was used to investigate the effect of a shorter exposure time. The LC shutter suffered from slow light transmission response times. It did have very good frequency and pulse duration control. Useful ESPI images could only be captured with pulses as short as 2ms, but the long pulse duration and low light transmission ruled it out as a pulsing method.

The large disc, LN shutter and camera shutter were then used to investigate the consequence of vibration on ESPI inspection. The LN shutter was able to provide pulses as low as 0.1ms at which point the lack of laser power became the prevailing factor. It was found to have a light transmission of approximately 30% and the shutter's polariser was predominantly responsible for this. The LN shutter has some benefit over the camera shutter because it is able to provide an unlimited range of pulse widths and frequencies, while the camera shutter can only provide eight shuttering speeds. The ability to provide higher frequency pulses than normal may be necessary if specialised ESPI investigation such as Double-pulsed addition ESPI is to be performed. In this type of ESPI, both laser pulses are fired into a single camera field, which would be impossible with the camera shutter. The camera shutter has the benefit that it is built in and easy to operate. It does

not require additional electronics and components, nor does not suffer from transmission losses as the Lithium Niobate crystal does.

The blade was exposed to environmental vibration, simulated industrial vibration from a compressor and sinusoidal vibration from a loudspeaker. The effects of these vibrations were noted, and the influence that of each of the pulsing techniques had in eliminating these effects was investigated.

Environmental vibration only had a slight effect on the ability to capture successful ESPI images. It was possible to acquire successful images with no reduction in exposure time, although this was a hit and miss process. Out of a series of ten images captured at the full 20ms, only six were deemed acceptable. This increased to eight images when the exposure time reduced to 2ms and to ten when reduced to 0.5ms. The number of acceptable images obtained however decreased to eight for a 0.1ms exposure time. The vibration levels experienced in the lab where the testing took place were much lower than those that could be expected in an industrial environment would be. In real-life conditions, normal ESPI inspection may be impossible without the appropriate application of vibration isolation.

It was much more difficult to capture acceptable images without pulsing the laser when the compressor excited the object. Out of ten images captured over 20ms, only one was acceptable in terms of fringe clarity. However, by reducing the shuttering period to 2ms, the amount of acceptable images increased to nine, but decreased to seven for a shuttering time of 0.5ms and five for 0.1ms.

When the loudspeaker excited the blade, nodal and anti-nodal regions were clearly visible on the ESPI images that were taken without any shuttering or laser pulsing. Fringe lines were only visible in the nodal regions, whereas no fringe lines were visible in the anti-nodal regions of the images captured at 20ms. When the pulse duration was reduced to 2ms, the nodal and anti-nodal regions were much less distinguishable, and eight out of ten successful whole field fringe patterns were obtained. This increased to nine acceptable fringe patterns for the 0.5ms and 0.1ms shuttering times.

The effect of a reduced exposure time on the probability of obtaining successful images appeared to be partly a function of the vibration levels that the object suffered. In cases of low vibration levels, the improvement in images was apparent, but not by any means exceptional. In the case of higher vibration levels, as in the case of the compressor and loudspeaker-induced vibration, the improvement was remarkable.

This was a clear demonstration of the effectiveness of using a short image capture period. Although a successful image was not guaranteed on every capture, the probability was found to be clearly higher with a lower exposure time.

The positive effect of shorter exposure times on ESPI in conditions of vibration has therefore been demonstrated. The shuttering speed needs to be as short as possible and the optimum pulse duration will vary for different vibration amplitudes and frequencies. There is clearly a loss of light intensity as the pulse duration decreases, which must be traded off against the requirement of a short exposure time.

The use of Ferroelectric Liquid Crystal (FLC) shutters should be investigated. These operate in the same manner as LC shutters, but are able to provide shuttering speeds of approximately 50μs. The advantage is that they operate at 12V instead of 1400V in the case of the Lithium Niobate shutter, and this would simplify matters considerably.

If the Lithium Niobate shutter is to be used, a polariser with better light transmission properties should be sourced. The laser needs to be much more powerful than the one used for this project. This will allow shorter pulse durations to be used and larger areas to be investigated at once. It will also improve the quality of the fringe patterns obtained. The laser used for this project was rated at 60mW, and would normally output at least 35mW, but was incorrectly calibrated and therefore only provided 8mW. This problem was however only noticed after all the completion this project. Increased laser power would solve many of the problems experienced with low light levels in this investigation. Suitable diode lasers are currently available with outputs up to 300mW.

Contents

List of Illustrations

List of Tables

Glossary and List of Symbols

	Description	Units
AC	Alternating current	
AGC	Automatic Gain Control	
CCD	Charge-coupled device. The part of a TV camera that is used to convert the light into an electrical signal.	
CCIR	Consultative Committee for International Radio. A standardised camera video format.	
Coherent light	This is light that has all its peaks and troughs in phase with each other.	
CW laser	Continuos Wave laser. A laser that emits laser light continuously.	
DC	Direct Current	
De-interlacing	Separation of image into separate fields, namely Field 1 and Field 2	
Duty Width	Time period that shutter remains open	ms
ESPI	Electronic Speckle Pattern Interferometry	
Global, rigid-body, or whole body motion	Motion of the whole object where each point of the object moves by the same amount	
HI	Holographic Interferometry	
LC/LCD shutter	(Electronic) Liquid Crystal shutter that darkens when a voltage is applied to it	
LED	Light Emitting Diode	

LN shutter	Lithium Niobate shutter. A shutter that darkens when a voltage is applied to it	
NDT/NDE	Non Destructive Testing/Evaluation	
NTSC	National Television Standards Committee. A North American video signal standard.	
S	Chord length of the cut-out	mm
t_{pulse}	Time period of the laser pulse(ms)	ms
Transmissibility	The percentage of light which is allowed to pass through the LC shutter	%
v_{tang}	Tangential velocity at the point on disc where the laser is chopped(m/s)	m/s
ω_{disc}	Rotational speed of the disc	Rads/sec

Chapter 1 Introduction

Electronic Speckle Pattern Interferometry or ESPI is a non-destructive optical interference technique that enables the user to measure very small changes in displacement or deformation of an object's surface as a result of an applied stress. The technique can be set up to measure a variety of static and dynamic variables such as displacement, strain, and vibration. It provides a useful tool for flaw detection, design evaluation and vibration amplitude and mode-shape measurement. It provides almost instantaneous results over the entire area being investigated at once, as opposed to other methods that inspect the object in a point-by-point fashion.

The ESPI equipment consists of a laser, a variety of optical components such as mirrors, beam splitters and beam expanders, a CCD TV camera, a framegrabber and a computer. A beam splitter is used to split a single laser beam into two separate beams. A beam expander is a diverging lens that expands light to cover a larger area. A framegrabber is used to capture the image information from the camera, digitise it and allow it to be viewed and stored on a computer.

The ESPI equipment captures two images of the object under investigation; a reference image in the object's natural state and another after the object's surface has been displaced or deformed, usually as a result of stressing. These two images are digitally compared with one another, and if there has been any change in surface displacement between them, a zebra-like fringe pattern is produced and displayed on the monitor. A typical fringe pattern is shown in Figure 1.1. The fringe pattern is essentially a 'contour map' of the object's surface displacement change, and each of the lines in the fringe

pattern represent areas of equal displacement on the object's surface. The displacement amplitude can be calculated by adding the number of fringes from a known point and applying the relevant formula. ESPI has the ability to measure displacements in the region of half the wavelength of light, (0.316μm for Helium-Neon laser), which is equivalent to approximately $1/300$ of the width of a human hair.

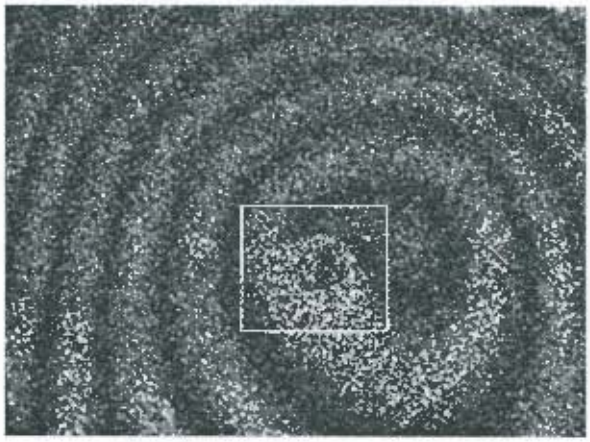

Figure 1.1 A typical ESPI fringe pattern

Flaws are indicated by a rapid change of density or direction in the fringe pattern, as in the highlighted area in Figure 1.1. These patterns can be saved on the computer for later viewing, and can be enhanced using a variety of techniques if necessary.

Because of ESPI's ability to measure such small displacements, it is very sensitive to movement caused by vibration. Care must therefore be taken to ensure that neither the object under inspection nor the optical components of the ESPI system are exposed to vibration. This may be done using holographic tables, although this usually confines the technique to a laboratory. If vibration cannot be avoided, an alternative is the use of pulsed lasers, which act to provide a freezing effect through stroboscopic illumination. The disadvantage of these pulsed laser systems is that they are bulky and expensive.

This project aims to investigate the effect of vibration on ESPI, as well as investigating methods of eliminating its effect on the successful completion of ESPI inspections. This

enable ESPI to be performed in real-world situations, and hence provide a useful tool for industrial Non Destructive Testing (NDT) investigation.

This thesis was limited by the lack of knowledge in this field. Although substantial work has been done on pulsed laser systems, little has been done on the pulsing of CW lasers. The exposure times aimed for in this project are also different to those employed in traditional pulsed ESPI inspection. CW lasers are generally of much lower power than pulsed lasers. Very short pulse durations associated with traditional pulsed ESPI would be insufficient for the low-power CW lasers to provide enough illumination for the camera to image the object. The exposure times would therefore fall between those of pulsed ESPI systems (approx. 20ns) and CW laser ESPI systems (20ms).

Chapter 2 Problem statement

By its very nature of operation, ESPI is very susceptible to vibration. Because of vibration, the object under investigation moves, and this masks or overshadows the surface displacements that result from the actual stress applied. This motion occurs either during the exposure time when the camera captures each individual image (typically 20ms for CCIR/PAL TV systems), between the capture of the two fields that make up the image or between the capture of the reference image and subsequent image. If the movement occurs during the image acquisition process, the resultant fringe lines are poorly defined in much the same way as motion blur reduces the image clarity in photography.

Figure 2.1(a) below shows the typical fringe pattern of a slit flaw obtained using ESPI. The slit flaw is indicated by the irregular fringe pattern in the highlighted area. Figure 2.1(b) shows the ESPI image of the same flaw captured without the benefit of vibration isolation and demonstrates the resultant loss of fringe definition due to vibration. This loss of clarity clearly makes ESPI investigation impractical if not impossible in circumstances under which vibration conditions are expected.

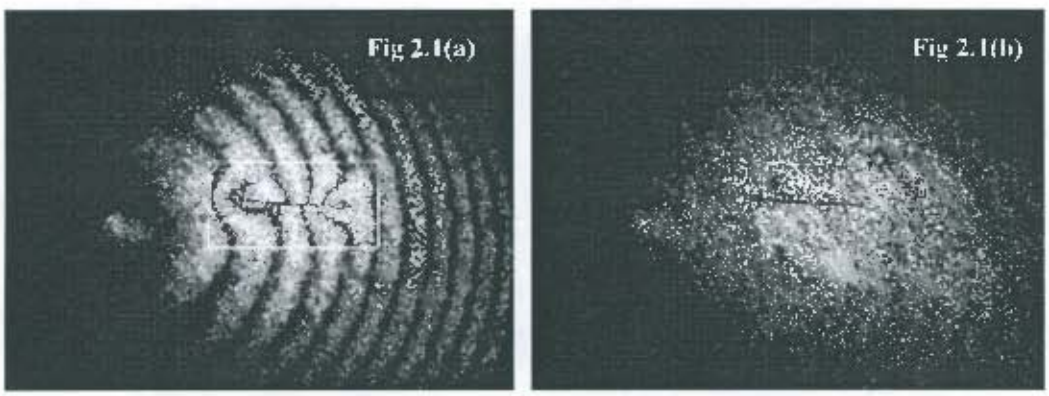

Figure 2.1(a) (b) ESPI images of flaw with and without vibration isolation (UCT)

Two methods are commonly used to overcome this vibration problem.

The most common method in practice is that ESPI is performed on a vibration isolation table and a typical example is shown in Figure 2.2. These tables are typically large steel slabs that rest on air cushions, which damps most of the vibration out. The object, camera and optical components are magnetically fastened to the table, reducing the effects of airborne vibration. The stiff steel slab also greatly reduces relative motion between the optics, the camera and the object. These tables are however large and bulky, and not transportable, meaning that this arrangement is laboratory bound only.

Figure 2.2 ESPI vibration isolation table at UCT

The second technique used to overcome the vibration problem is the use of pulsed lasers, which are analogous to a stroboscope. These allow the camera to capture a 'snapshot' of the object while it vibrates, essentially freezing whole body motion. Pulsed lasers also have their limitations, and are usually very bulky, costly and complicated compared to their continuous wave (CW) counterparts. The pulsed laser system at the University of

Figure 2.3 Pulsed ruby laser equipment at UCT

Cape Town (UCT) with its components is shown in Figure 2.3. These pulsed lasers and switching mechanisms are capable of providing laser pulses from as little as 20ns up to 2ms.

The purpose of this thesis was to investigate the influence of a reduced exposure period on ESPI image capture of objects under vibration. This included the feasibility of using a pulsed CW laser in order to mimic a traditional pulsed laser system. There are many possible applications where this technique may be of use in industry, where there is not the luxury of vibration-damping equipment, and hence the interest in pursuing this field. CW lasers are available in much smaller sizes than pulsed laser systems, which would be beneficial if a compact system was desired. If the camera CCD is exposed to illumination for a much shorter duration than the usual 20ms, the object motion can effectively be frozen, and the negative effects of vibration on ESPI during the capturing of the image can be eliminated. The effect of object stressing between the capturing of the reference image and subsequent images will not be explored in this thesis, and forms a part of the broader research being performed in the Department of Mechanical Engineering at UCT.

In the literature consulted, it was indicated that pulses of below 1ms are short enough to isolate objects that are vibrating at frequencies of 100Hz or less. [5] This was used as a starting point since the majority of vibrations in industrial environments were expected to be below 100Hz. The source of much of the vibration that is expected would be machinery, which would generally be operating at below 3000rpm (50Hz).

On a similar vane to the use of pulsed lasers is the use of ultra-high speed CCD cameras. Examples of ESPI inspections with cameras having exposure times of approximately

0.22ms have been noted. [24,25] These short exposure times made it possible to capture ESPI images of objects subjected to vibration with CW lasers without needing to employ vibration-isolation systems. The reduction of camera exposure time was investigated by the use of the camera's built-in shutter.

Chapter 3 Background and Literature review

3.1 Electronic Speckle Pattern Interferometry

Electronic Speckle Pattern Interferometry (ESPI) has its origin in Holography Interferometry (HI) and replaced it as technology advances allowed for the use of computers and CCD cameras. Both techniques are based on optical interference and the essential difference between the two is that the images are stored chemically on photographic plates in HI, while in ESPI the images are captured using a TV camera, digitally manipulated and stored in a computer. ESPI was first demonstrated in 1971 by Butters and Leendertz [1]

ESPI provides a contour map of the change in surface displacement of an object that occurs as a result of an applied stress. It can be used qualitatively as a flaw detection technique through the highlighting of weakened areas. Any flaws (including sub-surface flaws) that affect the object's deformation to an applied stress are potentially detectable. The technique can also be used to provide quantitative displacement information, which can be compared to theoretical results if the loading conditions are known. Almost any conceivable object can be inspected, and by way of example, ESPI has been used as a diagnostic tool to inspect the condition of ancient art pieces [2,3,4] and to test for delaminations and debonds in aircraft components [5,6,7]. ESPI can also be used as a component design tool, locating areas subjected to stress concentration or high loads in a virtually unlimited variety of structures, including biomedical components, engines and gearboxes [1,8,9,10]. It can be also used to study vibration effects on objects and the

and the location of nodes and anti-nodes as well as the quantification of vibration amplitude. [11,12,13].

The major benefit of the technique is that no contact of the ESPI equipment is required with the object. Because of the extreme sensitivity of ESPI, the stresses required to perform the investigation need only be very small. As a result, the risk of damaging fragile or valuable objects is greatly reduced.

3.1.1 Laser Speckle

As the name implies, Electronic Speckle Pattern Interferometry involves the interference of speckle patterns. A speckle pattern is created when a laser beam is expanded and illuminates an object with an optically rough surface. The speckle is a grainy psychedelic pattern of light and dark spots that seems to float on the object surface. This speckle pattern is unique for the observer's position relative to the object, and the speckle size depends on the size of the aperture through which it is viewed. An optically rough surface is defined as one whose height variation is of the order of or larger than the wavelength of the illuminating light [1]. The speckle observed is a result of certain properties of the laser light used to illuminate the object, namely that it is coherent (all the peaks and troughs of the light are in phase with each other) and monochromatic (it is of only one wavelength or frequency). An illustration of the typical appearance of speckle is shown in Figure 3.1 below.

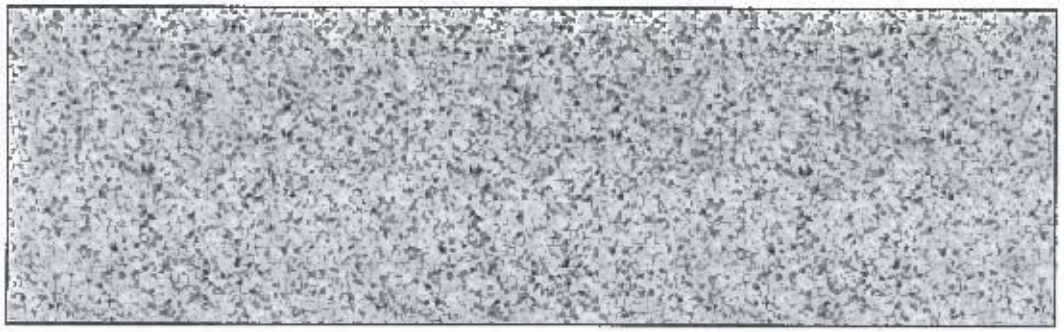

Figure 3.1 Typical speckle pattern observed on object surface

The phenomenon of the speckle observed can be explained by the principle of superposition of light waves, which states: "If two or more wavefronts are travelling past a given point, the total amplitude of the displacement at that point is given by the sum of the individual displacements of the wavefronts." [14]

The expanded laser light strikes the object and is reflected and scattered in random directions due to the peaks and troughs on the object's surface. Because of this scattering, the viewer sees light from all over the object's surface. Some of these beams will cross each other, and where they do, they will interfere either constructively or destructively, depending on their relative phase. This is shown in Figure 3.2. The surface roughness has been exaggerated for clarity, and the regions of interference are highlighted.

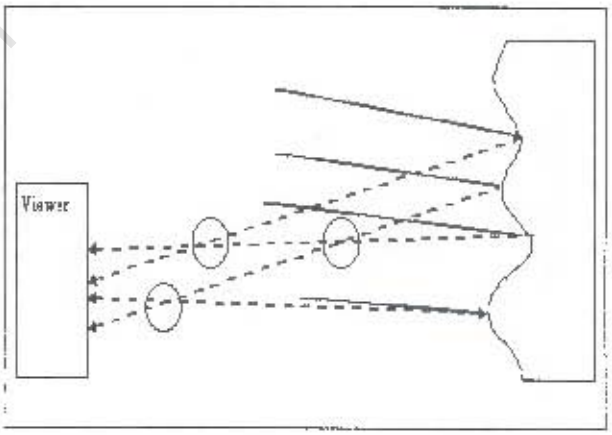

Figure 3.2 Illustration of light scattering by rough surface

Light travels as a sinusoidal wave, and when two light waves are added together, they give rise to either constructive or destructive interference, depending on their relative phase. Because the light is monochromatic, bright spots appear when constructive interference occurs, and dark spots when destructive interference occurs. In the case of white light, which is made up of wavelengths across the visible spectrum, this constructive and destructive interference still takes place, but is not noticeable doe to the combination of all the different wavelengths. [1]

The speckle size and quality that are imaged by the camera CCD are affected by several factors, which include aperture size and coherence length.

Aperture opening

The size of the speckle depends partly on the aperture size of the camera iris. Opening the aperture decreases the average speckle size, and increases the amount of light entering the camera. If the speckle becomes too small the camera CCD is no longer able to image it, and ESPI investigation becomes impossible. This is because the speckle becomes smaller than the size of the CCD pixels. Ideally the speckle needs to be two or three times the size of the pixels in order to be imaged. Closing the aperture increases the speckle size, but decreases the amount of light entering the camera. Eventually there will be insufficient light falling on the CCD to record the necessary information. A compromise must therefore be reached between a suitable speckle size and sufficient levels of illumination.

The size of the speckle imaged by the CCD can be calculated by

$$d_{sp} = \frac{2.4\lambda v}{a}$$ **Eqn 3.1**

Where d_{sp} is the speckle diameter imaged by the CCD

λ is the wavelength of the light used

v is the distance from the lens aperture to the CCD

a is the diameter of the iris. [1,15]

Coherence Length

One of the requirements of the laser light for ESPI is that it has to be coherent for the production of speckle. The frequency of the beam of laser light being emitted from the laser itself varies slightly with time, and because of this, the light is no longer coherent with the light that was emitted earlier. [5]

The coherence length is defined as *' the distance that light leaving the laser can travel before there is a shift in instantaneous laser frequency sufficient to produce light that is no longer coherent with that which left the laser initially'*. [5]. The coherence length is generally defined as the distance in which the interference visibility falls to $1/e^2$, where e is the natural log base (2.7183)[16]. In order to obtain fringes of the highest contrast, the difference in path lengths between the reference beam and the object beam should be less than the coherence length of the laser light, and as close to zero as possible. [1,17]

3.2 ESPI set-up

Only out-of-plane and in-plane interferometers will be dealt with here but there are many other arrangements that are used.

3.2.1 Out-of-plane displacement

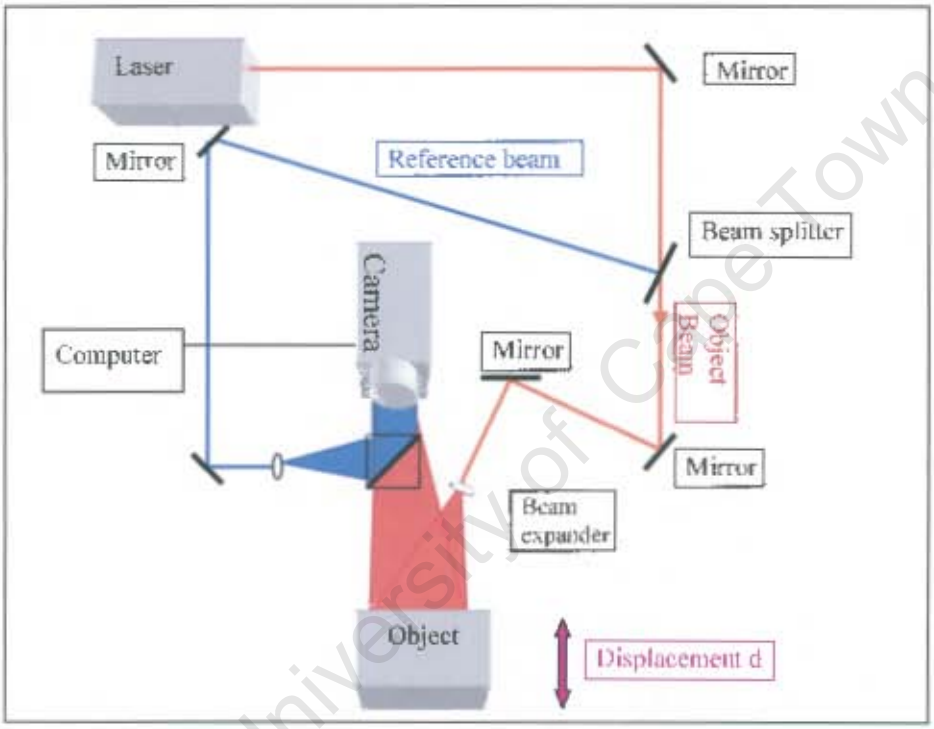

Figure 3.3 A typical out-of-plane ESPI arrangement

This arrangement is used to measure surface displacement parallel to the surface normal of the object. A laser beam (see Fig 3.3) is split into a reference beam and an object beam by the beam splitter. The object/reference beam split is typically 95 - 5%. The reference beam is directed to the camera CCD without reflecting off the object and is then expanded. Because the reference beam does not strike an optically rough surface, no speckle is produced, and it is referred to as being smooth. The object beam is expanded by an expanding lens and illuminates the object. After the object beam has struck the

object's surface, it is scattered in random directions as diffuse reflection. Part of this is reflected towards the camera, and as it enters, is made to interfere with the incoming smooth reference beam by means of a prism. The light intensity reaching the CCD is therefore the sum of the object beam and the reference beam components. This interference means that the speckle pattern is unique for the object's current position. If the object or part of the object moves at all, a new speckle pattern is produced.

Gryzagoridis et al [16,17] give the equation below for out-of-plane surface displacements. These displacements have a sensitivity corresponding to half the wavelength of the laser light used and are dependant on the angles of the incident beam and camera to the object's surface normal. The change in displacement of a point on the object's surface relative to another is calculated by counting the number of fringes generated between the points and applying the following formula:

$$d_n = \frac{n\lambda}{\cos\theta_i + \cos\theta_c} \qquad \textbf{Eqn 3.2}$$

For small angles of camera and illumination this equation can be simplified to

$$d_i = \frac{n\lambda}{2} \qquad \textbf{Eqn 3.3}$$

Where n is the number of fringes observed
λ Is the wavelength of light used
θ_i is the angle of illumination to the surface normal
θ_c is the angle of the camera axis to the surface normal of the object

3.2.2 In-plane displacement

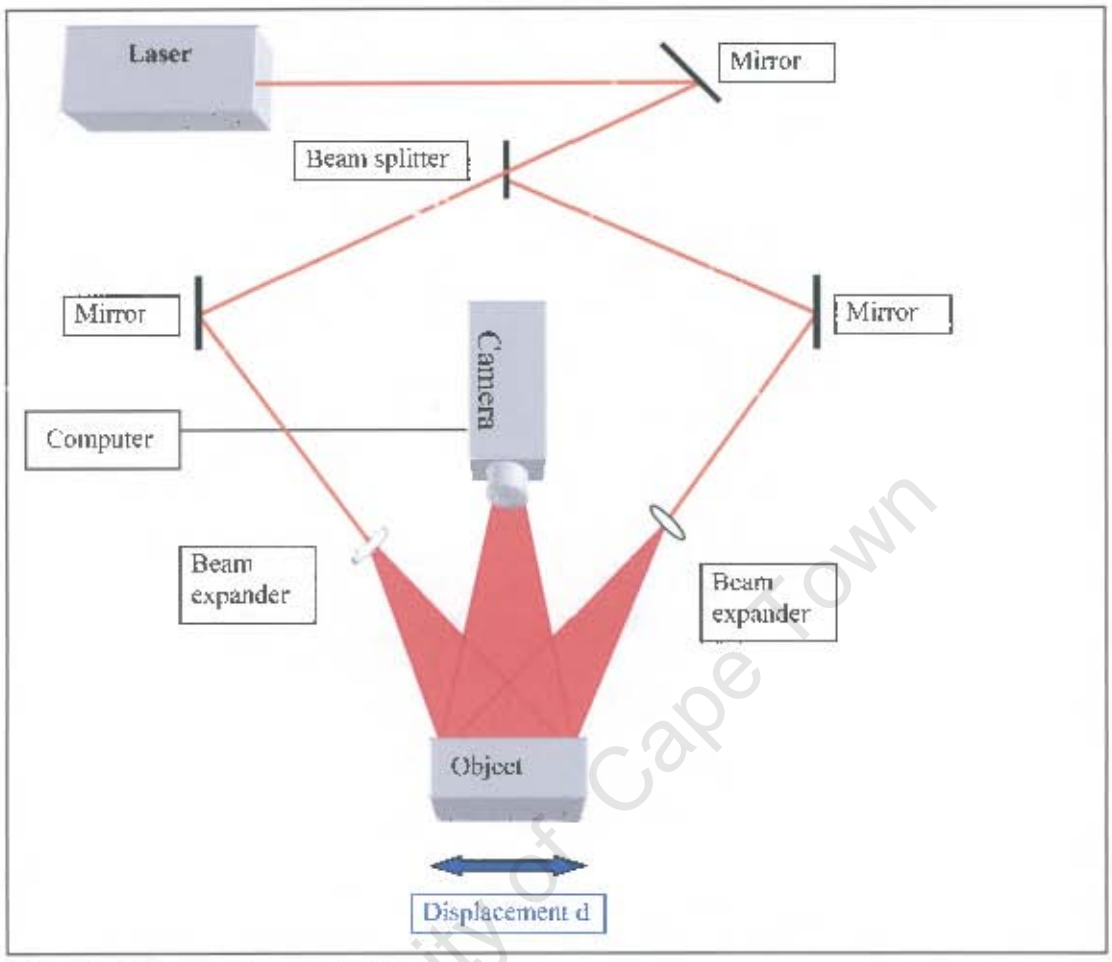

Figure 3.4 A typical in-plane ESPI set-up

This arrangement is used to measure displacement perpendicular to the object's surface normal. When measuring in-plane displacement, the object is illuminated by two laser wavefronts at equal and opposite angles to the surface normal. These two wavefronts interfere with each other after being reflected off the object's surface. This interference results in the formation of a speckle pattern that is imaged by the camera CCD. The sensitivity of in-plane ESPI depends mainly on the angle of the wavefronts and the wavelength of light. [9]

Gryzagoridis et al [16,17] gives the following equation for calculating the in-plane displacement of the object surface.

$$d_i = \frac{n\lambda}{2\sin\phi} \qquad \textbf{Eqn 3.4}$$

Where n is the number of fringes observed
λ is the wavelength of light used
ϕ is the angle of the illumination from the normal

Equations 3.2 to 3.4 can be derived using the single ray approach. See Appendix 1and 2

Figure 3.5 below summarises the ESPI inspection procedure that is used to generate the fringe pattern in both the above arrangements.

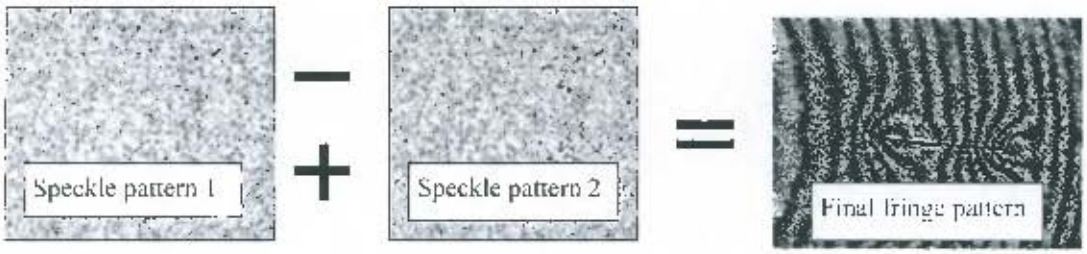

Figure 3.5 Visual representation of ESPI inspection procedure

An image of the object is captured in its unstressed state. This image is in the form of an arbitrary speckle pattern. (Speckle pattern 1). The intensity of this pattern is given by:

$$I_1 = A_1^2 + A_2^2 + 2\sqrt{A_1^2 A_2^2}\cos(\phi_1 - \phi_2) \qquad \textbf{Eqn 3.5}$$

where A_1 and A_2 are the complex amplitudes of the object and reference beam wavefronts and $(\phi_1-\phi_2)$ is the phase difference between them at the point of interest. [1,18]

The object is then stressed by one of a variety of techniques that include external mechanical forces, heating, acoustic vibration or the application of a vacuum or pressure. The stressing technique chosen is specific to the object under investigation and is designed to generate maximum displacement of the flawed area. (See Section 3.2.3). Because of this stress, the surface deforms a small distance d, and another image (speckle pattern 2) is captured. Speckle pattern 2 is also a speckle pattern, but is different to the first because the deformation has changed the path length of the object beam, while leaving the reference beam unaffected. The intensity of this speckle pattern can be given by Equation 3.6:

$$I_2 = A_1^2 + A_2^2 + 2\sqrt{A_1^2 A_2^2}\cos(\phi_1 - \phi_2 + \Delta\phi) \qquad \textbf{Eqn 3.6}$$

Where

$$\Delta\phi = \frac{4\pi}{\lambda} = 2\pi n \qquad \textbf{Eqn 3.7}$$

$\Delta\phi$ is the change in the phase angle of the object beam due to the change in path length that results from the object displacement.

n is the number of fringes generated.

The computer software then processes these two images, either adding or subtracting them from each other. Subtraction is preferable to addition because areas where no displacement has taken place cancel each other out, leaving a black area. This reduces the amount of unnecessary information, as well as cancelling out the intensity of the reference beam and leaves only the object beam information. [1]

When the two images are subtracted from each other, the intensity of the light at corresponding points on the two speckle patterns is subtracted from each other. The resultant intensity at each point is the difference between the intensities of the same point in Speckle pattern 1 and Speckle pattern 2. The resultant intensity will thus be:

$$I_r = I_1 - I_2 = 4\sqrt{A_1^2 A_2^2}\sin\left\{(\phi_1 - \phi_2) + \tfrac{1}{2}\Delta\phi\right\}\sin\left(\tfrac{1}{2}\Delta\phi\right) \qquad \textbf{Eqn 3.8}$$

In the case of speckle pattern addition, the fringe pattern is given by:

$$I_r = I_1 + I_2 = 2(A_1 + A_2) + 4\sqrt{A_1^2 A_2^2}\cos\left\{(\phi_1 - \phi_2) + \tfrac{1}{2}\Delta\phi\right\}\cos\left(\tfrac{1}{2}\Delta\phi\right) \qquad \textbf{Eqn 3.9}$$

The electrical output voltage V_s of the camera CCD is proportional to the intensity of light falling on it, as given by Equation 3.6 above. The brightness B of any point on the monitor is given by:

$$B \approx |V_s| = 4K\left(I_1 I_2 \sin^2\left((\phi_1 - \phi_2) + \tfrac{1}{2}\Delta\phi\right)\sin^2\left(\tfrac{1}{2}\Delta\phi\right)\right)^{\frac{1}{2}} \qquad \textbf{Eqn 3.10}$$

Where K is a constant [1]

The brightness varies between B_{max} and B_{min}. It is maximum for $\Delta\phi = (2n+1)\lambda$ and minimum for $\Delta\phi = 2n\lambda$. Points of equal displacement on the object surface will have equal phase change. Fringes will therefore be generated along lines of equal displacement. [1,5,16,18,30]

The result of this is an image of a zebra-like fringe pattern composed of light and dark bands, which is displayed on the monitor. The fringe pattern is a 'contour map' of the object's surface displacement. A distinctive fringe pattern is generated around a flaw, usually indicated by an irregular change in fringe density or direction. This is because the area around a flaw will deform more than usual as a result of the weaker mechanical properties associated with it, and the more the surface displaces, the denser the fringe pattern will be.

3.2.3 Methods of stress application

There is a wide range of techniques that can be used to stress the object. The technique chosen must produce sufficient deformation of any flawed regions present, and at the same time, it should not cause excessive global or rigid body motion. Excessive rigid body motion will cause speckle decorrelation, and no fringe pattern will be obtained. A detailed description of these methods is given in the ASM Handbook [5]

- Acoustic stressing
  - Standing acoustic waves
  - Travelling acoustic waves
- Thermal stressing
  - Radiant heat sources (e.g. heat lamp)
  - Electrical resistance heating tape or heat gun which applies heat to a specific area
  - Resistance heating of the object itself
  - Hot air or liquid nitrogen cooling
- Pressure or vacuum stressing
- Mechanical stressing
- Forced vibration of the object by piezoelectric crystal, loudspeaker or similar. [5]

3.2.4 Advantages of ESPI

ESPI has several advantages, which are summarised below.

- ESPI provides almost instantaneous and easily interpretable results, which can be later enhanced and manipulated.
- Real time viewing of the object's response to stress is possible with ESPI. This is beneficial when the applied stress varies with time. If thermal stressing is used for example, the results can be monitored as the object cools and captured when suitable results are observed.
- ESPI can be applied to any type of solid material, regardless of its composition or its mechanical or electrical properties, e.g. metals, plastics, ceramics or composites.
- ESPI can be used on objects of almost any size, limited by laser capacity and a suitable stressing technique.
- Pulsed laser techniques allow inspection in unstable or hostile environments.
- ESPI is able to measure displacements in the order of half the wavelength of light (0.3μm when using a Helium-Neon laser, equivalent to approximately $1/300$ of the width of a human hair.). With the application of special techniques, it is possible to improve sensitivity up to 1000 times. [5] It is also possible to reduce the fringe sensitivity to 100μm, depending on the specific requirements.
- Large areas can be studied at once, not requiring a time-consuming point-by-point investigation. [5]

3.2.5 Disadvantages of ESPI

- Often the flaw under examination cannot be accurately quantified with regard to size, shape and precise location.
- Rigid-body motion or displacements as a result of spurious external environmental vibrations often mask flaws. [1,5,9,18]
- Set up of equipment can be time-consuming as the reference - object beam path lengths must be matched in order to meet the coherent length requirements.
- Special coatings may be required to increase surface reflectivity of dark or matt objects.
- Embedded flaws in a stiff structure are not easily detected because they often do not affect the surface displacement.[1]
- The images obtained are sometimes not well defined and 'grainy' due to a reduction in resolution. [16,20] This is because the CCD which the camera uses to record the image has a limited number of pixels per area. The density of pixels obviously influences the spatial resolution of the image obtained. [1]

3.3 Types of lasers used

Two different types of laser are commonly used for ESPI NDT investigation; continuous-wave (CW) lasers and pulsed-lasers.

3.3.1 Pulsed lasers

Pulsed lasers emit pulsed laser light at relatively high power, and usually over a very short interval. The increased power is necessary to get sufficient light onto the photographic plate or CCD in a shorter period. Pulsed lasers are used when the inspection is not performed on a holographic table and when the object under investigation is not stable. They can also be used when the most effective stressing procedures involves dynamic loading. The most common lasers used for ESPI applications are flash lamp pumped solid-state lasers such as ruby and frequency-doubled neodymium-doped yttrium aluminium garnet (Nd: YAG). These provide a pulse typically 1 to 2 ms in duration. [5].

3.3.2 Continuous Wave (CW) lasers

CW lasers emit laser light continuously, at relatively low power, and are usually used when care has been taken to ensure that the object remains stationary throughout the duration of the exposure. This usually involves performing the entire procedure on a special table that has been isolated from vibration. [5]

3.4 ESPI methods

There are several different variations of ESPI inspection methods available to the investigator. A brief introduction is given below:

3.4.1 Real time Interferometry

This technique compares the deformation of an object that is being perturbed in real time to a previously recorded image of the object in its undisturbed state. An initial image is captured and stored by the computer. Stresses are applied to the object and the fringes observed on the monitor are a live indication of the displacement profile relative to the initial reference image. As the stress loading changes (e.g. the object cools when thermal stresses are applied) the fringe pattern will also change and when a suitable fringe pattern is observed it can be captured. It is thus possible to monitor the effects of applied loads to the object as they are happening and make adjustments accordingly. The technique is only possible with the use of CW lasers.

By way of an example, Albrecht [2] used ESPI to inspect the condition of antique Italian paintings. Thermal stresses were applied to the paintings by radiation from a spotlight, and out-of-plane displacements were measured. Both micro-cracks and debonded areas were detected by the technique.

3.4.2 Double or multiple exposure Interferometry

Double or multiple exposure Interferometry involves the recording of two or more images, one in the unstressed state and one or more in the stressed state. The technique is primarily suited to pulsed ESPI, but can be performed just as easily with CW lasers. The stress may be applied dynamically and could be generated by impacting the object between exposures.

Two pulses of 1 to 2 ms are used to record images. These pulses are short enough to isolate objects that are vibrating at frequencies of 100Hz or less, and perform time-averaged studies at frequencies of 1000Hz of higher. If the pulse separation period is less than a few hundred microseconds, vibrational effects below 1000Hz are eliminated. In most industrial environments, the major components of the vibration spectrum would be below this level. [5]

Pedrini et al [20] developed a multi-pulse ESPI system. They used a ruby laser that was pulsed by a Q-switch in order to provide four pulses of 100μs with a pulse separation of between 20μs and 100μs. They used three separate CCD cameras in order to record the four separate interferograms. The use of three cameras was necessary because the normal imaging time of a CCD camera is 40ms, during which only one image is recorded. (For an explanation of CCDs and cameras, see Section 3.5) The light reflected off the object was split into three paths using prisms, and directed onto the three CCDs, so that each camera had exactly the same view of the object. Each camera was triggered in succession to capture the successive images. CCD1 was reset just before the first pulse was fired. After the first pulse was fired, the charges from CCD1 were transferred into the shift

register. CCD2 was then reset and the second pulse was fired. The charges from CCD2 were then transferred into the shift register. CCD3 was then reset and the third pulse was fired. The charges from CCD3 were then transferred into the shift register and the fourth pulse was fired. The images associated with the first, second and third pulses were stored in the shift registers of CCD1, 2 and 3 respectively, and the fourth pulse was stored in the photo-sensor of CCD3. It was possible to obtain six fringe patterns associated with the deformations between the pulses (1,2), (2,3), (3,4), (1,3), (1,4) and (2,4). Pedrini et al used this system to study the propagation of shock waves in a metal plate after a steel ball was dropped on its centre, as well as the vibration of a loudspeaker amongst others.

Férnandez et al. [19] used a Nd: YAG laser to perform experiments in both a Double-pulsed Addition and a Double pulse-subtraction mode, which was used to study the propagation of a mechanical wave. They concluded that if the laser pulses could be made to freeze an instant of the object's transient deformation, it would produce a fringe pattern representing the instantaneous deformation of the object's surface. In the first case, both pulses were fired within a single TV frame (double-pulse addition ESPI). In the second case, the laser was synchronised to the camera CCD refresh rate of 60Hz(NTSC). The system waited for an even TV field (see Section 3.6) and stored it. During the following odd field, a solenoid struck the object, after which another field was stored. The two stored speckle patterns were subtracted from each other, and the fringe pattern generated. Due to relatively large elapsed time between the image capture, the system was still susceptible to external vibration in the subtraction mode, which was overcome in the double pulse addition mode. [19]

3.4.3 Time-averaged Interferometry

Usually used to study an object under periodic motion, this technique highlights nodal and antinodal areas. Either a CW laser or a pulsed laser is used where the laser pulse duration is much larger than the period of the object's motion. The fringes generated are of a zeroth order Bessel square function. The brightest fringe corresponds to nodal regions or regions of small or zero vibration. Subsequent bright fringes correspond to areas of constant vibrational amplitude. The fringe order (density) increases as one approaches antinodal regions (regions of large amplitude), and fringe visibility diminishes if the vibration amplitude is too high.

Anderson et al [23] give the equation describing the brightness of a point on the monitor as

$$I_m(r_d) = CJ_0^2\left(\frac{4\pi a_0(r_0)}{\lambda}\right) \qquad \textbf{Eqn 3.11}$$

Where r_d is a position vector on the CCD detector
C is a constant
J_0 is the Zeroth order Bessel Function
r_0 is a position vector on the object
a_0 is the amplitude of the applied vibration
λ is the wavelength of light used

Time averaging has been used to inspect the condition of ancient works of art, which suffered from debonding of the painted plaster layer from the supporting wall. A loudspeaker was used to induce minute vibrations of the plaster that caused debonded

regions to vibrate at their own natural frequencies. By performing time averaged ESPI these flaws could be located. [1,3,5,13,23]

When using a CW laser to perform ESPI, time averaging occurs over each video cycle (typically 20ms, depending on the camera used) if the object is made to vibrate at a frequency higher than the frame rate of the camera. [23]

3.4.4 Stroboscopic ESPI

This technique of pulsed interferometry that is used for analysis of objects under harmonic vibration. The object is made to vibrate at a known frequency, which is much higher than the camera frame rate. The laser is pulsed at the same frequency but for a much shorter time, typically with a duration of 5 to 10% of the overall period. [21] This can be increased to 20% if the pulses are timed to coincide with when the object is at the extremes of its motion when velocity is a minimum. By exposing the object to such a short period of illumination, its motion is effectively frozen. [23]

The fringes generated are no longer a square Bessel function, as in the case of Time-Averaged ESPI, but are of a cosine function, and represent regions of constant displacement. The laser is either pulsed with a Pockel's cell (pulsed laser) or an optical modulator (CW lasers) [1,12,21,23]

Anderson et al [23] studied stroboscopic ESPI, and used a vibrometer to modulate the injection current of a diode laser. A vibrometer is a probe that measures the motion of a point on an object's surface and outputs it as a voltage. The vibrometer was used to

synchronise the laser pulse with when the object was at the peak or trough of its vibration. Anderson et al compared the fringe patterns obtained when using time averaged ESPI, and those obtained using stroboscopic ESPI, and found a large improvement in the fringe quality and order when stroboscopic illumination was used. In this case, the laser pulses were timed to coincide with the minima of the object's vibration. The pulsing of diode lasers is discussed further in section 3.4.6.

Steinbichler [21] successfully used stroboscopic ESPI to investigate vibrating car engines, railway bridges, turbine blades, disc brakes and car bodywork. He modulated the laser beam with a Pockel's cell at a pulse duty width of 5-10% and synchronised the vibration of the object with the laser pulses.

3.4.5 Other techniques

Some of the literature that was consulted indicated other techniques that have been employed in ESPI investigations with CW lasers that are relevant to this thesis and are described below.

CW lasers can be modified to produce a pulsed output, either directly by controlling their injection current or by introducing a physical obstruction in the beam's path. Anderson et al. [23] showed that diode lasers can be made to pulse by controlling their injection current, but this method was found to be unstable for frequencies lower than 10MHz. The instability was the result of changes in the thermal properties of the diode laser as the current was switched on and off and required an electronic equalisation circuit to compensate for this. This required that the circuit resistance and capacitance had to be matched with the particular diode laser. This matching is only specific for a particular frequency and pulse duration, and if a different frequency or pulse duration is required, the circuit must be correspondingly altered. [23]

A CW laser and a CCD camera with very high imaging rates can be used instead of a pulsed laser. Moore et al [24,25] used a camera with a maximum imaging rate of 40 500 frames per second giving an exposure time of 24μs, instead of the typical 25 frames at an exposure time of 20ms. This was aimed at reducing the effects of vibration on ESPI inspection and negating the need for a pulsed laser. Using simple mathematics, they were able to calculate the maximum possible exposure time that could be tolerated for any given vibration amplitude and frequency. Moore was able to perform ESPI on a plate vibrating at 198Hz using an imaging rate of 4500 frames per second, at an exposure time

of approximately 0.22ms. The camera was not synchronised with the vibration frequency, effectively meaning that the object was in random motion. Moore et al also performed analysis on a car door vibrating as a result of the engine running without vibration isolation for the interferometer. Again these were recorded at 4500 frames per second, and yielded good results. These cameras that are capable of high imaging rates are however much more expensive than normal. The resolution of the CCD (number of pixels per unit area) decreases with increasing imaging rates. Thus the shorter the capture period of the image, the lower the image intensity will be.

Sciammarella et al [35] designed a portable in-plane ESPI system that was capable of eliminating rigid body motion that resulted from environmental vibration. It used a phase compensation technique to eliminate environmental vibrations, which worked as follows: A laser beam was split into two paths of equal intensity along a fibre optic cable. One of these paths went to a piezoelectric crystal, and is then expanded onto the object. The other path was expanded directly. A photo detector detected the phase change of a small area on the object's surface, which sent a corresponding signal to an electronic circuit, which inverted it. The inverted signal was sent to the piezoelectric crystal, which expanded or contracted accordingly. The change in dimension of the crystal caused the optical fibre's length to change, and hence the optical path length of the beam changed. In this way, environmental vibrational effects were eliminated.

The system also allowed much larger stresses than normal to be measured by compensating for the rigid body motion that occurs during loading. Normally these stresses would not be measurable by the ESPI system, because the large deformations would cause decorrelation of the images obtained. This was done by monitoring the

change in position of two points on the object when a load was applied. The camera was mounted on a platform with three degrees of freedom, and was moved by a similar amount. In this way, the excessive whole body motion was eliminated.

3.5 Camera and CCD operation

The Charge-coupled Device (CCD) is the part of the camera that is used to obtain the image and convert it into an electrical signal. It is effectively a highly sensitive photon detector, and is divided up into many small areas, known as pixels. These are used to build up an image of the scene of interest. A pixel is about 10-20μm in size, and CCDs typically have between 524 pixels high x 524 pixels wide and 1024 x1024 for commercial closed circuit security cameras, but are much higher for scientific and specialised cameras (e.g. 4096 x 4096 pixels). CCDs with rectangular aspect ratios are also common. [26]

A typical pixel construction is shown in Figure 3.6 below.

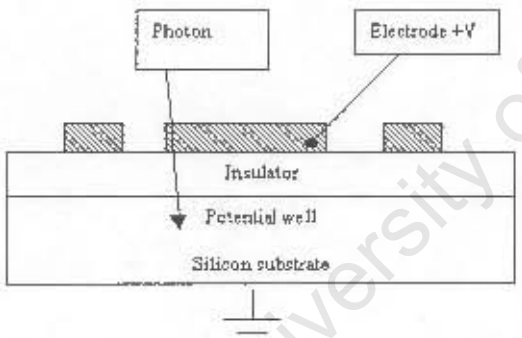

Figure 3.6 Individual CCD pixel construction (Side view)

A pixel is made up of a semi-conducting layer of silicon, covered by an insulating layer and a positively charged electrode. This electrode creates a "potential well" near the surface of the silicon layer. If a photon incident on the electrode has sufficient energy, it can create an electron-hole pair in the in the silicon substrate. The photon-generated electron is attracted towards the potential well that is formed under the positive electrode. The number of electrons collected by each pixel is thus directly proportional to the intensity of light falling on it and in this way a "charge packet" is formed. [15]

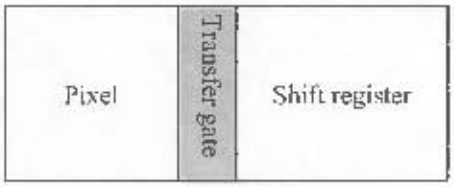

Figure 3.7 Individual CCD pixel construction (Front view)

After a predetermined period, the charge in each pixel is read out and transferred from the CCD into the light-shielded shift register where they remain separated from the pixel area. (See Fig 3.7) After the charge packets have been removed from the pixel area, the pixels are empty again, and begin to fill with electrons as incident light falls on them until the next transfer process. The charges are then transferred into the second shift register, which transfers them line by line to the sensor output. This output is converted into a corresponding voltage by an amplifier. The voltage is filtered to remove noise and output to a storage device or digitiser. [15]

There are two different CCD arrangements commonly in use, namely *Interline Transfer* and *Frame Transfer*. The difference between them lies in the position of the shift register in relation to the pixels, and hence the direction that the accumulated charge takes from the pixel to the sensor output.

3.5.1 Interline Transfer

In this kind of CCD, the charge is transferred from the pixels directly across the transfer gate into a vertical shift register, which takes approximately 1μs. Horizontal rows of charge packets are simultaneously transferred vertically down into the horizontal shift register, and subsequently transferred to the output. Figure 3.8 shows the layout of an interline transfer camera.

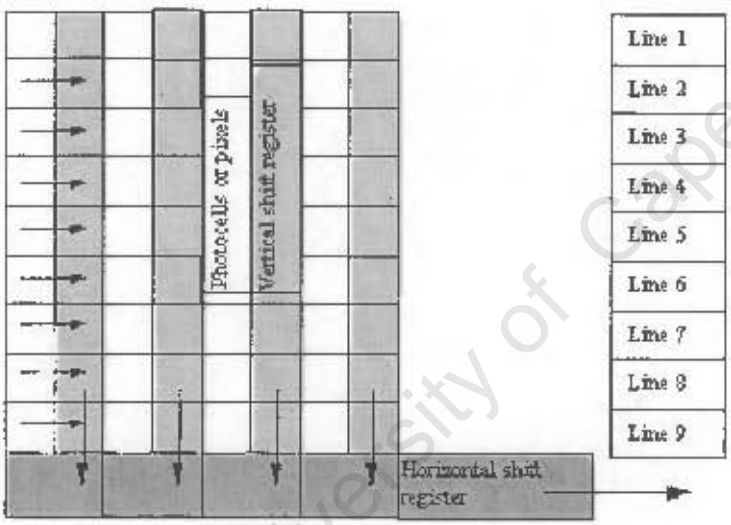

Figure 3.8 Interline Transfer CCD

3.5.2 Frame Transfer

In this type of CCD, the shift register is situated below the pixels. After the integration period, the charge packets are transferred line by line to the vertical shift register, a process that takes approximately 300μs [15]. The charges are then read out consecutively through a horizontal shift register. Figure 3.9 shows the layout of a frame transfer CCD camera.

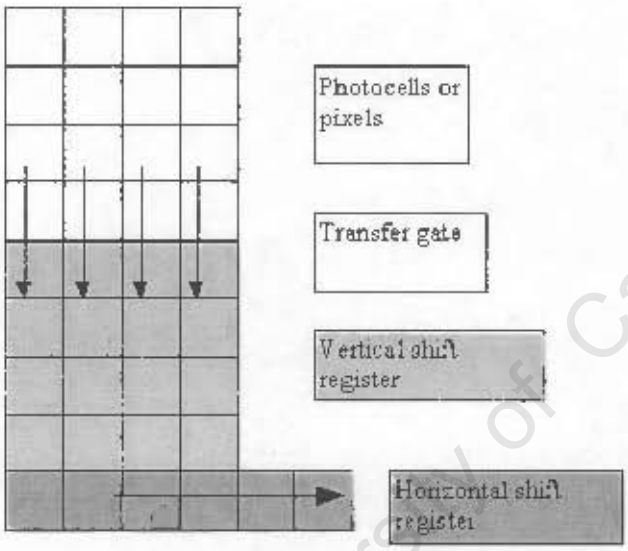

Figure 3.9 Frame Transfer CCD arrangement

3.5.3 Interlacing of fields

When the signal from the CCD output is adapted to a public broadcasting standard, odd and even rows of pixels are read alternatively after a total integration time of either 40ms for CCIR or 33.3ms for NTSC, which are the two most common standards.

These half images are known as fields. Field 1 would consist of line 1,3,5,7 and field 2 would consist of line 2,4,6,8 and so on. The odd fields are imaged and read out after the first 20ms of the cycle, and the even fields are imaged and read out during the second 20ms for the CCIR standard. There are thus 50 fields (at 20ms per field) and 25 frames (at 40ms per frame) recorded per second. These two fields are recombined into a full image known as a frame. This procedure is known as interlacing, and is done in order to avoid flickering on the monitor.

3.5.4 Application to ESPI

Spooren [15] investigated various aspects of the application and requirements of standard CCD cameras when used for ESPI inspection. The following points are of relevance:

- Integration time control

  It is possible to reduce the integration time (time during which the CCD receives and quantifies incident light), and in order to provide a "shuttering effect" and investigate objects with a CW laser under unstable conditions. When pulsed lasers are used, shuttering in synchronisation with the laser pulses is a way to remove background

light. The integration time of some interline and frame transfer cameras is adjustable from 1/50000s to infinity.

- Read out synchronisation

  It is possible to synchronise the laser pulse and camera pixel clock. The laser pulse can thereby be synchronised so that it occurs during the active period of the CCD, and not when the pixels are being read out, which would result in a loss of information. It is also possible that if the laser pulse and the camera imaging are not synchronised, part of the laser pulse is recorded during the end of one active period, and the remainder is recorded during the beginning of the next.

Spooren [15] also compared the benefits and drawbacks of interline and frame transfer methods with regard to ESPI investigation. He said that Interline transfer cameras are better suited to pulsed ESPI than frame transfer cameras because:

- The time taken for the charge in each photocell to be transferred to the shift register is much less for an interline camera (1μs) compared to that for a frame transfer camera (300μs).
- Interline-transfer cameras are cheaper than frame-transfer cameras for similar specifications.

3.6 LC shutter operation

Liquid Crystal (LC) shutters work in much the same way as LC displays that are commonly found in watches, laptop screens and instrument displays etc. They consist of a sheet of liquid crystal material that is sandwiched between two orthogonally crossed polarisers. They are normally transparent, but when a voltage is applied across them, they darken, allowing little or no light to pass though them. By applying a suitable signal, a shuttering effect can be obtained.

They come in three forms, namely Nematic liquid crystal, Ferro-electric crystals (FLC) and Twisted Nematic (TN) crystals. They all use the same basic principle and the difference between them is the construction of the liquid crystal material.

Conventional LCD's found in watches and displays make use of nematic crystals, while FLC crystals make use of Smectic C liquid crystals. The smectic C crystals are much more ordered than the nematic crystals, making the FLC shutters capable of shutting speeds of three orders of magnitude higher than conventional LCs. FLC shutters would typically take 15μs to change from either clear to black or black to clear, while conventional shutters would take typically 2 or 3 ms [27, 28]. FLC shutters are, however, substantially more expensive than the others.

The LC material has the ability to change the axis of polarisation of the light passing through it, depending on whether or not a voltage is applied across it, as illustrated in Figure 3.10.

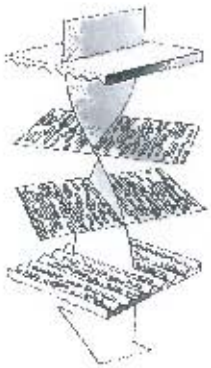

Two microscopically grooved surfaces are arranged orthogonally to each other. The crystals line themselves up with grooves on the surfaces, gradually twisting through 90° from one surface to the other. When light passes through the crystals, the light's polarisation orientation follows the crystal orientation, and is also twisted through 90° [27]

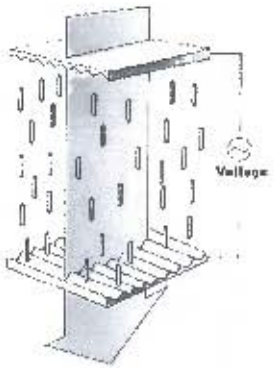

When a voltage is applied, the crystals rearrange themselves as shown above. The light then passes through the material and the polarisation orientation is unaffected.[27]

Figure 3.10 (a), (b) Rotation of light polarisation by LC crystal

When a thin layer of liquid crystal material (either nematic or FLC) is sandwiched between two linearly crossed polarisers, it becomes a shutter, as shown in Figure 3.11 below.

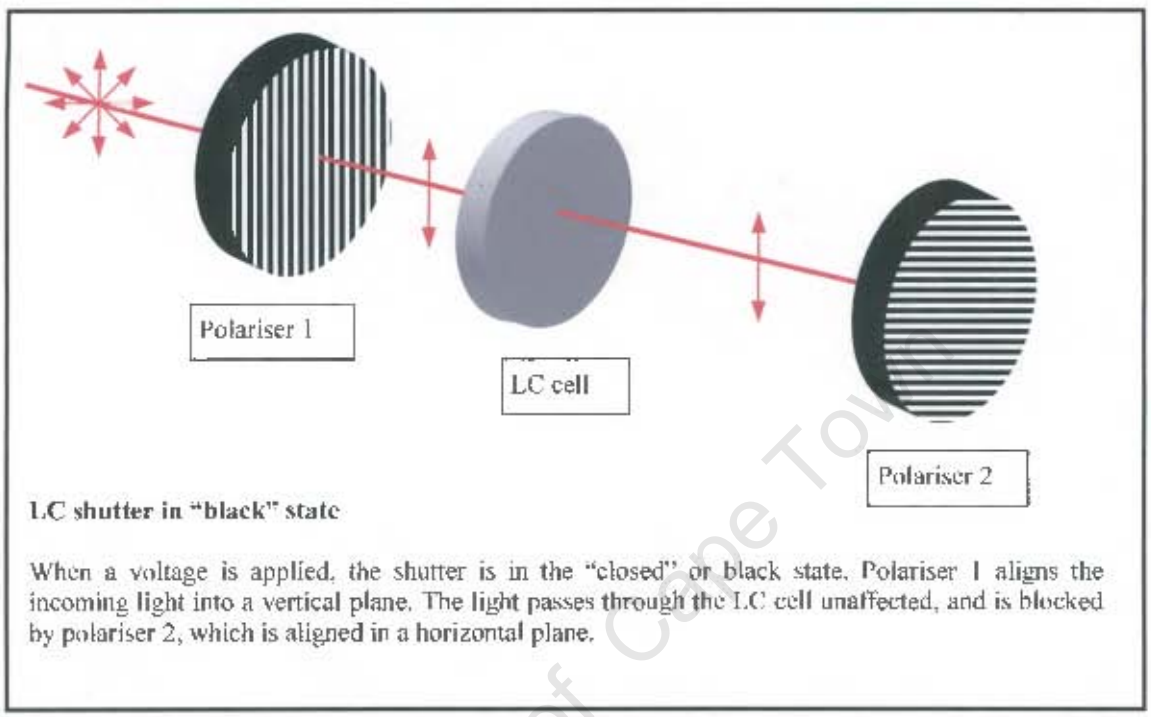

LC shutter in "black" state

When a voltage is applied, the shutter is in the "closed" or black state. Polariser 1 aligns the incoming light into a vertical plane. The light passes through the LC cell unaffected, and is blocked by polariser 2, which is aligned in a horizontal plane.

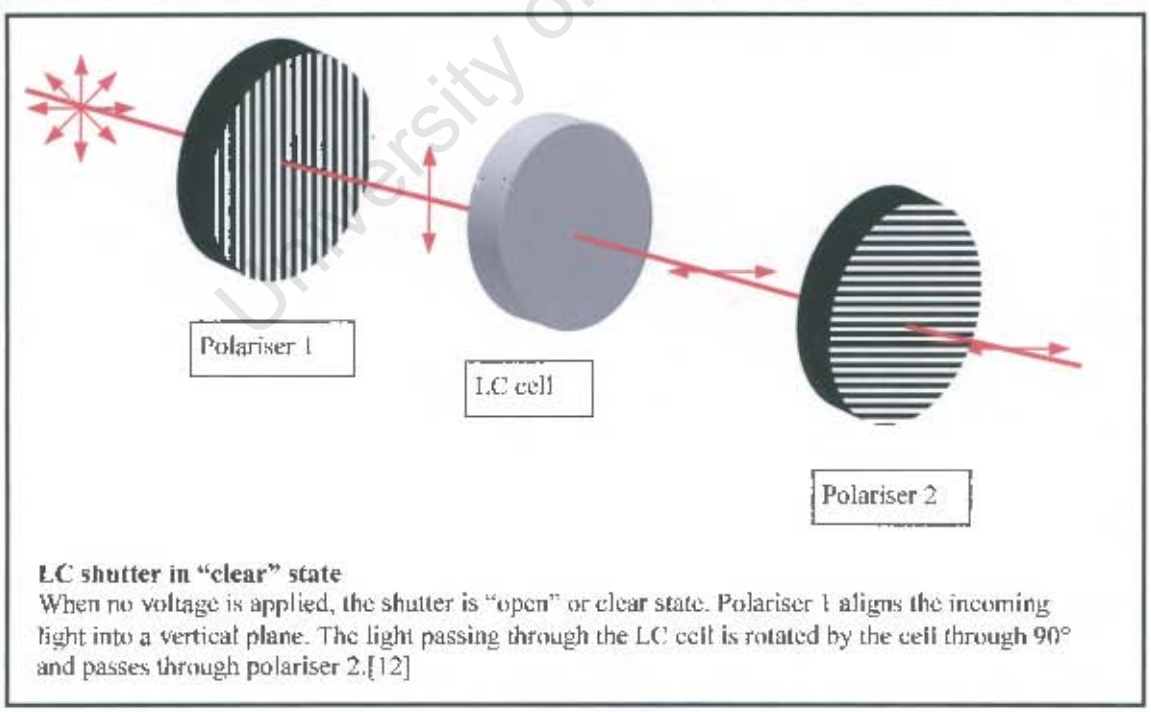

LC shutter in "clear" state

When no voltage is applied, the shutter is "open" or clear state. Polariser 1 aligns the incoming light into a vertical plane. The light passing through the LC cell is rotated by the cell through 90° and passes through polariser 2.[12]

Figure 3.11(a) (b) Shuttering of light by LC shutter in opaque and transparent states respectively

3.7 Lithium Niobate crystal operation

Lithium Niobate (LN) is a substance that has the ability to change the direction of polarisation of light passing through it when a voltage is applied to it. It requires much higher voltages to do so than the LC shutter described above. It operates on the Pockel's effect or electro-optic effect, which is described by Yariv [36].

The crystal can be used in conjunction with two linearly crossed polarisers in order to form a shutter and modulate a beam of light passing through it. The principle is the same as that described in Figure 3.11 above, except that in this case the light only passes through the shutter when the voltage is applied, not when it is removed as in the case of the LC shutter. Figure 3.12 shows the principle of the LN shutter. [36]

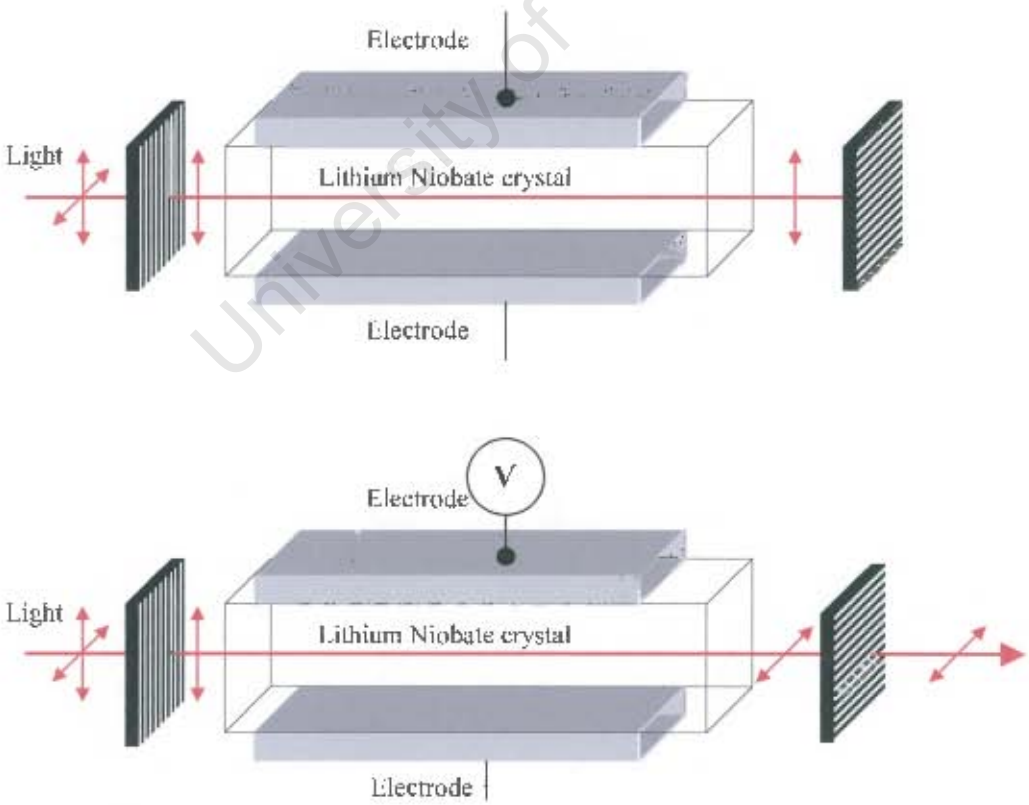

Figure 3.12(a) (b) Shuttering of light by LC shutter in opaque and transparent states respectively

3.8 Insulated Gate Bipolar Transistor (IGBT)

In order to control the Lithium Niobate shutter, a voltage in the order of 2000V was required. This voltage had to be switched on and off accurately and at a suitably high rate. IGBTs were investigated as a possible switching mechanism.

An IGBT is a transistor that is capable of switching very high voltages on and off. (Approximately 1200v, although this varies from model to model) Current is allowed to travel from the collector to the emitter if a voltage is applied to the gate terminal. The amount of current that is allowed to pass through the transistor is proportional to the voltage applied to the gate.

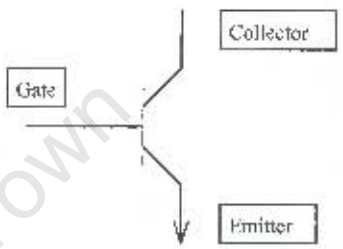

Figure 3.13 Illustration of IGBT connections

By modulating the gate voltage, IGBTs can be made to modulate the collector-emitter voltage, and thus replicate voltage cycles, for example square waves.

If the collector-emitter voltage required is larger than the maximum rated voltage of the IGBT, it is possible to connect several IGBTs in series, and divide the voltage among each of them. [32] This, however, requires special control to ensure that they each receive equal voltages, or there is a risk of damaging the IGBT.

Chapter 4 Experimental procedure

4.1 Theoretical approach

The intention of this project was to reduce or eliminate the effect of vibration on the successful capture of ESPI images and two techniques were investigated for this purpose. Both techniques essentially had the same objective, namely to reduce the duration of the camera CCD exposure period, thereby creating a shuttering effect. If this period were sufficiently short, the object's motion would be frozen, and would no longer present a problem.

The first technique was the amplitude modulation or pulsing of a Continuos Wave (CW) laser. This was done using two different slotted discs, a Liquid Crystal shutter and a Lithium Niobate shutter. The second technique investigated was the use of the camera's built-in shuttering capability.

4.2 ESPI Inspection

4.2.1 On Table Inspection

ESPI inspection of the object was initially performed on an optical table at UCT using the different shuttering methods to investigate the effect of various parameters, including the characteristics of each of the shuttering methods. In order to allow comparison between these conditions, the ESPI set-up was constructed in the same way in each case. The layout is shown in Figure 4.1 below.

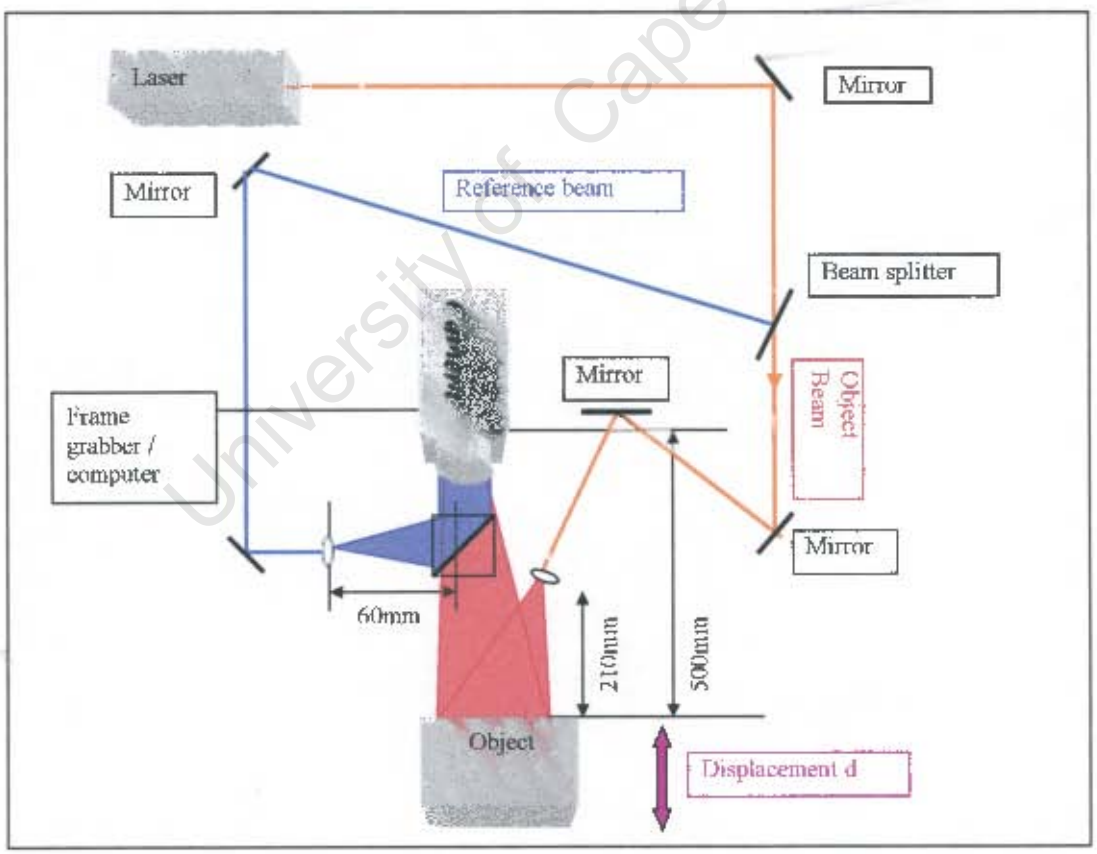

Figure 4.1 ESPI arrangement used during on table inspection

The laser used was a He-Ne with an output of approximately 8mW. The expanding lenses were 40x microscope objective lenses and the camera was a Sony SSC M-370CE. The camera's Automatic Gain Control (AGC) was on for all the images that were captured. The computer used custom software that was written by Mr D Findeis of the Department of Mech Eng at UCT to perform the inspection procedure. The software allows the user several options, such as real-time ESPI and double exposure ESPI, amongst others. The program is also able to provide light intensity plots of the ESPI image that is obtained along either rows or columns. It also allows the ESPI images to be saved as TIFF image files.

Once the pulsing methods had been tested on the table, the object was placed on the ground, and inspection under various vibration conditions was performed. Inspection was carried out while the object was at rest and while a compressor and loudspeaker were exciting it. In this way three different vibration environments could be investigated, namely naturally occurring environmental vibration, simulated industrial vibration from the compressor and loudspeaker vibration.

The laser, camera and optics remained on the holographic table. This was done in order to simulate a portable vibration resistant ESPI system that was under development at UCT. In this system, the optics (including the camera, beam splitter, mirrors and expanding lenses) were to be mounted on a firm platform that would be supported on a tripod. The tripod would rest on inflatable tyres in order to eliminate or reduce the vibrations transferred to the optics. The object under inspection would rest on the ground without any vibration isolation.

4.2.2 Environmental Excitation

While the test specimen (a section from a helicopter tail rotor blade) was off the holographic table, ESPI images were captured using a selection of the pulsing methods. The vibration experienced by the test specimen were recorded, allowing for comparison and making it possible to observe the effects that environmental vibration had on ESPI inspection.

4.2.3 Compressor Excitation

A small portable compressor was run near the object in order to induce vibration and simulate an industrial environment. The laser was pulsed using the large disc, LN shutter and camera shutter, and ESPI performed.

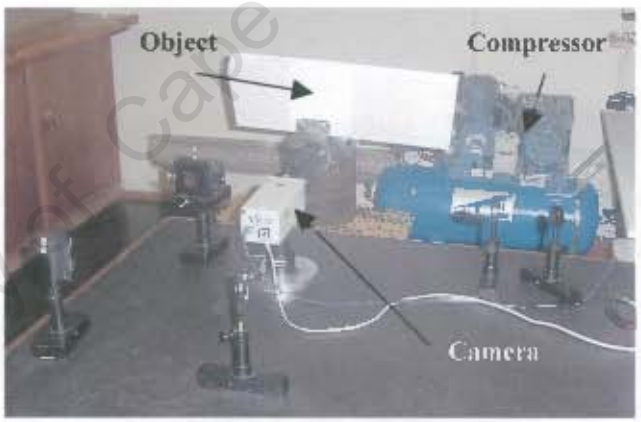

Figure 4.2 Off-table ESPI arrangement with compressor to excite test specimen

4.2.4 Loudspeaker excitation

A loudspeaker was used to excite the object under investigation. The loudspeaker excited the test specimen at 214Hz, having a period of 4.67ms, and the vibration level recorded.

Figure 4.3 Test specimen excited by loudspeaker

4.3 Specimen inspected

A section from a helicopter tail rotor blade with two deliberately induced flaws on its surface was inspected. One of the flaws is a pinhole of approximately 0.5mm and the other is a slit approximately 30mm long and 0.5mm wide as shown in Figure 4.6. Although these were all visible surface flaws the technique is just as suited to subsurface flaws, as long as the defect affects surface displacement.

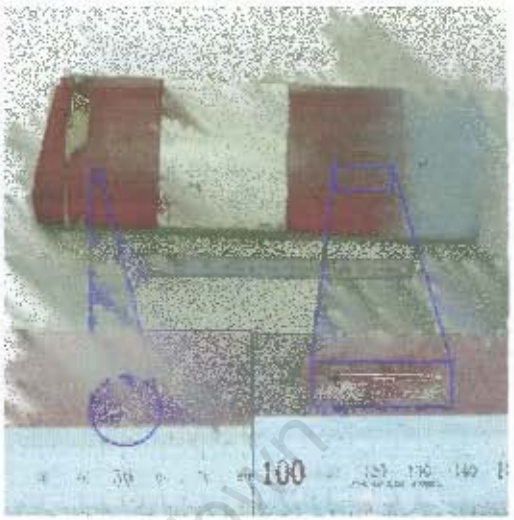

Figure 4.4 Tail rotor showing flaws

Figure 4.3 shows the construction of the rotor. It comprises of an outer skin that is bonded to the spar at the leading edge and clamped at the trailing edge. The rest of the rotor section is filled with an aluminium honeycomb structure. The spar determines the leading edge shape, and the honeycomb provides a measure of structural strength. The slit and pinhole flaws were in the outer skin, where it is bonded to the honeycomb section.

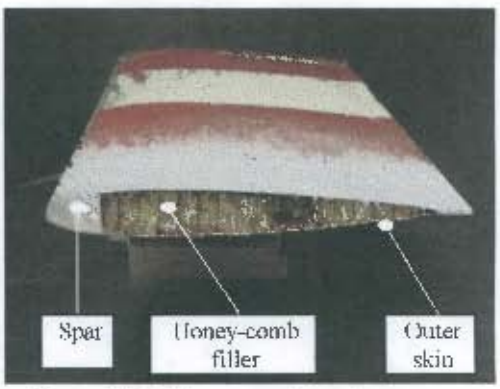

Figure 4.5 Tail rotor construction

Thermal stresses were applied to the tail rotor by a blowing hot air from a hairdryer onto the region around the flaw.

4.4 Vibration simulation and measurement

An accelerometer was attached to the helicopter tail rotor blade to enable the vibration of the blade to be measured. The accelerometer outputs a voltage that is proportional to the acceleration that the accelerometer experiences. The voltage was measured and recorded on a computer using a Handy-Scope. A Handy-Scope is a digital oscilloscope that connects directly to a computer. The Handy-Scope provided values of voltage and corresponding time, which were inserted into a Microsoft Excel spreadsheet. The voltages obtained were converted into acceleration values in the spreadsheet using the voltage/acceleration value of 100mV/g, or 10.19mV/m/s^2. The specification sheet of the accelerometer is included as Appendix 4.

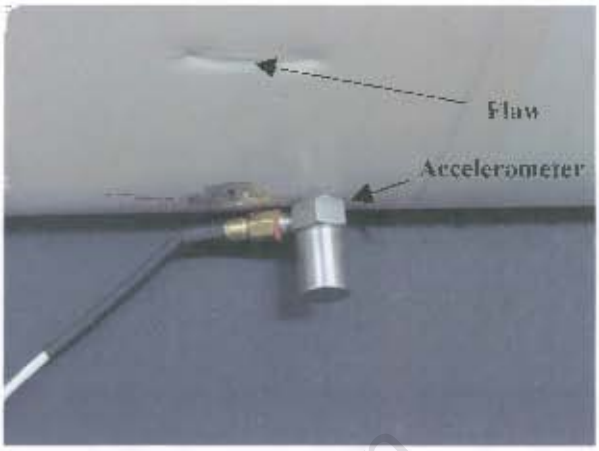

Figure 4.6 Accelerometer mounted on rotor section

A simple equation was used to calculate the instantaneous velocity and displacement. These equations could not be applied to random vibration, because the vibration is made up of a spectrum of frequencies.

$$v = \frac{a}{2\pi f} \qquad \textbf{Eqn 4.1}$$

$$d = \frac{a}{4\pi^2 f^2} \qquad \textbf{Eqn 4.2}$$

Where a is the instantaneous acceleration of the object

v is the instantaneous velocity of the object

d is the instantaneous displacement of the object

f is the frequency of the applied vibration [33]

These equations did not take the phase shift that occurs when acceleration is integrated into velocity, or when velocity is integrated into acceleration into account. This shortcoming could be overlooked since the magnitude of the displacement was of importance, and not its phase.

4.5 Laser pulsing using an electric motor and large slotted disc

A simple apparatus was set-up consisting of a circular disk with two triangular holes in it, a DC motor and a variable power supply, as shown in Figure 4.8 below.

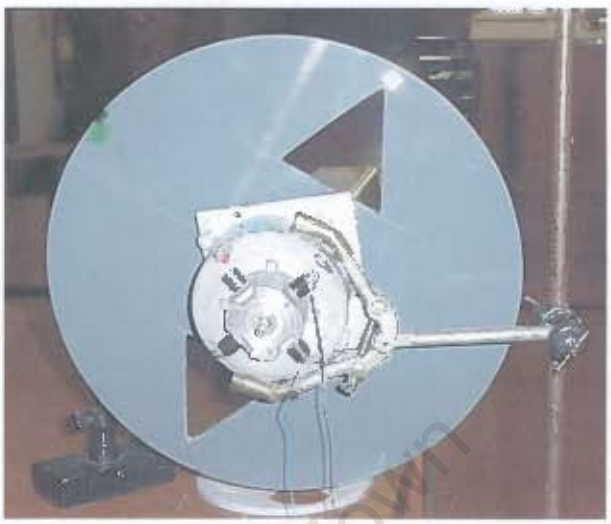

Figure 4.7: Large disc and motor

The disc was placed in front of the laser aperture, and the laser light was disrupted as the disc rotated. The intention was to show that ESPI images could be satisfactorily captured using a "pulsed laser", without having to go to the expense of a more specialised system. A motor was found that was able to maintain the required speed to an acceptable degree of accuracy. The motor spun the disc at 1500rpm(25rps), which would provide 3000 pulses per minute, or 50 pulses per second. This speed was chosen in order to co-ordinate the laser pulses with the camera field rate. The holes were shaped in such a way that it would be possible to vary the laser pulse duration easily by simply changing the position of the laser along the radius of the disc, while maintaining the same pulse frequency.

The effective period of the laser pulse was calculated as follows:

$s = v_{tan\,g} t_{pulse}$ **Eqn 4.3**

Which gives $s = r\omega_{disc} t_{pulse}$ **Eqn 4.4**

Solving for t gives $t_{pulse} = \frac{s}{r\omega_{disc}}$ **Eqn 4.5**

Where: s is the chord length of the cut-out,

v_{tang} is the tangential velocity at the point where the laser is chopped

t_{pulse} is the duration of the laser pulse.

ω_{disc} is the rotational speed of the disc

r is the point on the disc radius through which the laser shone

A Microsoft Excel spreadsheet was used to perform these calculations, and is given as Appendix 3.

4.6 Laser pulsing using a stepper motor and a slotted disc

A stepper motor was also investigated and a small model out of a printer (a uni-polar Epson SM-LO40) was located. The model selected was much smaller than the motor used with the previous disc, and would be capable of higher speed accuracy due to the nature of its construction. The stepper motor required much more complicated electronics to control it than the motor previously used. The disc and controlling circuit can be seen in Figure 4.8. The electronic circuit was built and provided by Mr S Graber of the Department of Mechanical Engineering at UCT.

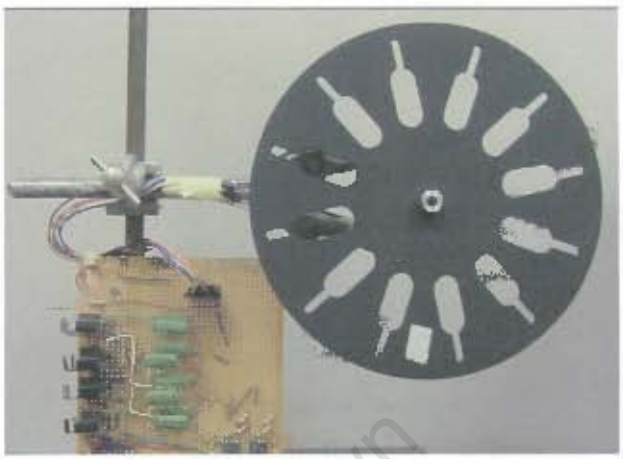

Figure 4.8 Stepper motor, disc and controller circuit

In order to reduce the rotational speed at which the disc would operate, and still maintain the correct pulse rate, more slots were cut into the disc. Twelve slots would provide the required 50 pulses per second, if the disc were rotated at 250rpm instead of two slots at 1500rpm. Again the slots were designed to make the pulse width adjustable, and the pulse duration was calculated using Equation 4.5. The drawing of this disc is attached as Appendix 5

4.7 Laser pulsing using a Liquid Crystal (LC) shutter

The next shutter that was investigated was an electronic liquid crystal (LC) shutter. This is effectively a window that is normally clear, but when a voltage is applied across it, it darkens, allowing little or no light to pass though it. These shutters are compact, and units 10mmx10mm are commercially available.

The clear advantage of these shutters over the motor arrangement is their small size and vibration-free characteristics. They would also be much easier to control if a customised pulsing sequence was needed. Whereas the disc-motor set-up can only pulse in an on-off-on-off sequence, the shutter can provide any sequence that is desired.

A LC shutter was sourced from a pair of 3-D goggles. One of the shutters was removed and is shown in Figure 4.9.

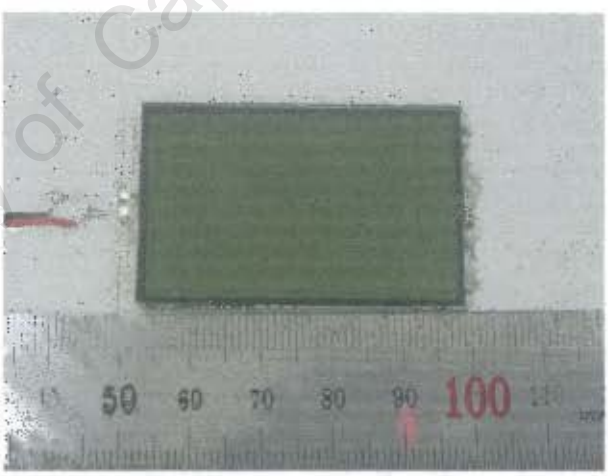

Figure 4.9 LC shutter

These goggles are usually used to allow computer games to be viewed in 3D when worn by the user. Two of these shutters operate together, and darken alternatively. While the left shutter is blocked, the right shutter is clear, and the computer monitor displays the image as would be seen from the right eye's perspective. The right shutter then darkens and the left shutter becomes clear. The computer monitor then refreshes and displays the image as it would be seen from the left eye's perspective. The shutter then reverses again and the

cycle continues. By using a sufficiently high alternating rate, the user has the perception that he is seeing in three dimensions. These goggles typically refresh at 50Hz, meaning the shutter opens and closes once during the 20ms period.

Optimal contrast between the clear and black states of the shutter was obtained when it was oriented at 45° to the horizontal. A possible reason for this is that the crossed polarisers were oriented at 45° and 135° respectively, while the laser beam was vertically polarised.

A pulse generator was used to supply a 12v square wave voltage to operate the shutter. This particular pulse generator allowed the frequency as well as the duty width or pulse duration to be varied. The duty width, duty cycle or pulse width all refer to the amount of time that the shutter is open compared with the amount of time that it is closed, and can be expressed as a percentage.

4.7.1 Characterisation of the LC shuttering ability

The light transmission and dynamic response of the shutter to the applied voltage was measured with a laser, an oscilloscope and a light sensitive diode, as illustrated in Figure 4.10 below. The light that was emitted from the laser was shone through the shutter and measured by the light sensitive diode. The diode outputs a voltage proportional to light incident on it, and this voltage was compared to the high voltage applied to the shutter. One oscilloscope channel was used to measure the voltage applied to the shutter, and the other was employed to measure the response of the light sensitive diode. In this way, a direct comparison could be made between the two. By simple proportion of the voltage across the light sensitive diode, the transmission of the shutter in its transparent state and black state were calculated using equation 4.6 and 4.7 below.

$$Transmission(clear) = \frac{Voltage_{clear}}{Voltage_{Noshutter}} \qquad \textbf{Eqn 4.6}$$

$$Transmission(Black) = \frac{Voltage_{Black}}{Voltage_{Noshutter}} \qquad \textbf{Eqn 4.7}$$

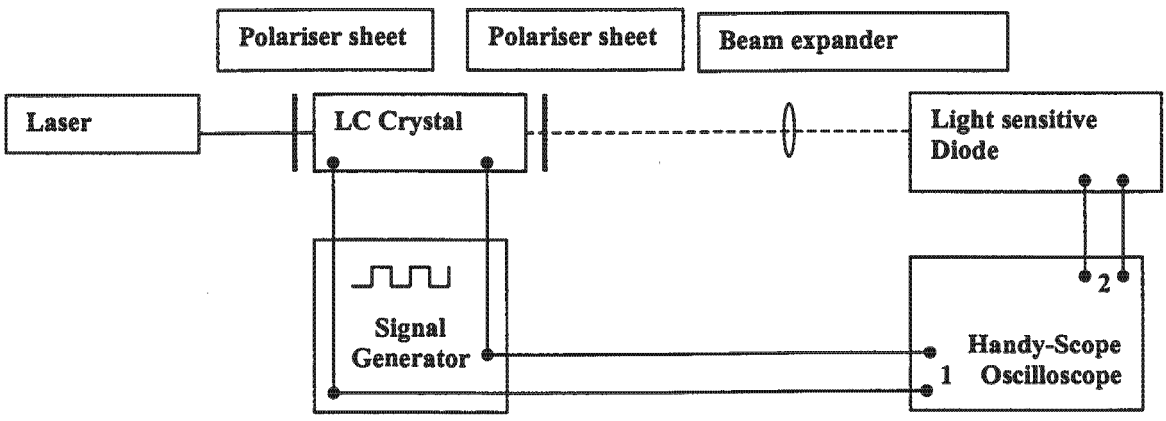

Figure 4.10 Procedure to measure LC characteristics

4.8 Laser pulsing using a Lithium Niobate (LN) crystal shutter

A Lithium Niobate (LN) crystal shutter was also investigated. The principle used to investigate it was the same as that for LC shutter, except that only a single polariser was necessary because the laser being used emits polarised light. The Lithium Niobate crystal and plastic mounting is shown in Figure 4.11

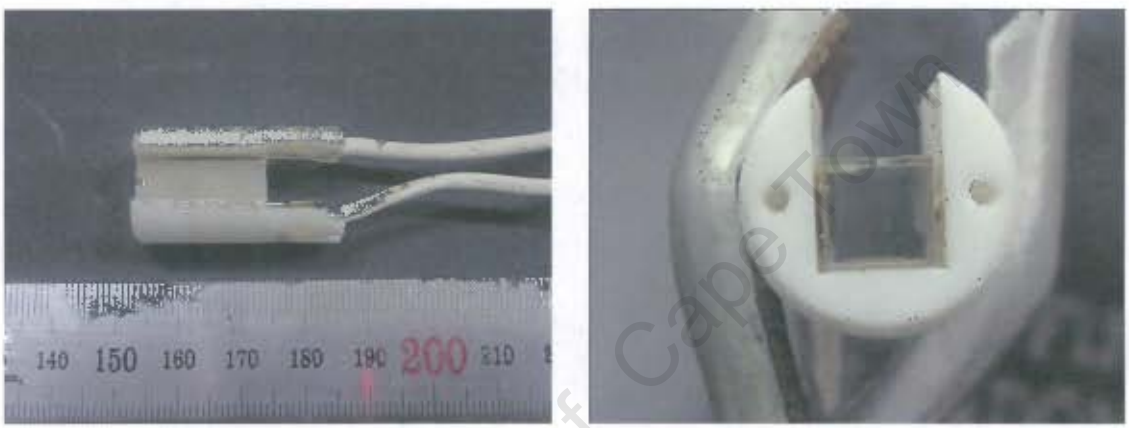

Figure 4.11(a) (b) Lithium Niobate crystal side and end view

4.8.1 Construction of the Lithium Niobate (LN) control circuit

Lithium Niobate crystals require very high voltages (approximately 2000V) in order to operate. This voltage can be Alternating Current (AC) or Direct Current (DC), DC being the preferable option. In this case, DC was essential because of the wide range of pulse widths that were to be investigated. The degree of polarisation rotation, and hence the shuttering ability depend on the voltage applied. This voltage will not be consistent at the peaks if AC is used. By using a DC signal, the same voltage would be applied to the shutter during the entire time that it was open, regardless of the pulse width.

The Electrical Engineering Department of UCT supplied a suitable transformer that would provide up to 3000VAC from 110VAC input. The input voltage was supplied by a variac, which is effectively a variable transformer, and is capable of providing an adjustable range of AC voltages.

A high voltage rectifier and an ultra fast switching system using Insulated Gate Bipolar Transistors (IGBTs) was built based on the circuit diagram illustrated in Figure 4.12. It was only possible to obtain IGBTs (GT8Q101 IGBTs) with a maximum rating of 1200v, so it was necessary to stack several IGBTs in series to reach the required voltage. Three IGBTs were used, because at the time that the circuit was built, little was known about the crystal's properties, and voltage that would be required. A conservative estimate of 3000V was initially predicted.

The IGBTs used had the following switching time characteristics: [31]

	Typical time (µs)	Maximum time (µs)
Rise time	0.3	0.6
Turn-on time	0.4	0.8
Fall time	0.3	0.5
Turn-off time	0.8	1.5

Table 4.1 IGBT characteristics

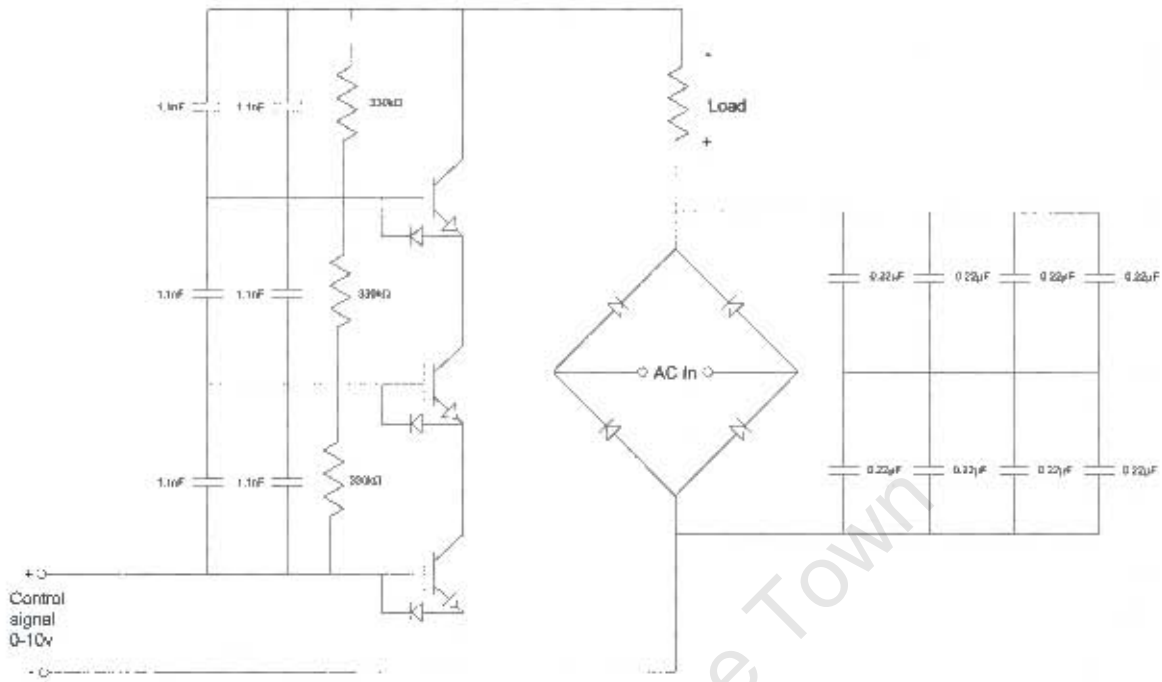

Figure 4.12 Rectifier and IGBT circuit

The right-hand branch of the circuit is a rectifier that converts the incoming AC voltage into DC voltage. The AC voltage is supplied by the output of the transformer. The left-hand side of the circuit is the switching side. The capacitors on the IGBT side were necessary to ensure that each of the IGBTs had the same voltage across them and none of them experienced an excessive voltage spike during switching on or off.

The circuit was housed in a box to ensure minimal contact of the operator and surroundings with the high-expected voltages. Two of the connections were for the incoming AC voltage from the transformer, and the other two were for the output of the rectified and switched DC voltage which was to be applied to the shutter. The BNC connection was the signal input from the signal generator that controlled when the circuit would apply the voltage to the shutter.

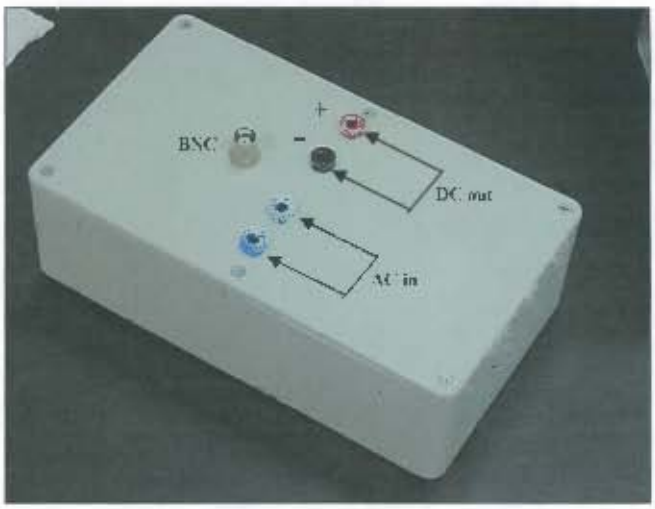

Figure 4.13 Lithium shutter control box

4.8.2 Characterisation of the High voltage circuit

Once the circuit was built and the initial problems resolved the IGBT circuit response was analysed. This was done by using an oscilloscope to measure the applied voltage signal from the signal generator in relation to the high voltage coming out of the circuit and onto the shutter, as shown in Figure 4.14. The high voltage was measured with a high-voltage probe from the Electrical Engineering Department.

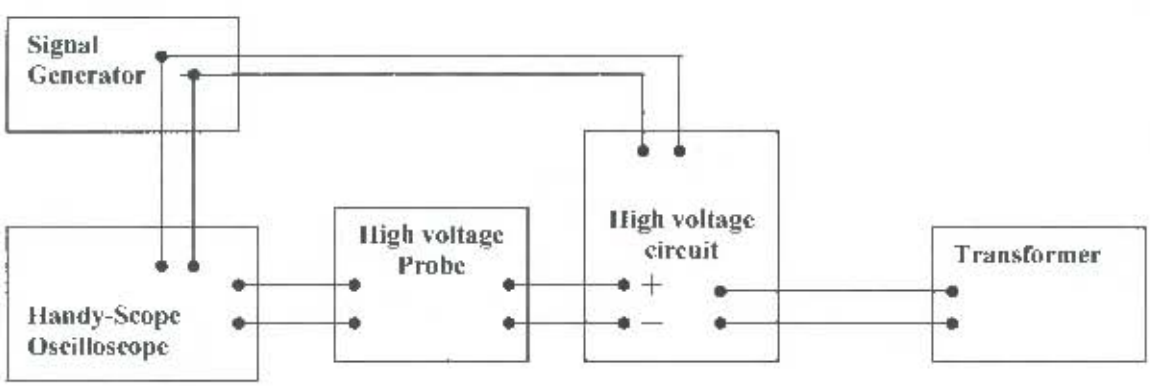

Figure 4.14 Procedure to measure circuit response

4.8.3 Characterisation of the Lithium Niobate crystal's shuttering

The light transmission response of the shutter was then measured using the procedure in Figure 4.15. A He-Ne laser was shone through the crystal and the output measured with a light sensitive diode. The diode outputs a voltage proportional to light incident on it, and this voltage was compared to the high voltage applied to the shutter. Equation 4.6 and 4.7 were used again to calculate the light transmission through the shutter.

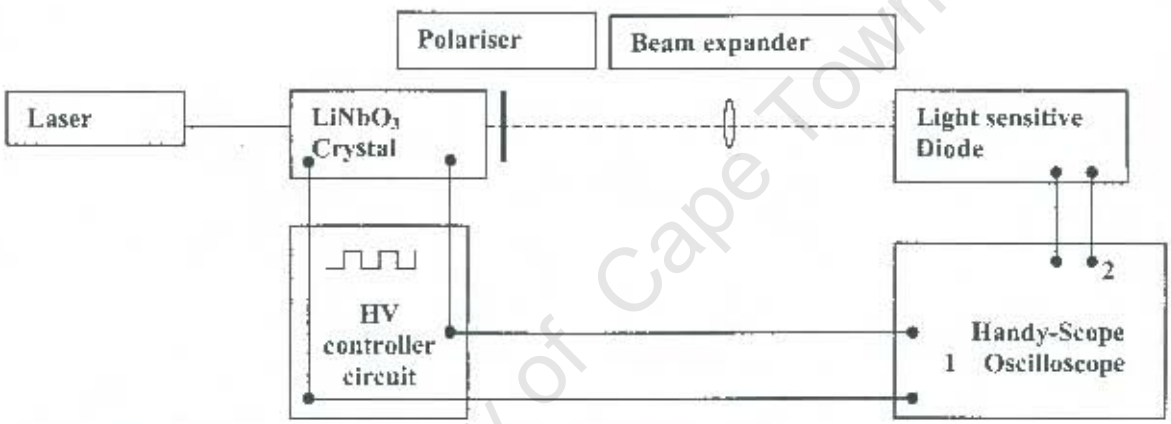

Figure 4.15 Procedure to measure LN shutter characteristics

4.9 Shuttering using the camera's built-in shutter facility

The camera used to record the ESPI images was a Sony SSC M370CE black-and-white TV camera. It is an interline transfer camera with a CCD area of 6.3 x 4.7mm. The CCD has 752 x 582 pixels giving a pixel size of approximately 8μm, including the transfer gate and shift register. It captures images at 25 frames per second, and each frame is comprised of two fields, giving a field rate of 50Hz. The camera has a built-in Automatic Gain Control (AGC) facility, which can be used in low light conditions to improve the sensitivity of the CCD. It also has a built in shuttering facility with eight shuttering times that can be selected through a dial within the camera. The shutter time determines the period of time for which the camera picks up image information during each of the 20ms field capture periods. Thus, when the shutter is set to 4ms, the camera captures the image information for only 4ms out of the total 20ms and is idle for the rest of the field's duration. These shuttering times are 20ms, 8.33ms, 4ms, 2ms, 1ms, 0.5ms, 0.25ms and 0.1ms. The camera also has a synchronisation facility, so that the camera image capture can be synchronised to an external device or vice versa.

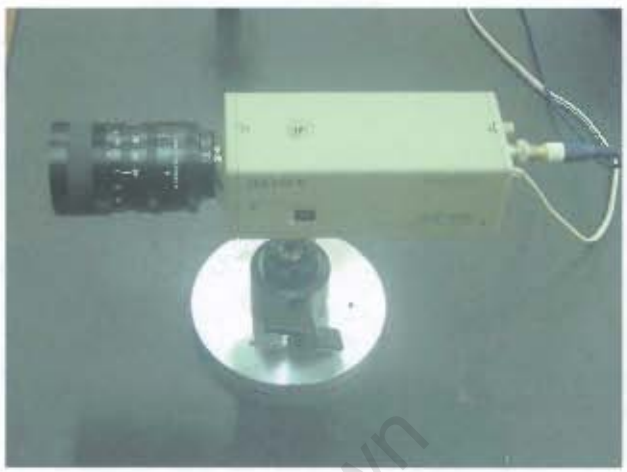

Figure 4.16 Camera used to perform ESPI inspection (Sony SSC M370 CE)

The built in shutter facility was investigated as a possible method of reducing the CCD exposure time.

4.10 Image Editing

The ESPI images captured were edited after being captured in order to improve their clarity. It was necessary to adjust the brightness and contrast levels to make them visible, sometimes quite substantially.

The CCD is 752 pixels wide x 582 pixels high and is digitised by a frame grabber that is 512 x 512 pixels. Consequently, the fringe pattern is not an actual representation of the object's proportion. The images obtained were therefore widened by 33% in order to correct their aspect ratios.

Graphs of light intensity variation of the final fringe pattern were also obtained. These were taken along a single line of the ESPI images, which is indicated by a white line on the images themselves. The plots are shown in a bar graph format that is scaled from 0 to 255. On this scale, 0 indicates a completely black pixel, and 255 indicates a completely white pixel. Values between these extremes are varying shades of grey.

Chapter 5 Results

5.1 Calibration and evaluation of equipment characteristics

5.1.1 Accelerometer calibration

An accelerometer was used to quantify the magnitude of the object's response to various vibrational conditions. It was calibrated in order to ensure that accurate results were obtained using a calibration device that provides a very specific vibration to the accelerometer.

Figure 5.1 below shows the accelerometer calibration curves for acceleration, velocity and displacement. The curves correlate well with the applied vibration of 159.2Hz (±1%), with a maximum acceleration of 10m/s^2 (±3%), a velocity of 10mm/s (±4%) and a displacement of 10μm (±5%). The accelerometer and formulae used to calculate the object's velocity and displacement can therefore be considered sufficiently accurate.

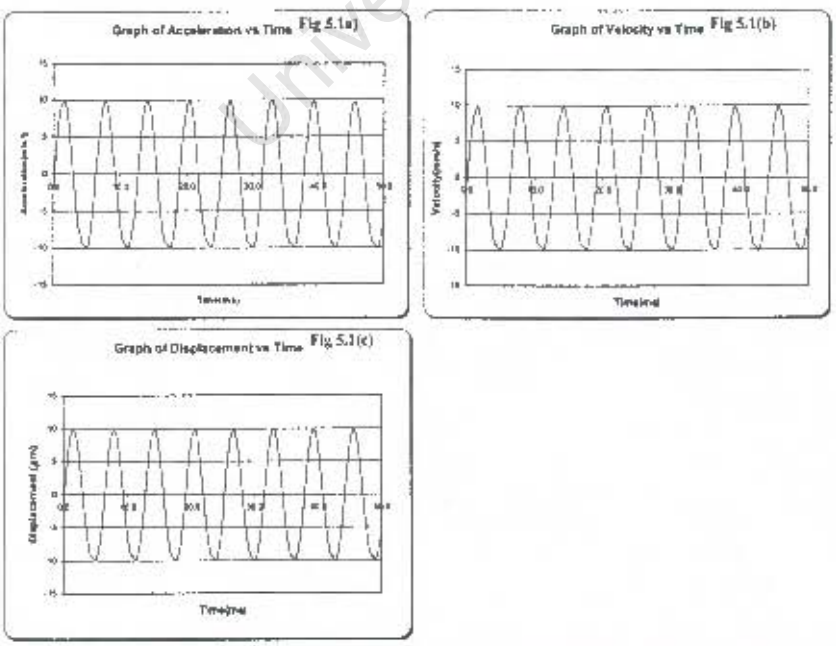

Figure 5.1(a) – (c) Calibration graphs of Acceleration, Velocity and Acceleration response for accelerometer when subjected to specific calibration vibration

5.1.2 Characterisation of the Liquid crystal (LC) shutter

The LC shutter's effectiveness was tested using the procedure described in Section 4.7.1 and the following results were obtained for the He-Ne laser light (632nm).

Condition	Voltage (V)	Transmissibility (%)
No shutter present	0.4075	100
Shutter open	0.325	79.8
Shutter closed	0.000	0

Table 5.1 Transmissibility of light through LC shutter

Figure 5.2(a) – (c) on the following page shows graphs of the shutter's light transmission response to the applied control voltage with respect to time. Note that the voltage scale is inverted to allow direct comparison with the light transmission curve. When the 12v signal is applied to the shutter, it darkens. This is shown by a decrease in the light transmission through the shutter. Figure 5.2(a) gives an overall indication of the shutter response. As indicated in Figure 5.2(c), the shutter responds relatively quickly when the voltage is applied, and darkens in approximately 0.9ms. This is not the case when the voltage is removed and the shutter opens, as illustrated in Figure 5.2(b). In this case, the shutter takes approximately 2ms to reach the first plateau. This occurs when the transmission of the shutter has reached approximately of its 80% open state value, and a further 3.5ms to reach its maximum transmission condition.

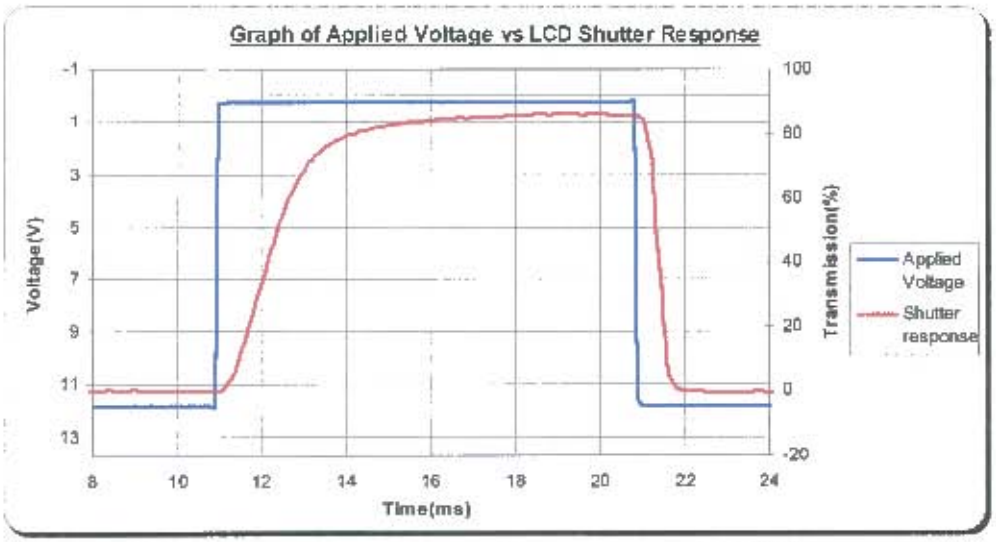

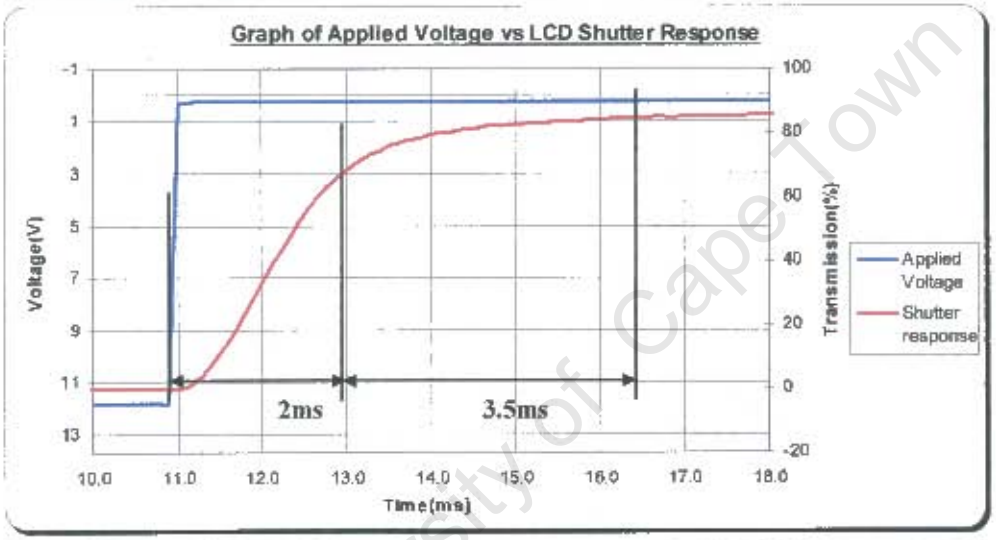

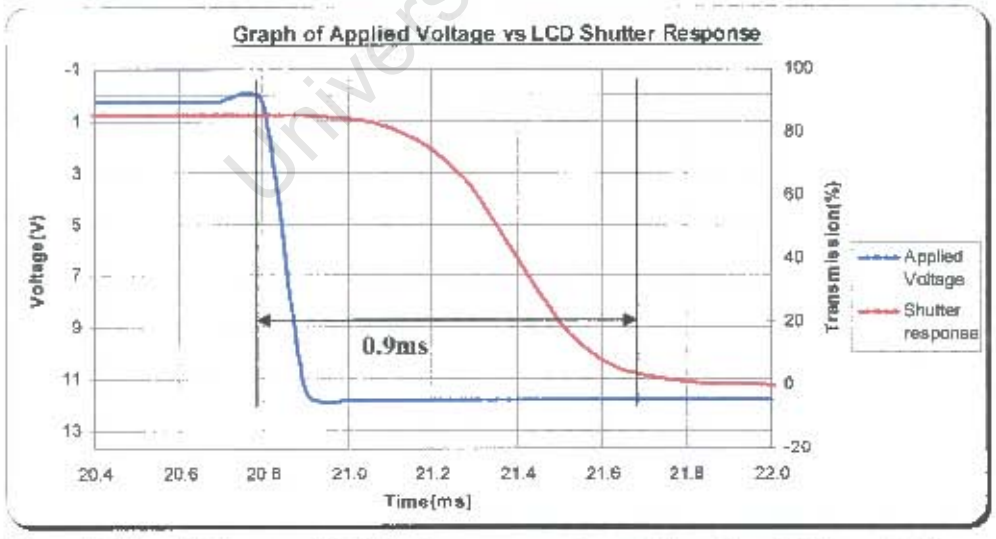

Figure 5.2(a) – (c) Graphs of LC shutter response to applied voltage (a) Overall (b) LC opening and (c) LC closing respectively

5.1.3 Characterisation of the high voltage circuit

The response characteristics of the circuit that would be used to control the LN shutter were investigated using the procedure described in Section 4.8.2. An oscilloscope was used to measure the input control signal (10V) from the signal generator in relation to the high-voltage output signal (up to approximately 2000V), which it supplied to the LN crystal. The circuit was tested at a frequency of 50 Hz and over a range of pulse widths. The results are shown in Figure 5.3(a) – (f).

The circuit was able to provide a moderately stable square wave for pulse widths as low as 0.1ms and up to approximately 2ms. Below 0.1ms, the pulse became rounded due to the slow high voltage decay (approx. 0.1ms) as the voltage decreased, as shown in Figure 5.3(a). Consequently, the pulse was not square as desired for short pulse widths. This was probably caused by the capacitors on the IGBT side of the circuit that were holding charge, and thus slowing the decay after the IGBTs switched off. Attempts were made to rectify this problem by lowering the capacitance of these capacitors, but did little to improve the situation. The IGBT circuit requires some capacitance to eliminate possible voltage spikes across the IGBTs during switching, as well as to ensure that the voltage was shared equally between all the IGBTs. For this reason, the capacitors could not be made too small or be removed entirely. As the pulse width increased beyond 2ms, the circuit was no longer able to maintain the square pulse shape. This is because the capacitors of the rectifier circuit that are used to smooth the rectified AC voltage were being drained to a point where they were unable to hold sufficient charge to sustain the square shape. The result is that the voltage decreases by approximately 3% over a pulse duration of 2ms as shown in

Figure 5.3(c). This is more evident in Figures 5.3(d) and (e) that had pulse widths of 10ms and 15ms respectively. In these cases, there is a component of the rectified AC voltage is imposed on the output. This becomes very apparent if the pulse width is increased further. This is illustrated for a pulse width of 20ms in Figure 5.3(f).

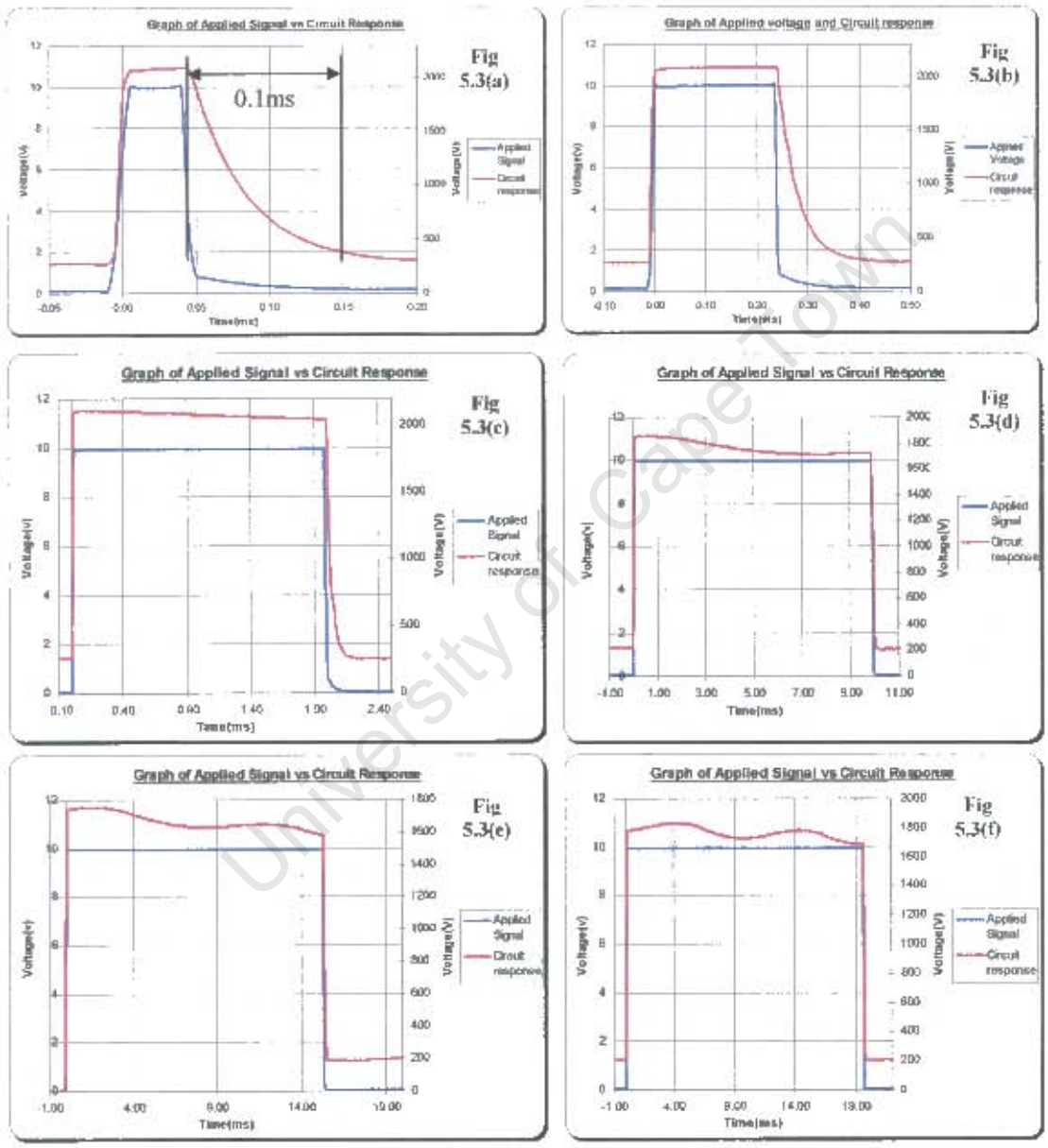

Figure 5.3(a) - (f) Graphs of circuit response to applied signal vs. Time for 0.05ms, 0.23ms, 2ms, 10ms, 15ms and 20ms respectively

5.1.4 Characterisation of the Lithium Niobate (LN) crystal shutter

The light transmission of the LN shutter was investigated using the procedure detailed in Section 4.8.3. The following results were obtained. The polariser transmission was measured with the polarisation direction in the same plane as the laser polarisation (i.e. the maximum transmission orientation).

Condition	Voltage (V)	Transmission (%)
No shutter present	0.708	100
Polariser only	0.287	40.5
Shutter open	0.216	30.6
Shutter closed	0.0023	0.33

Table 5.2 Light transmission through LN shutter

There is a significant loss of light due to this polariser, reducing the effective light passing through the shutter to 40% alone. This had serious implications on the ability to capture ESPI images, especially at short pulse durations.

The light shuttering response of the LN shutter to applied voltage was measured. The optimal voltage that was applied to the crystal was found experimentally by varying the voltage until the light transmission was maximised. The voltage that provided the highest light transmission was found to be approximately 1400V.

A curious phenomenon was observed when using the crystal. The light transmission through it varied dramatically by simply moving the orientation of the crystal relative

to the laser beam. It was found that to minimise this effect, and to obtain the highest degree of transmission, the LN crystal's surface should be perfectly perpendicular to the incoming laser beam.

Figure 5.4(a) to (f) below shows the crystal's response to an applied voltage for pulse widths of 0.05, 0.1, 0.5, 3, 10 and 20ms respectively.

In Figure 5.4(a) the shutter was still opening when the voltage was removed, evidenced by the fact that the shutter had not reached the maximum transmission value of approximately 34%. In Figure 5.4(b) and (c) the shutter has opened completely and this took between 0.1 and 0.15ms, where as it took between 0.15 and 0.2ms to close. These responses are thought to be delayed by the slow voltage rise and decay, and if this can be improved, an improvement in the shuttering times would be likely.

Figure 5.4(d) and (e) shows that the shutter's light transmission does not deviate excessively from the maximum values, although the applied voltage varies slightly.

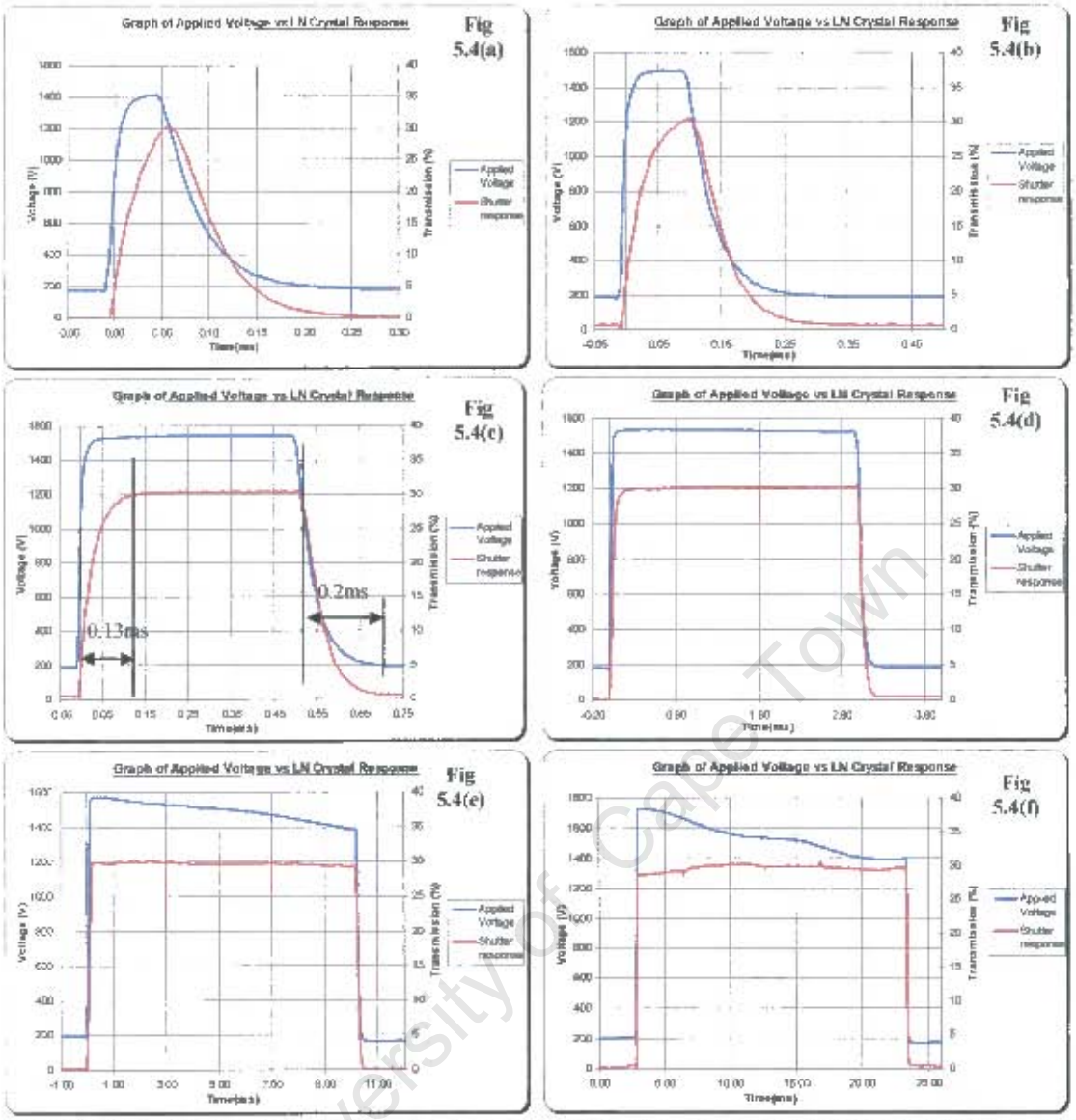

Figure 5.4(a) –(f) Graphs of LN shutter response to applied voltage vs. Time for 0.05, 0.1, 0.5, 3.0, 10.0 and 20.0ms respectively

5.2 Editing of ESPI images

As the laser pulse width decreased, the brightness of the ESPI images that were captured decreased accordingly. This was due to a reduction in the amount of light captured by the camera CCD as the effective light integration time decreased. Some of the images obtained needed to be edited after being captured in order to obtain the correct brightness and contrast ratios and enhance the fringe definition. In extreme cases, the brightness and contrast of the images had to be increased to such a level that background noise in the images and camera electronics became a dominant feature, and overrode the object image itself. Normally this background noise would be at such a low level compared to the object image that it would not be noticed.

Intensity plots were acquired from the ESPI program, measured along a single row or column of the image. They are an indication of the light intensity before image enhancement was performed, and is therefore an indication of the actual light levels reaching the camera CCD, although not a conclusive value. The light levels reaching the CCD are determined by the amount of light passing through the pulsing mechanism, the size of the camera iris and the light level of the reference beam.

5.3 ESPI inspection with no external vibration

ESPI inspection was performed on the holographic table with no applied vibration in order to illustrate of the effect of decreasing the exposure period. It also enabled a comparison of the results obtained when no vibration was applied with results obtained when vibration was introduced. The effect of vibration isolation methods such as pulsed ESPI was also considered.

The light levels of the disc pulsed images should be the same or similar to those obtained when the camera shutter is used, since there is no light lost when the light passes through the disc. This would not be the case for the LC and LN shutters, since they each have their own inherent transmission loss.

5.3.1 ESPI inspection with no excitation of object using large disc

Figure 5.5(a) – (f) below shows the ESPI images of the blade recorded when it was mounted on the table. The images were captured using the large disc and motor to pulse the laser between 20ms and 0.5ms. The light intensity plots show the decrease in intensity levels as the pulse duration decreases. This is mirrored in the unedited ESPI images on the left, which became steadily darker as the shuttering time decreased. In the enhanced images, the fringe patterns remained clear and well defined (although there was a loss of definition) to as short as 0.5ms, which was the shortest duration that could be achieved with the large disc.

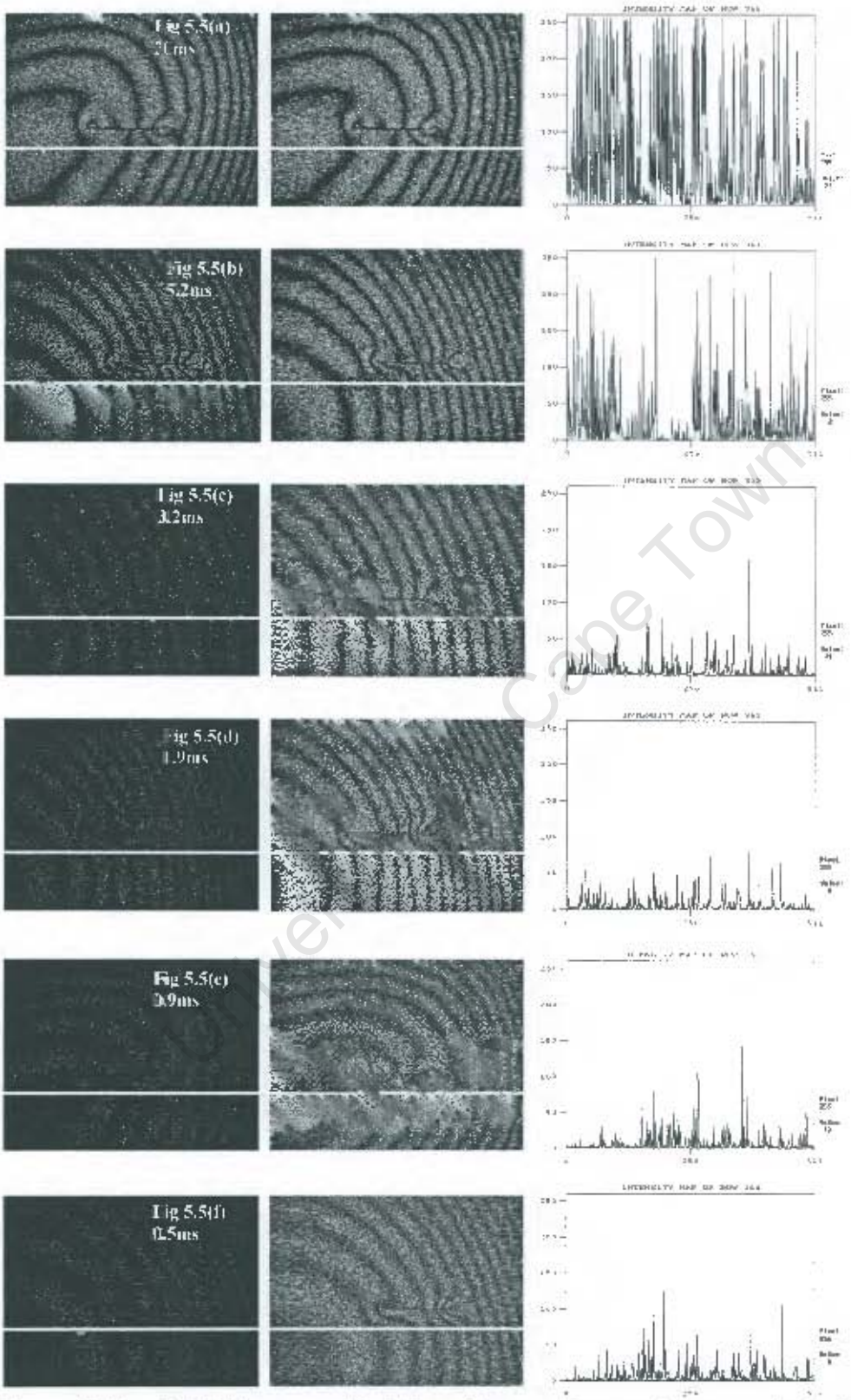

Figure 5.5(a) - (f) ESPI images and light intensity plots of test specimen on optical table using mechanical shutter (large rotating disc) to pulse laser at 20, 5.2, 3.2, 1.9, 0.9 and 0.5ms respectively

5.3.2 ESPI inspection with no excitation of object using stepper motor and disc

Figure 5.6(a) -- (f) shows the ESPI images of the blade captured while it was on the holographic table. The laser was pulsed by the stepper motor and disc for durations of between 20ms and 1.1ms. Again, the decrease in light in the unedited images and intensity maps is apparent as the pulse duration decreases. The clarity of the images is good throughout the series for the enhanced images, although the unedited images are only clear to 2.4ms, whereas in the case of the large disc it was clear for the 1.9ms image.

The light levels are lower than those recorded with the large disc and motor (Figure 5.5) for similar exposure periods. The reason for this is unclear, although it is possible that the set-up was slightly different on the two instances, e.g. the iris may have been more open in the first case, or the reference beam intensity may have been higher.

The enhanced images all show clear fringe patterns across the series.

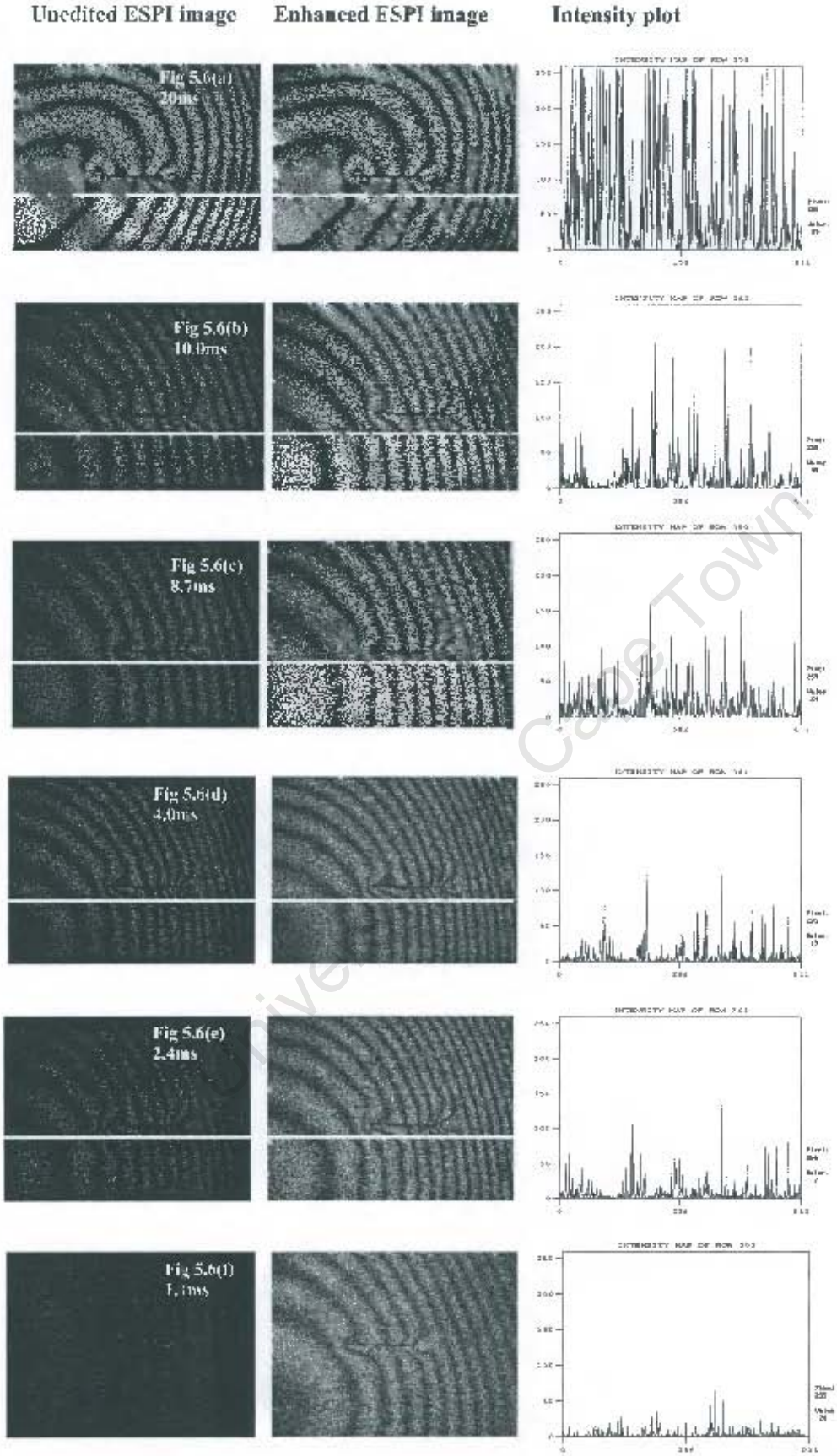

Figure 5.6(a) – (f) ESPI images and light intensity plots of test specimen on optical table using mechanical shutter (rotating stepper motor disc) to pulse laser at 10.0, 8.7, 4.0, 2.4 and 1.1ms respectively

5.3.3 ESPI inspection with no excitation of object using LC shutter

Figure 5.7(a) – (e) shows the ESPI images of the blade captured while it was on the table, using the LC shutter to provide pulses between 10ms and 2.0ms. As the pulse duration is shortened, the images obtained show a general decrease in light intensity and fringe definition.

None of the unedited images are clear, and when compared to the images obtained using the large disc and motor as well as the stepper motor and disc (Fig 5.5 and 5.6), there is a clear reduction in light intensity levels for similar pulse durations. This indicates the effect of the lower light transmission and slow response time of the LC shutter. The enhanced fringe patterns are of reasonable clarity, although the images in Fig 5.7(d) and (e) are becoming unclear as a result of low light levels. The LC shutter was unable to pulse the laser below 2ms due to the reduced light transmission and poor response characteristics.

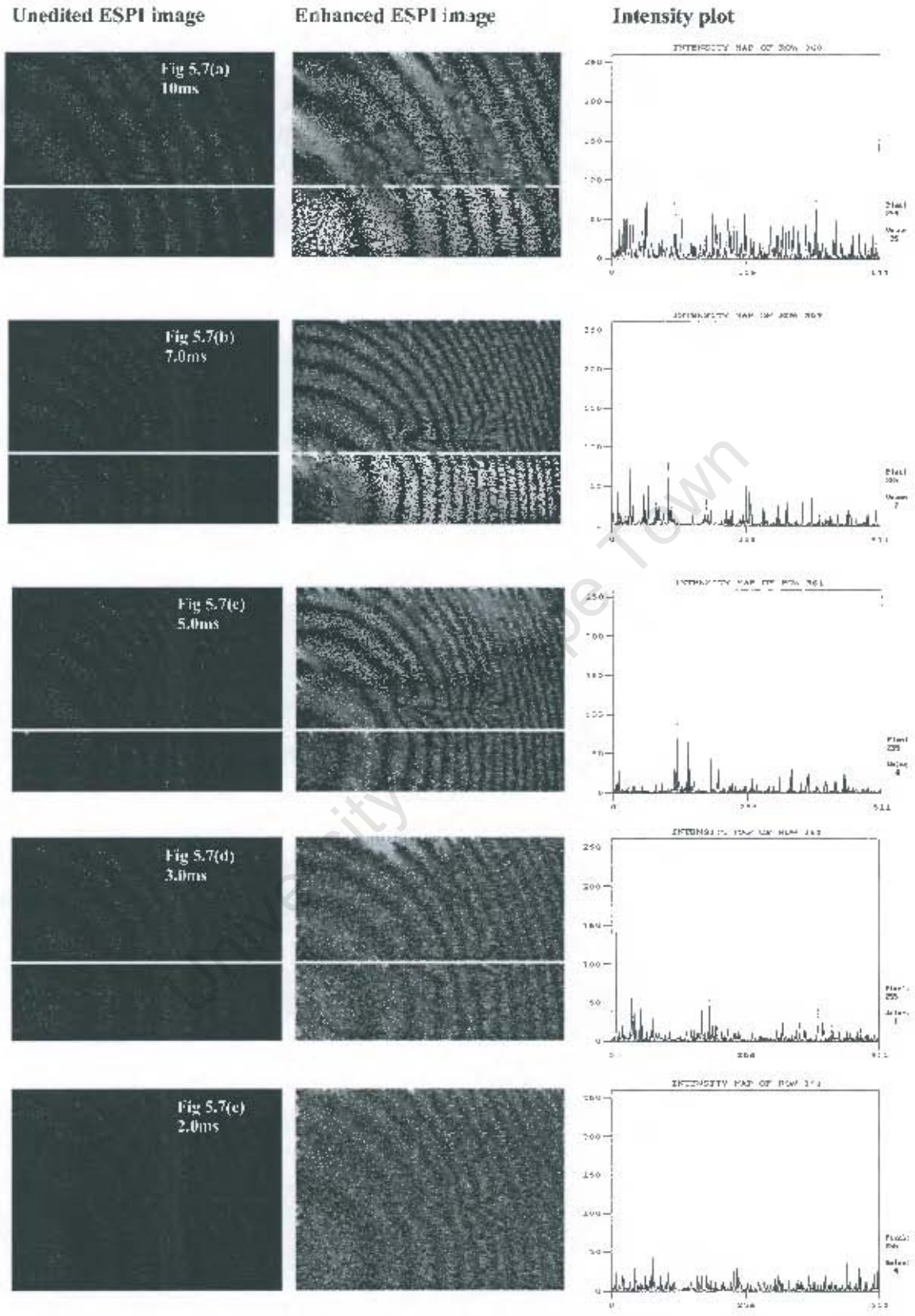

Figure 5.7(a) – (e) ESPI images and light intensity plots of test specimen on optical table using electronic shutter (LC shutter) to pulse laser at 10, 7.0, 5.0, 3.0 and 2.0ms respectively

5.3.4 ESPI inspection with no excitation of object using LN shutter

Figure 5.8(a)-(f) shows a series of ESPI images and intensity plots of the rotor blade that were captured on the table using the LN shutter to pulse the laser at various pulse durations between 10.0ms and 0.1ms.

The unedited images are completely incomprehensible because of low light levels. The intensity plots all show low levels of intensity, indicating the diminished light level that reached the camera. The enhanced images are visible, and the clarity is reasonable for pulses as short as 0.5ms. These poor light levels are due to the poor light transmission of the LN shutter.

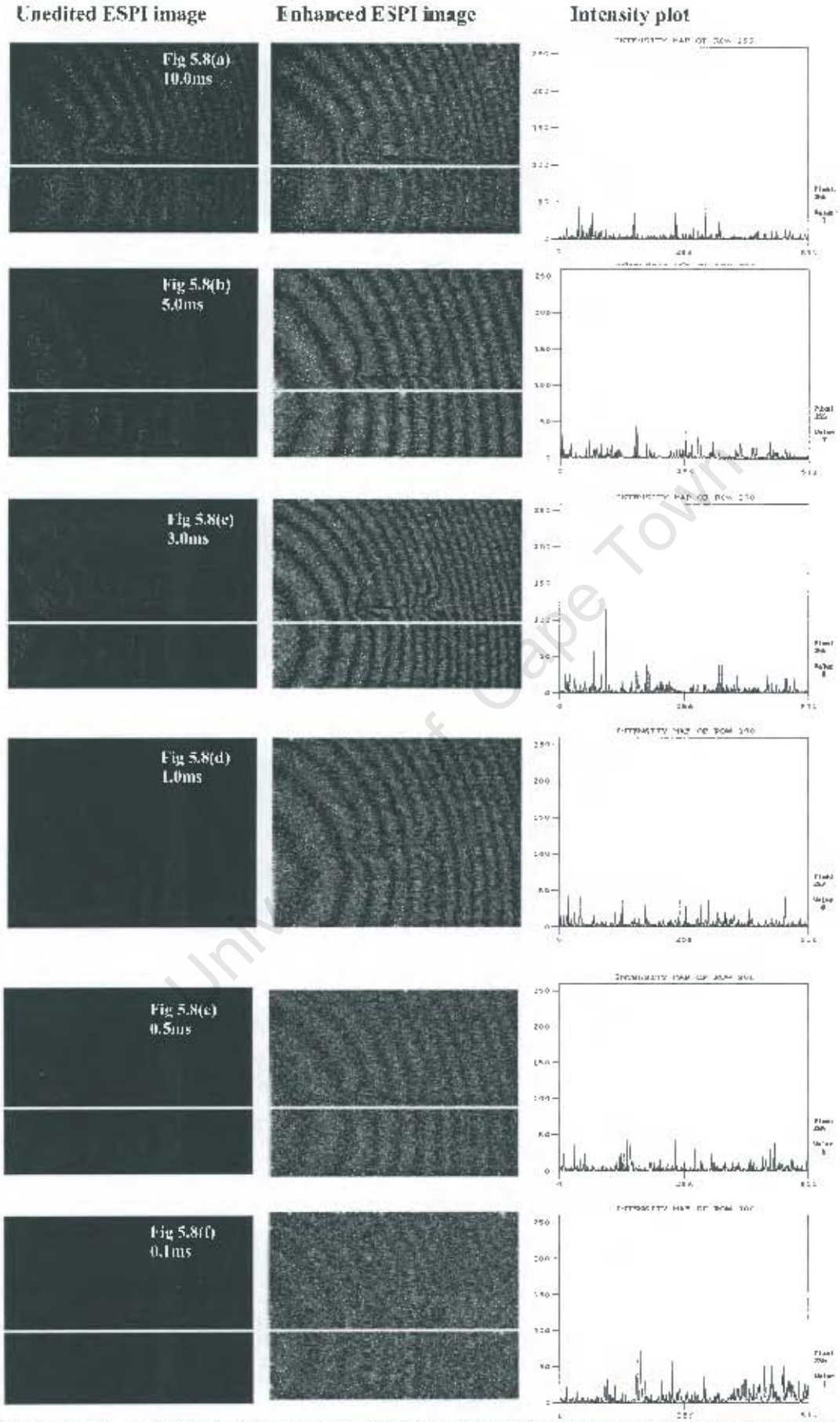

Figure 5.8(a) – (f) ESPI images and light intensity plots of test specimen on optical table using electronic shutter (LN shutter) to pulse laser at 5.0, 3.0 1.0 0.5, 0.25 and 0.1ms respectively

5.3.5 ESPI inspection with no excitation of object using camera shutter

Figure 5.9(a) – (e) below shows a series of ESPI images of the rotor blade that were captured while it was on the holographic table. The images were captured at 20ms, 8.33ms, 2ms, 0.5ms and 0.1ms using the built-in camera shutter.

There is a general decrease in light intensity in the unedited images and intensity plots. The unedited images are sufficiently well defined to as low as 2ms. They show similar intensities to those captured when the large disc was used to pulse the laser. (Fig 5.5). The enhanced images are clear for exposures as short as 0.1ms, which was the lowest shuttering speed of the camera.

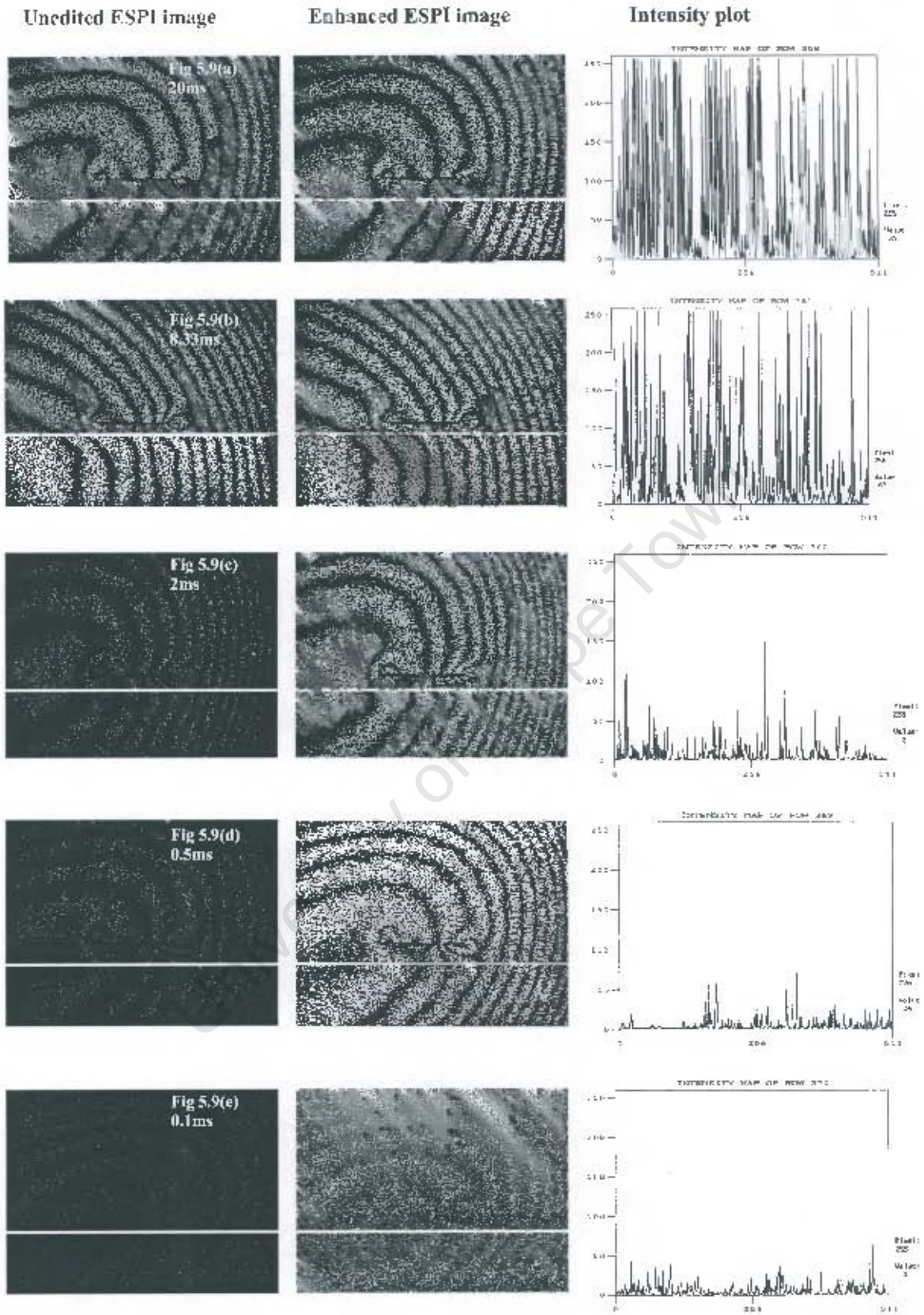

Figure 5.9(a)-(e) ESPI images and light intensity plots of test specimen on optical table using electronic shutter (camera shutter) to pulse laser at 20ms; 8.33ms; 2ms; 0.5ms and 0.1ms respectively

5.4 ESPI inspection with external vibration and reduced shutter time

ESPI was performed on the object for certain vibration scenarios, including environmental vibration, and excitation using the compressor and loudspeaker. The expanding lens was moved closer to the object in order to provide a higher illumination level and hence better quality images at very short shutter durations.

It became apparent that due to the random nature of the vibration the capture of acceptable fringe patterns was rather haphazard. For this reason, a series of 10 images were captured in order to illustrate the general trend that was occurring as a result of these different conditions. The images were all captured using the camera shutter because of its ease of operation and low light transmission losses.

These images were all enhanced to similar levels in order to enable comparison between those obtained at different shuttering periods.

Figure 5.10 below shows the graph comparing the vibration level experienced by the test specimen under the different conditions. The random characteristics of the environmental and compressor vibration are clearly shown in this graph.

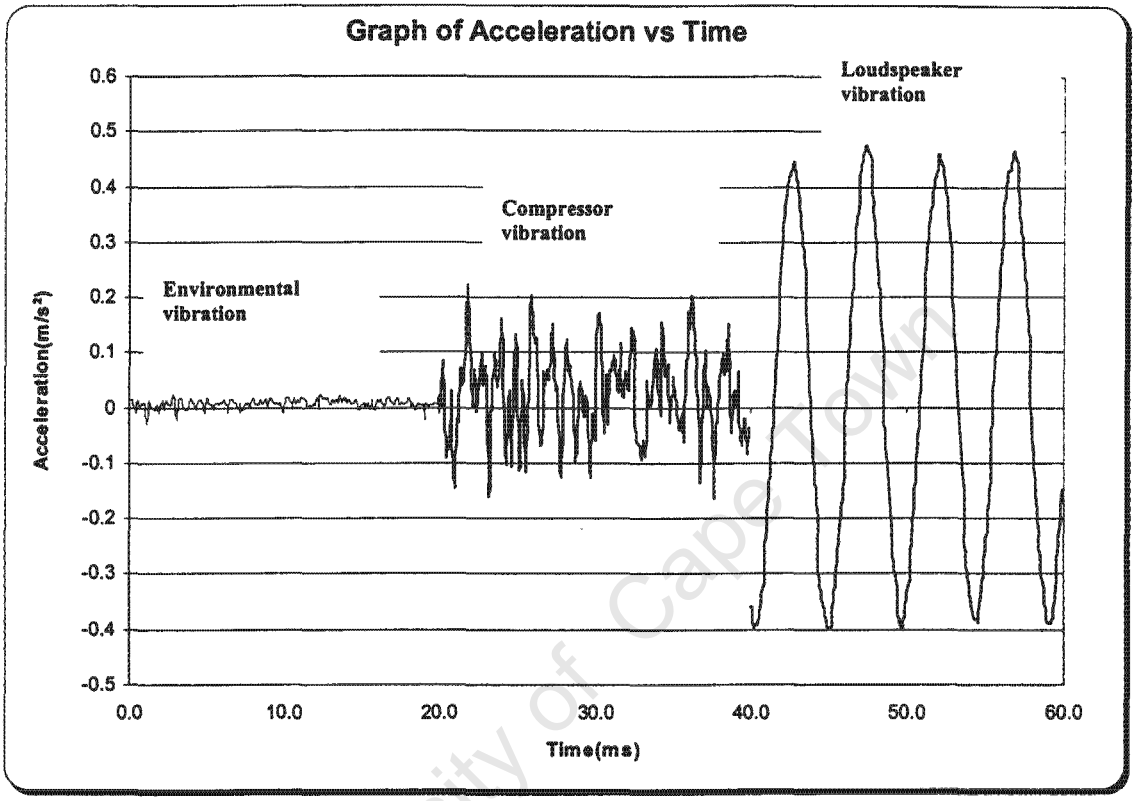

Figure 5.10 Graph of Acceleration vs. Time for environmental vibration, compressor vibration and loudspeaker vibration as experienced by the test specimen

5.4.1 ESPI inspection of object exposed to environmental vibration

The object's response to environmental vibration was measured. This vibration is clearly not constant over time, and results obtained are just an indication of the magnitude of expected vibration. The actual vibration of the object during any one of the ESPI inspections may therefore be different to that which was recorded.

Figure 5.11 below shows the Acceleration vs. Time graph for the object when environmental excitation was applied. Note the arbitrary "spike" in the middle of the graph.

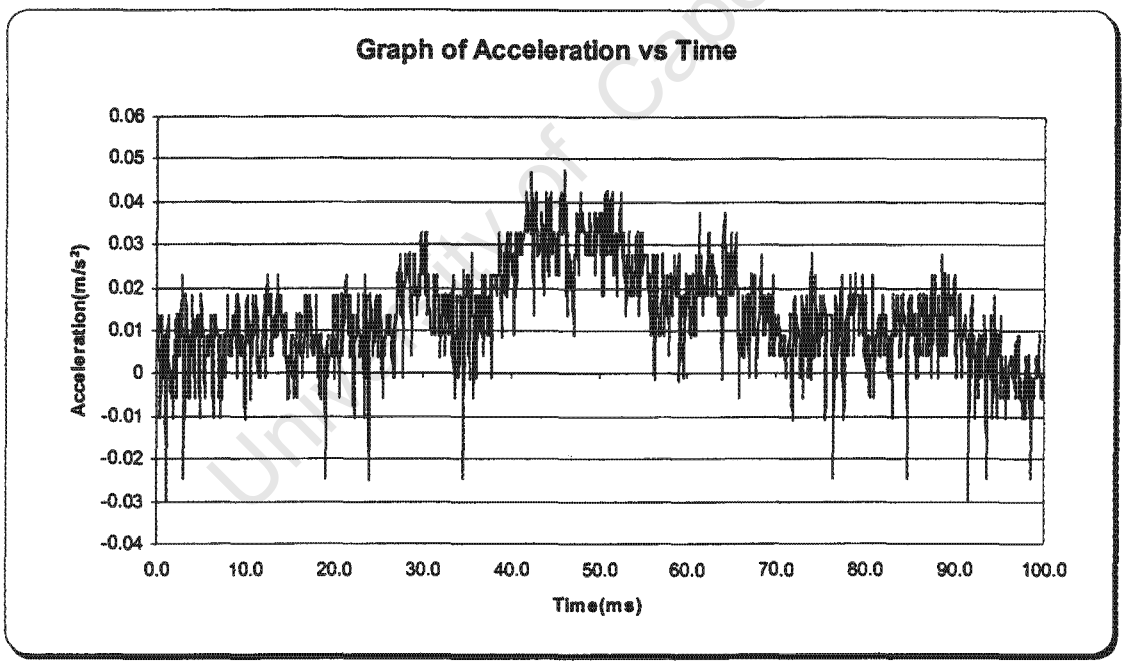

Figure 5.11 Acceleration vs. Time graph experienced by test specimen when subjected to environmental excitation

Figure 5.12 (a) – (d) below shows a series of 10 ESPI images of the test specimen exposed to environmental vibration that were captured with the camera shutter at periods of 20ms, 2ms, 0.5ms and 0.1ms.

When the shuttering time was 20ms, only six out of ten images obtained were thought to be acceptable. This increased to eight when the period was reduced to 2ms and to ten when the period was further reduced 0.5ms. It did however decrease to eight out of ten when the period was shortened to 0.1ms.

Figure 5.12 Series of 10 ESPI images of test specimen exposed to environmental excitation captured using camera shutter at shuttering times of 20ms, 2ms, 0.5ms and 0.1ms respectively

5.4.2 ESPI inspection of object exposed to compressor vibration

The compressor was used to excite the object in order to simulate a random vibration that could be expected in an industrial environment. Figure 5.13 below indicates the Acceleration vs. Time graph of the blade when it was mounted placed on the ground while the compressor was running nearby.

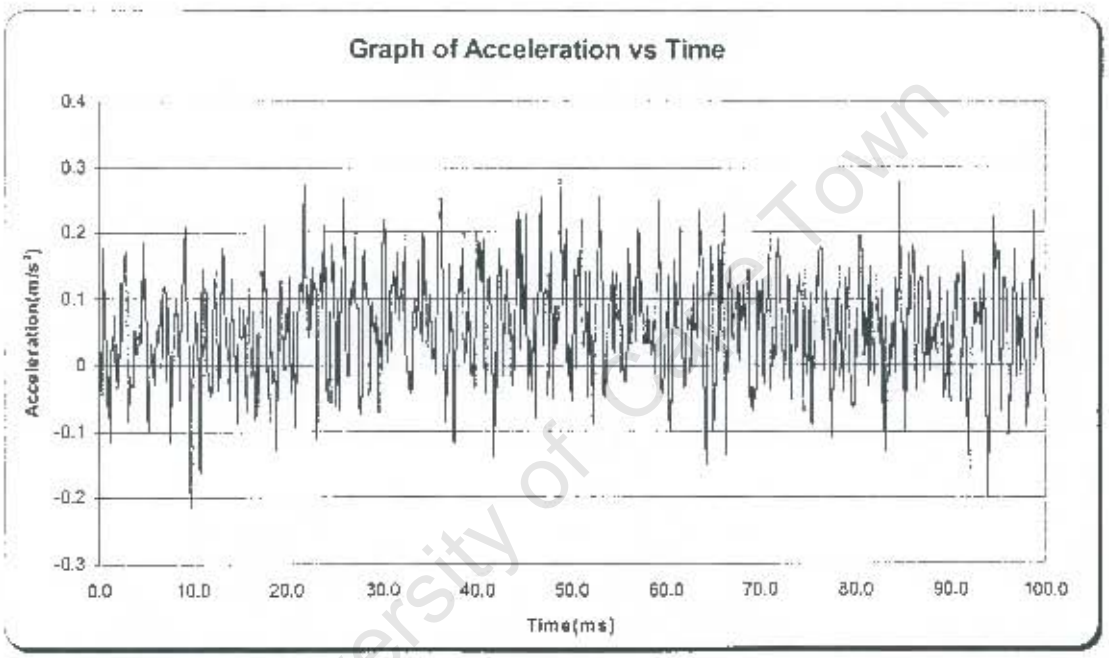

Figure 5.13 Acceleration vs. Time graph as experienced by test specimen when excited by compressor vibration

Figure 5.14 (a) – (d) shows a series of 10 ESPI images of the test specimen (blade) exposed to compressor vibration that were captured with the camera shutter for periods of 20ms, 2ms, 0.5ms and 0.1ms.

Of the images that were captured over 20ms, only two out of ten images can be considered successful although there is evidence of smudging in all of them. This improved significantly when the images were captured over 2ms, when a success rate of nine out of ten images was attained. Seven out of the ten that were captured were successful when the camera shutter was set to 0.5ms, and five out of ten successful for 0.1ms.

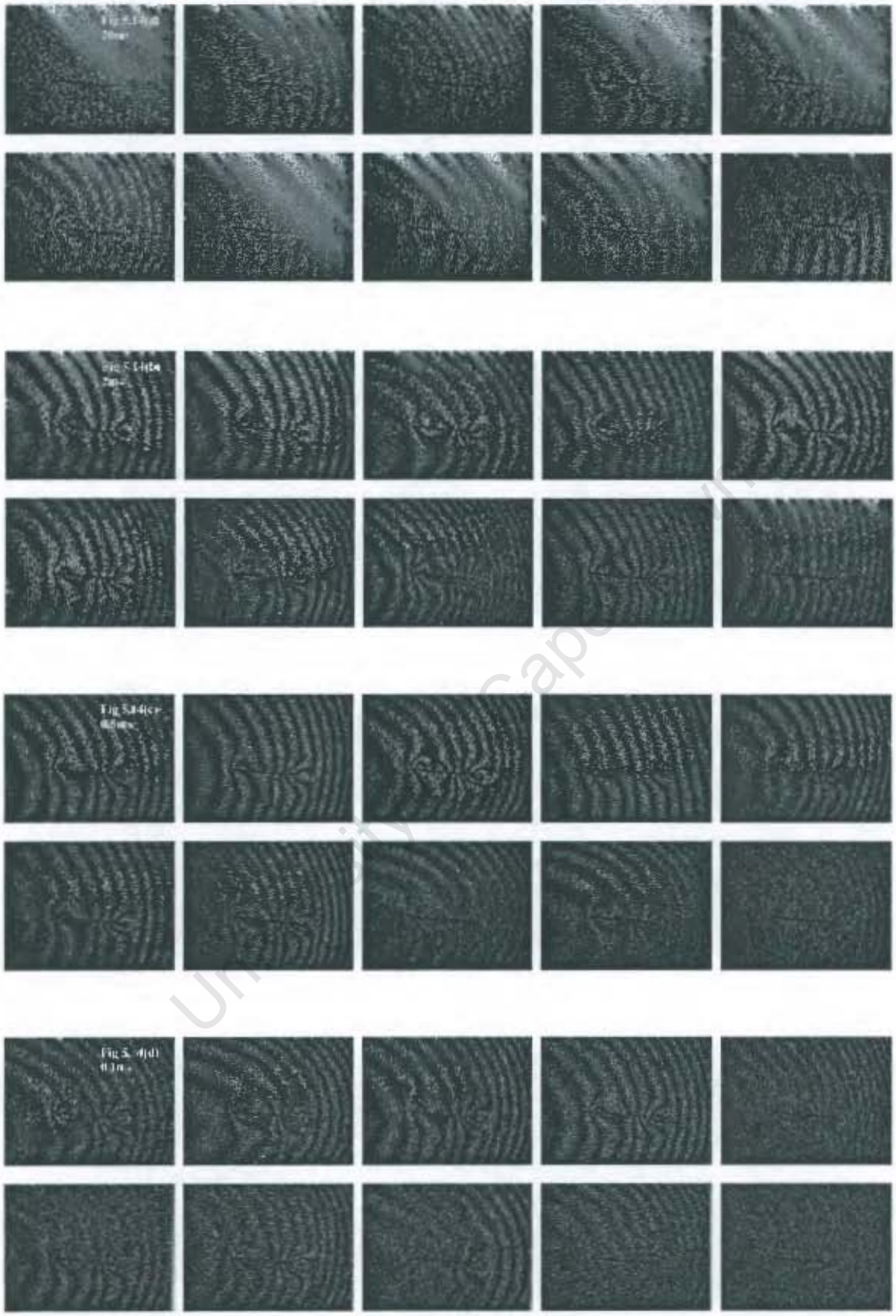

Figure 5.14 Series of 10 ESPI images of test specimen exposed to compressor excitation captured with camera shutter at exposure times of 20ms, 2ms, 0.5ms and 0.1ms respectively

5.4.3 ESPI inspection of object exposed to loudspeaker vibration

The blade's response to the applied excitation was measured and is illustrated in Figure 5.15(a)-(c) below. This shows the Acceleration, Velocity and Displacement response graphs of the test specimen when excited at 214Hz.

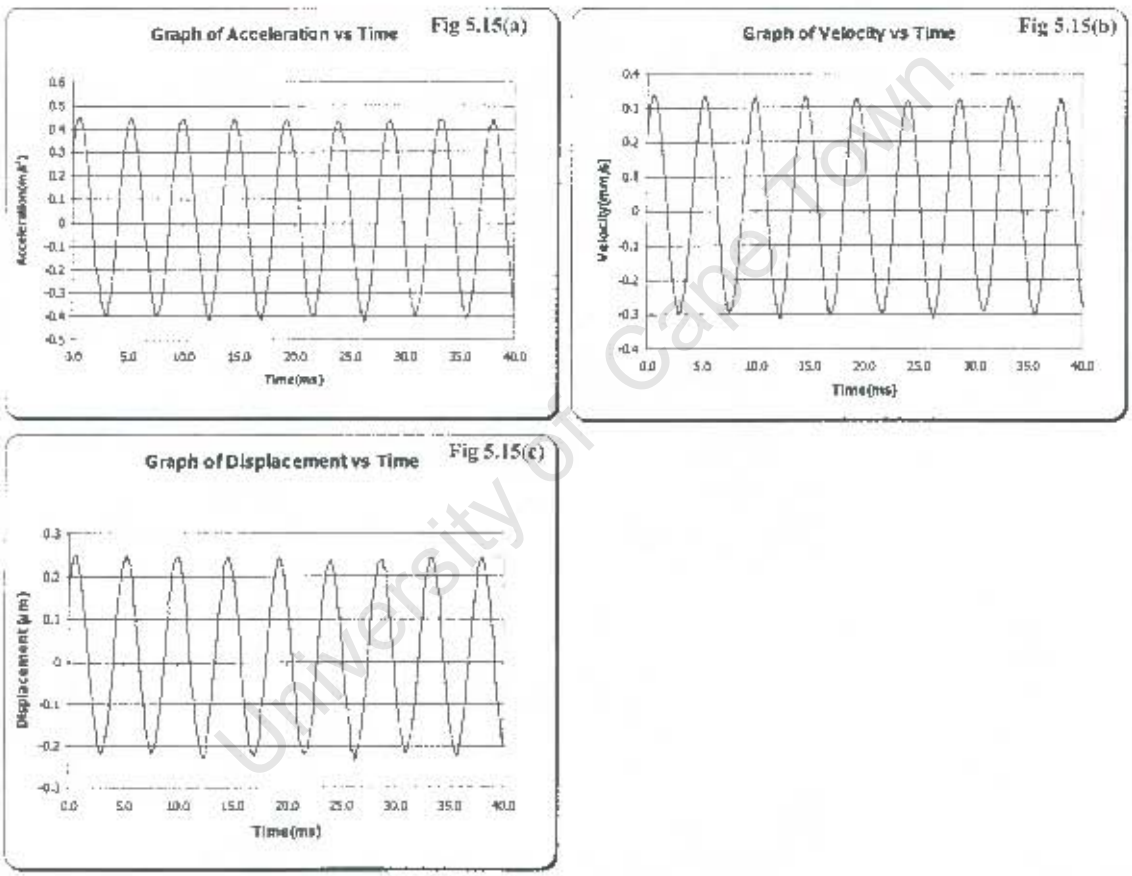

Figure 5.15(a) – (c) Graphs of Acceleration, Velocity and Displacement response vs. Time respectively as experienced by test specimen for loudspeaker excitation

ESPI inspection of the blade was performed while the loudspeaker excited it at 214Hz. Figure 5.16(a) – (d) shows a series of ten images of the object subjected to loudspeaker excitation, using the camera shutter with exposure times of 20, 2, 0.5 and 0.1ms respectively. The images captured at the full 20ms show two very distinctive areas. There are areas where the fringe lines are clearly visible, and areas where no fringe lines are formed at all. This is a result of the formation of standing waves in the test specimen. Fringe lines are visible in areas of the blade that correspond to nodal regions, and areas where no fringes are formed correspond to anti-nodal regions. During the 20ms period, the test specimen undergoes 4.3 cycles of oscillation due to the loudspeaker excitation. The movement that occurs as a result of this vibration smudges the fringe pattern and will obviously be more apparent in the anti-nodal region. As the shuttering period decreases, the fringe lines encroach steadily more into the anti-nodal regions. The reduced shuttering time means that there is less displacement of the object during the imaging period, and the smudging effects are eliminated. For 2ms, the test specimen undergoes 0.43 cycles, 0.11 cycles for 0.5ms and 0.0214 cycles for 0.1ms.

In Figure 5.16(a), which was captured at 20ms, the fringe patterns are only visible in the nodal regions and there are no fringes in the anti-nodal regions. Some of the fringe lines are however smudged. These images are therefore not satisfactory.

In the images captured at 2ms, there is a clear improvement in fringe clarity, although there is general smudging along the anti-nodal areas throughout the series. The fringe lines cover much of the anti-nodal regions that were previously not seen.

The images captured at 0.5ms are on average substantially clearer, although one is indecipherable. The fringe definition is better than that of Figure 5.16(b), captured at 2ms. The smudging is also less conspicuous.

The images captured at 0.1ms also show well-defined fringe lines, although there is smudging in three of them along the anti-nodal region.

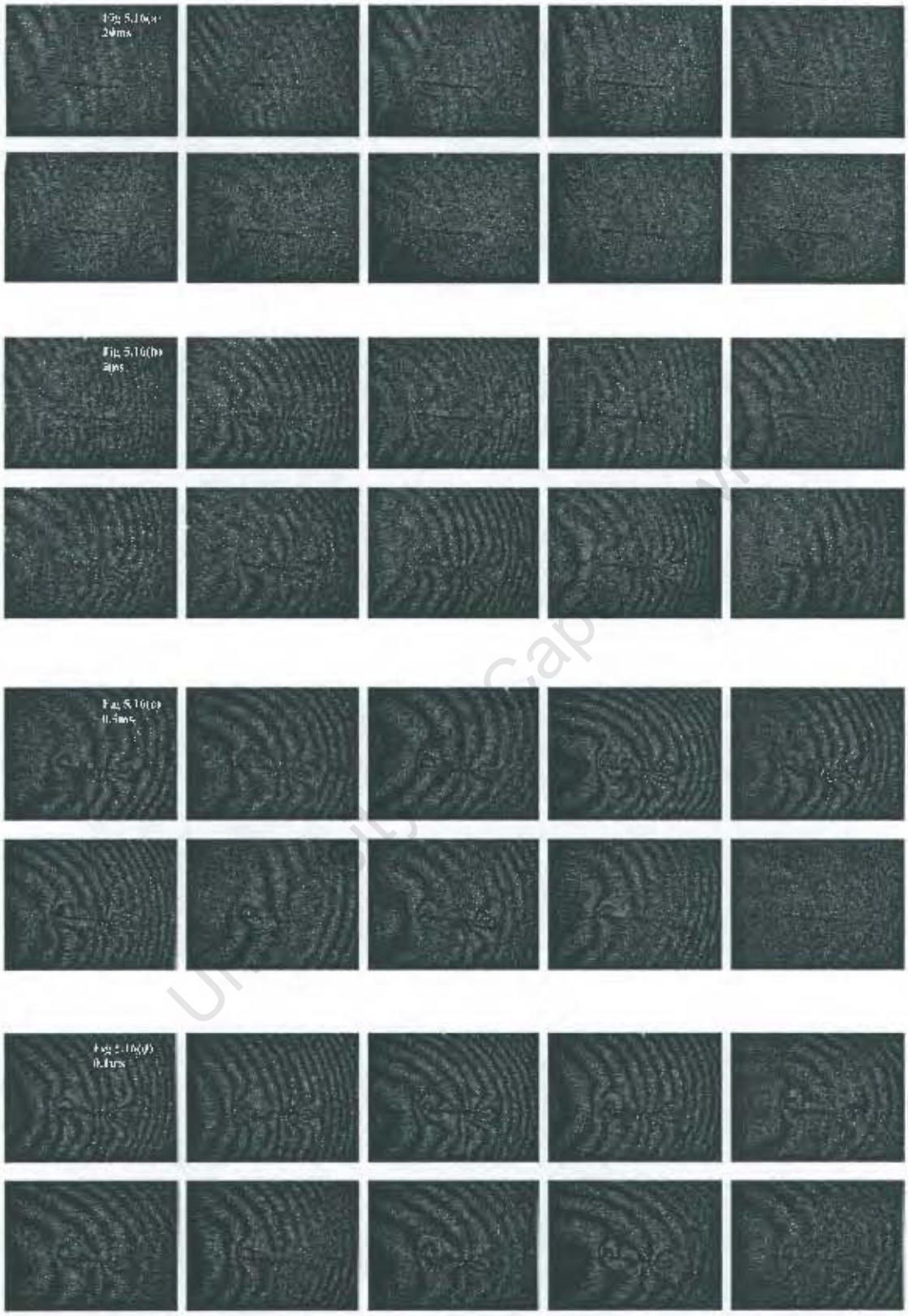

Figure 5.16 Series of 10 ESPI images of test specimen exposed to loudspeaker excitation captured using camera shutter at shuttering times of 20ms, 2ms, 0.5ms and 0.1ms respectively

5.5 The capture of ESPI images using selected pulsing techniques

ESPI inspection of the test specimen was performed under vibration conditions using the large disc, the LN shutter and the camera shutter to provide reduced exposure times. This enabled comparison of these methods and would assist in establishing which method was preferable to the others. It should be remembered that the capture of successful images was a hit and miss procedure. This was illustrated in Section 5.4. Therefore the images presented in this section do not reflect the optimum quality of images that could be obtained using any particular combination of exposure duration and shuttering technique.

The stepper motor and disc as well as the LC shutter were rejected as useful shuttering techniques. The minimum exposure period could not be shortened below 1.1ms because the stepper motor could not spin the disc faster than 500rpm. The large disc was however able to achieve a 0.5ms pulse duration. The poor response characteristics of the LC shutter meant that a minimum shuttering period of only 2ms was achievable, which was considered as too long when compared to rival pulsing methods.

5.5.1 ESPI inspection with object exposed to environmental vibration using large disc

Figure 5.17(a) – (e) shows the ESPI images of the test specimen that were captured under environmental excitation. The laser was pulsed using the large disc for durations between 20.0 and 0.5ms.

The image captured at 20ms is completely smudged as a result of the vibration, although a clear image could be obtained if sufficient images were recorded. This improves as the shuttering time decreases, and the remainder of the images show well-defined fringe lines. There is a decrease in the light intensity of the images for decreasing shuttering periods as expected.

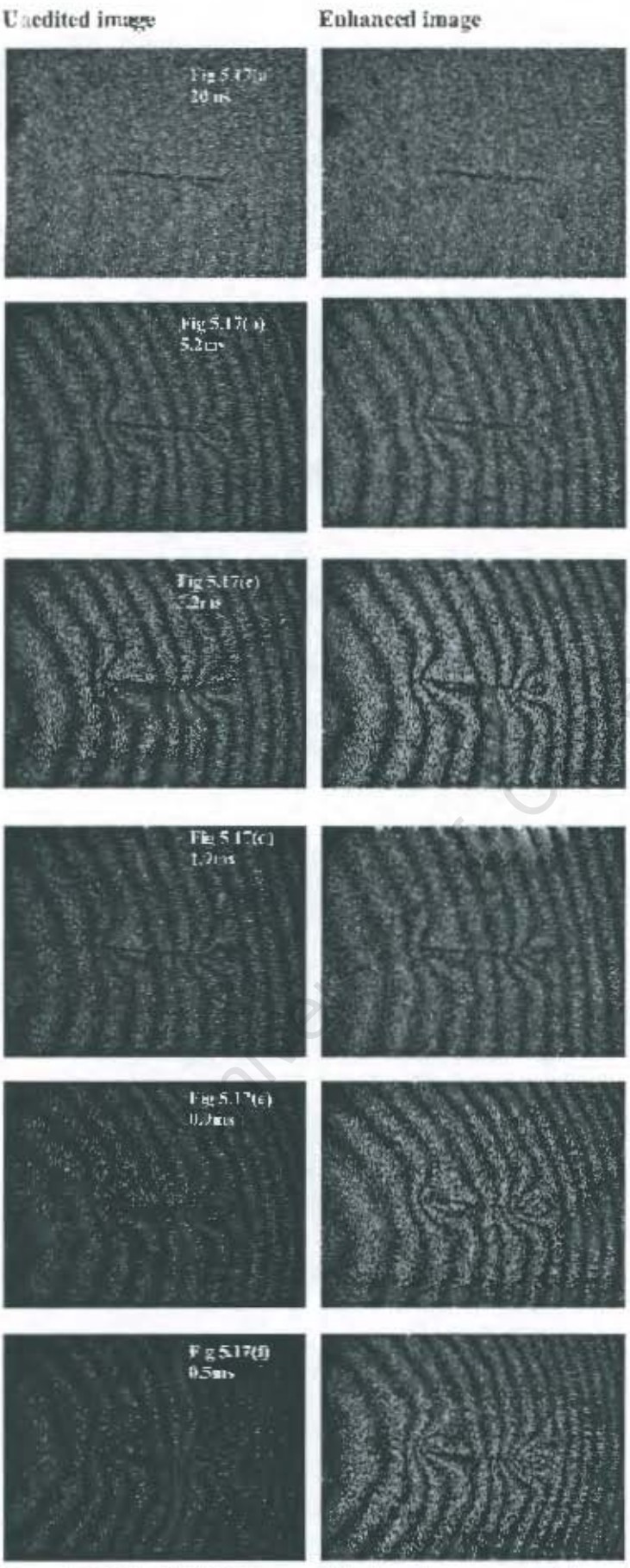

Figure 5.17(a) – (f) ESPI images of test specimen exposed to environmental excitation captured using mechanical shutter (large disc) to pulse laser at exposure times of 20, 5.2, 3.2, 1.9, 0.9 and 0.5ms respectively

5.5.2 ESPI inspection with object exposed to compressor vibration using large disc

Figure 5.18(a) – (f) shows a series of images of the object subjected to compressor vibration, using the large rotating disc to provide pulses of between 20ms and 0.5ms.

The images captured at 20ms and 5.2ms are badly smudged due to the object's motion. The image captured at 3.2ms is slightly smudged, but significantly clearer. The image captured at 1.9ms is very clear, but the two images captured at 0.9 and 0.5ms were less discernible as a result of smudging.

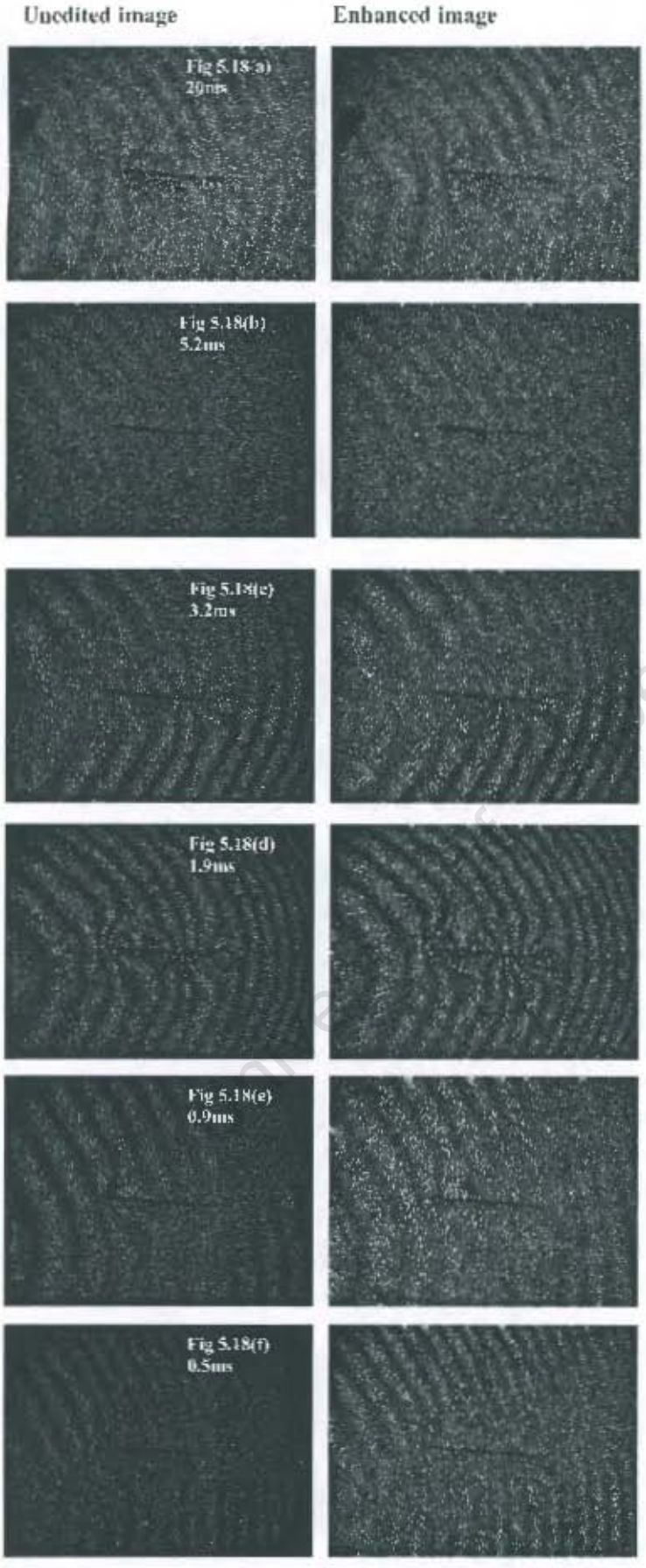

Figure 5.18(a) – (f) ESPI images of test specimen exposed to compressor excitation captured using mechanical shutter (large rotating disc) to pulse laser at exposure times of 20, 5.2, 3.2, 1.9, 0.9 and 0.5ms respectively

5.5.3 ESPI inspection with object exposed to loudspeaker excitation using large disc

Figure 5.19(a) – (f) shows a series of images of the blade subjected to loudspeaker excitation while the laser was pulsed with the large disc for durations of 20, 5.2, 3.2, 1.9, 0.9 and 0.5ms respectively.

The images captured at 20ms show the distinction between the nodal and anti-nodal regions clearly. The fringes are only apparent in the nodal region, and are well defined. The image captured at 5.2ms shows slightly smudged fringe lines in the nodal regions and no fringe lines in the anti-nodal regions, although there is evidence of smudging. The images captured at 3.2ms and 1.9 show clear fringe lines in the nodal region, with slight smudging in the anti-nodal region. The image captured at 0.9ms is smudged, while the fringe lines captured at 0.5ms are completely clear and extend throughout the image.

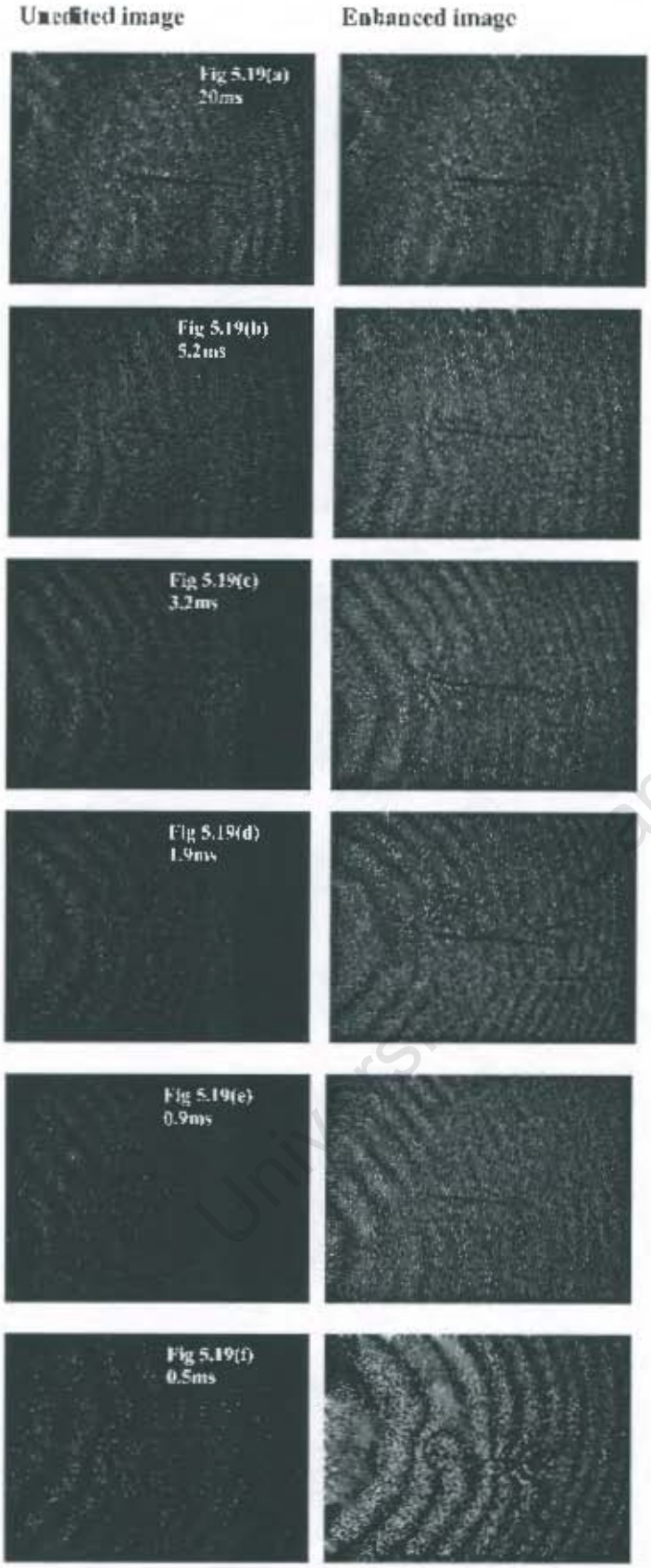

Figure 5.19(a) – (f) ESPI images of test specimen exposed to loudspeaker excitation captured at exposure times of 20, 5.2, 3.2, 1.9, 0.9 and 0.5ms respectively using mechanical shutter (large rotating disc) to pulse laser

5.5.4 ESPI inspection with object exposed to environmental vibration using LN shutter

Figure 5.20(a) – (f) shows the ESPI images of the test specimen under environmental excitation that were taken using the LN shutter to provide pulses of 10, 5, 3, 1, 0.5, and 0.1ms respectively.

The fringe lines in the enhanced images captured between 10ms and 0.5ms are not smudged, but show poor definition. No useful conclusion can be drawn for the image captured at 0.1ms.

There is only the slightest sign of a fringe line in the image captured at 10ms, and the other unedited images are completely black. The enhanced images are not well defined, and only discernible for shuttering periods as short as 0.5ms. This is a result of the poor light transmission of the LN shutter, and shows a similar trend to the images captured on the table when the LN shutter was used.

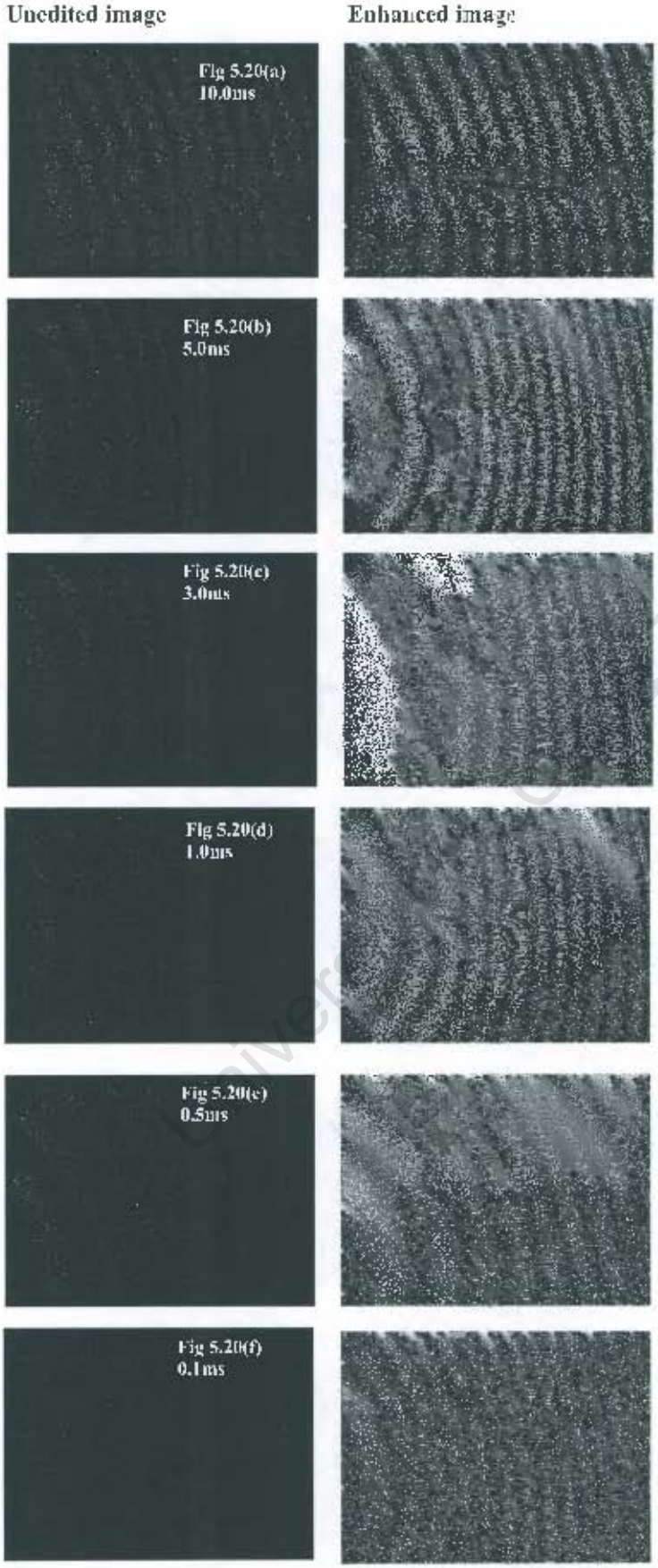

Figure 5.20(a) – (f) ESPI images of test specimen exposed to environmental excitation captured using electronic shutter (LN shutter) to pulse laser at exposure times of 10.0, 5.0, 3.0 1.0 0.5, and 0.1ms respectively

5.5.5 ESPI inspection with object exposed to compressor vibration using LN shutter

Figure 5.21(a) – (f) below shows the ESPI images that were captured while the blade was excited by the compressor captured using the LN shutter to pulse the laser at 10, 5.0, 3.0, 1.0, 0.5 and 0.1ms.

The unedited images are all too dark to provide any useful information, and the enhanced images are only clear to approximately 1ms. For exposure times shorter than 1ms, the images are unclear due to the amplification of background noise.

The images captured at 10ms and 5ms are smudged due to the compressor-induced vibration, but the image captured at 3ms is well defined. It is not clear whether the image captured at 1ms is smudged due to vibration or simply due to low light levels. The images captured at 0.5 and 0.1ms are unclear.

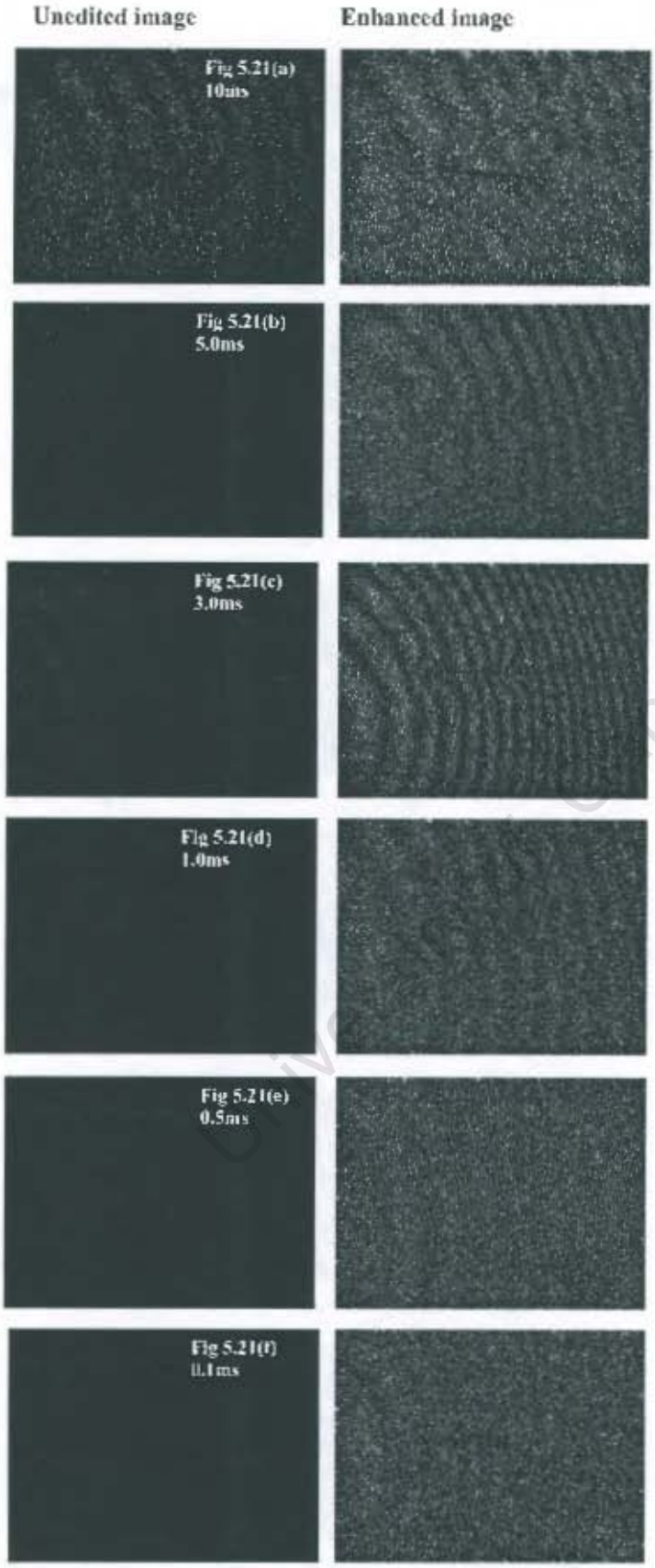

Figure 5.21(a) – (f) ESPI images of test specimen exposed to compressor excitation captured using electronic shutter (LN shutter) to pulse laser at exposure times of 10.0, 5.0, 3.0 1.0 0.5, and 0.1ms respectively

5.5.6 ESPI inspection with object exposed to loudspeaker excitation using LN shutter

Figure 5.22(a) – (f) shows the ESPI images of the test specimen excited by the loudspeaker that were captured using the LN shutter to provide pulses of 10.0, 5.0, 3.0, 1.0, 0.5, and 0.1ms respectively.

The images throughout the series are all of very low light level, as indicated in the unedited images. The enhanced images are also not well defined due to the amplification of background noise.

The images captured over 10ms and 5ms show clear fringe lines in the nodal region and nothing clear in the anti-nodal region. In the image captured at 3.0 ms, the fringe lines are starting to encroach into the anti-nodal region. The images captured at 1.0 and 0.5ms show whole-field fringe lines, which are of an extremely poor quality. No viable image was captured at the 0.1ms exposure time.

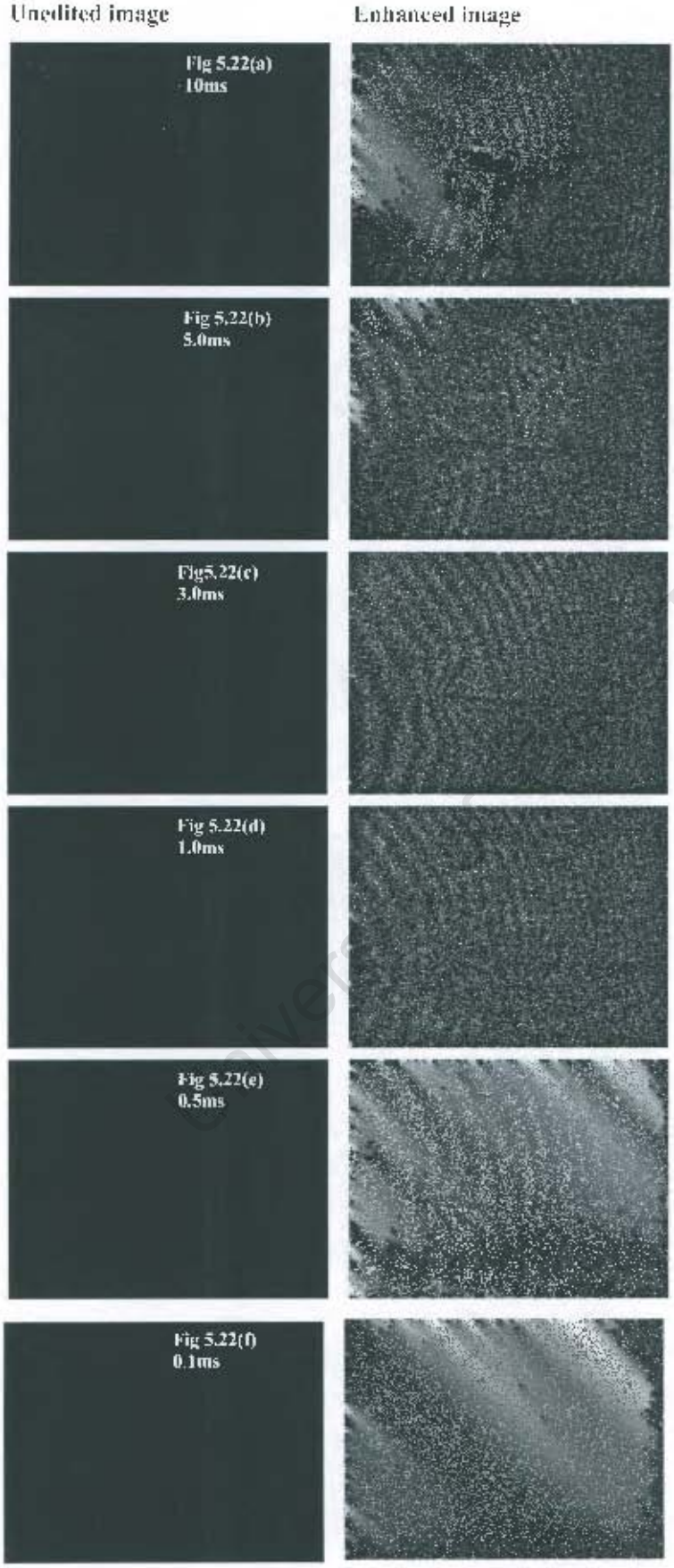

Figure 5.22(a) – (f) ESPI images of test specimen exposed to loudspeaker excitation captured at exposure times of 10.0, 5.0, 3.0 1.0 0.5, and 0.1ms respectively using electronic shutter (LN shutter) to pulse laser

5.5.7 ESPI inspection with object exposed to environmental vibration using camera shutter

Figure 5.23(a) – (c) below show the ESPI images of the blade captured under environmental excitation for camera shutter periods of 20.0, 8.33, 2.0, 0.5 and 0.1ms.

The images captured at 20ms and 8.3ms are both extremely smudged, but the quality of the images improves as the shuttering time decreases. The unedited images are clear up to 0.5ms, and the enhanced images to 0.1ms.

The light levels of the unedited images are good for durations as short as 2ms, and are clear throughout the range in the enhanced images.

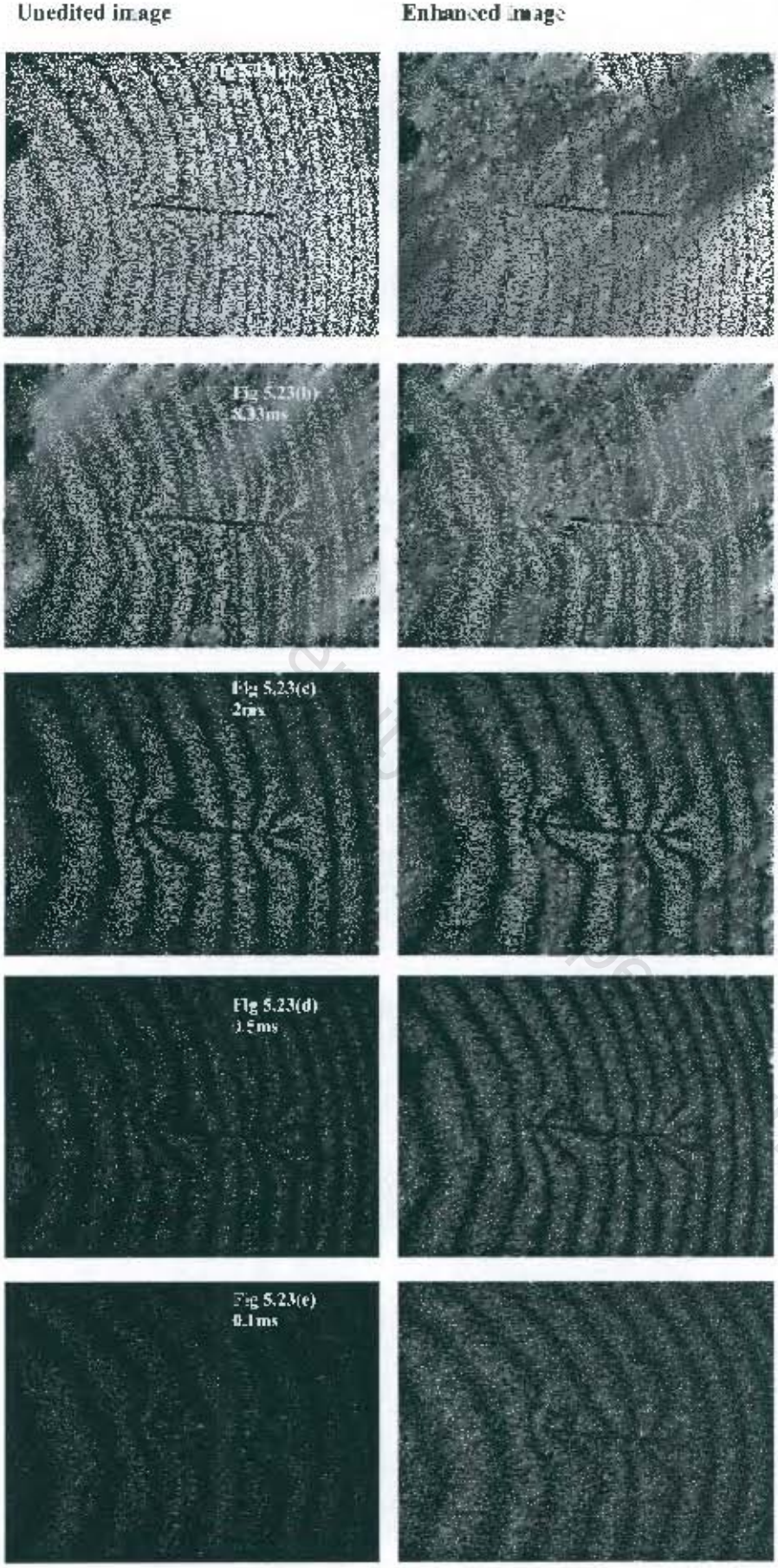

Figure 5.23(a)-(e) ESPI images of test specimen exposed to environmental excitation captured using electronic shutter (camera shutter) at exposure times of 20ms, 8.33ms, 2ms, 0.5ms, and 0.1ms respectively

5.5.8 ESPI inspection with object exposed to compressor vibration using camera shutter

Figure 5.24(a) – (e) below are the ESPI images that were captured using the camera shutter when the test specimen was excited by compressor vibration.

The images captured at 20ms, 8.33ms and 2ms show varying degrees of smudging. The image captured at 0.5 is distinctly clearer, and the one captured at 0.1ms is slightly smudged. The unedited images are clear to exposure times as short as 0.5ms, and with enhancement, the whole series becomes clear.

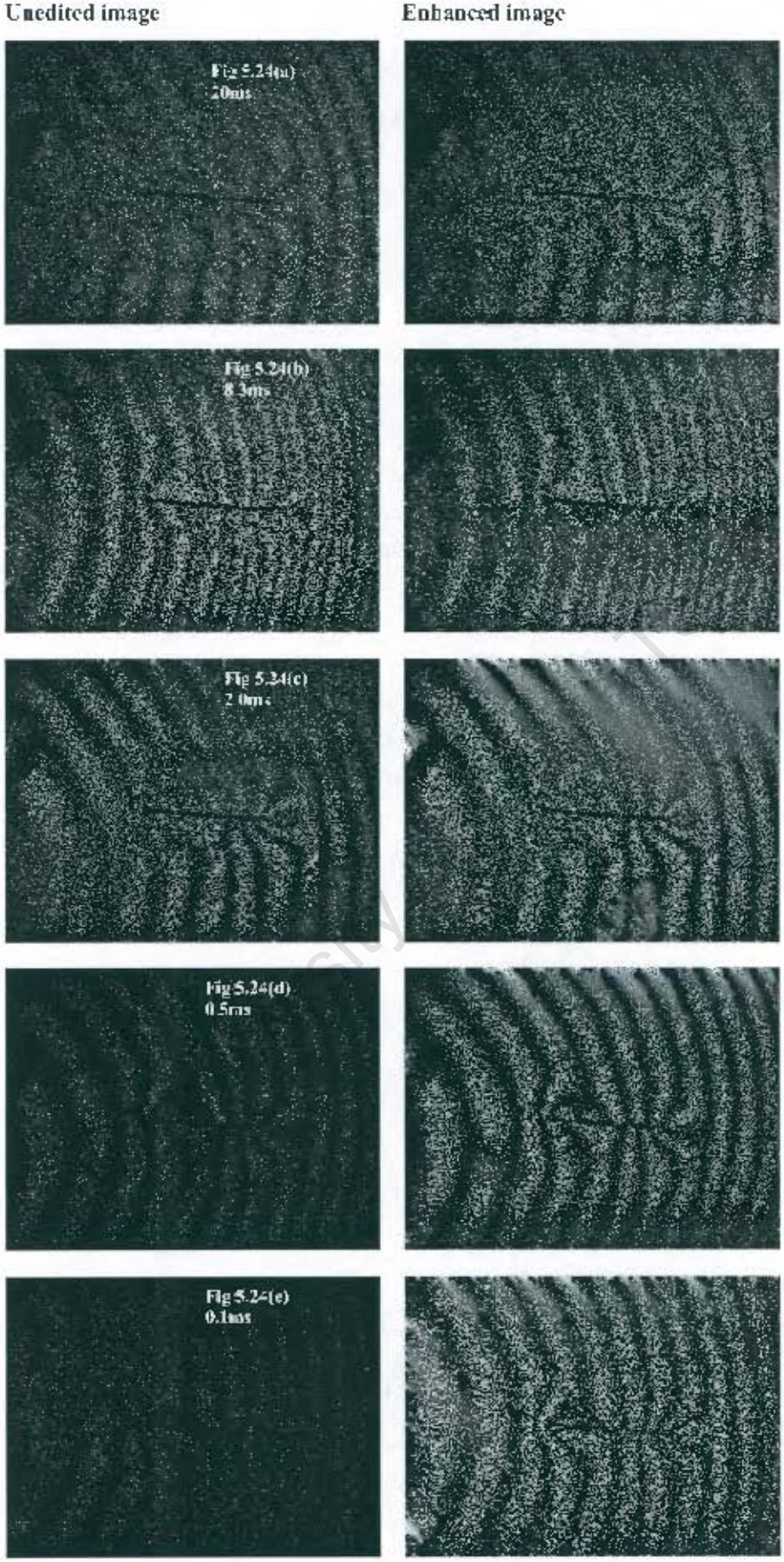

Figure 5.24(a)-(e) ESPI images of test specimen exposed to compressor excitation captured using electronic shutter (camera shutter) to pulse laser at exposure times of 20ms, 8.33ms, 2ms, 0.5ms, and 0.1ms respectively

5.5.9 ESPI inspection with object exposed to loudspeaker excitation using camera shutter

Figure 5.25(a) – (e) below shows the ESPI images for the blade captured using the camera shutter for periods of 20, 8.33, 2, 0.5 and 0.1ms while it was being excited by the loudspeaker.

The unedited images are clear for exposure times as short as 2ms only. The enhanced images are clear to 0.1ms, but of poor quality at these extremes.

The images captured at 20ms and 8.33ms show fringe lines in the nodal region, but nothing in the anti-nodal zone. The images captured at 2ms and 0.1ms show clear, whole-field fringe lines, but the one captured at 0.5ms is smudged along the anti-nodal line.

Unedited image

Enhanced image

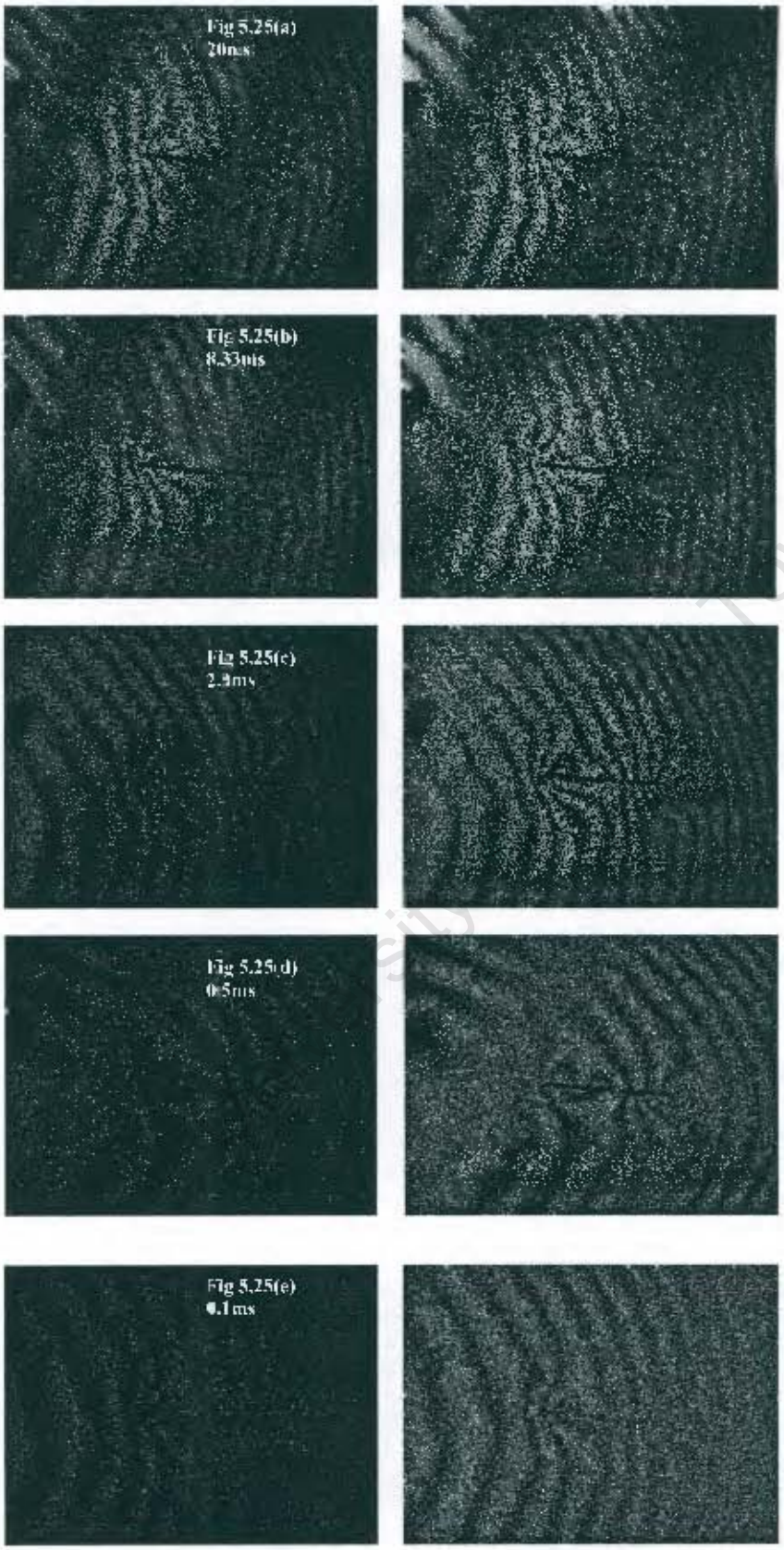

Figure 5.25(a)-(e) ESPI images of test specimen exposed to loudspeaker excitation captured at exposure times of 20ms, 8.33ms, 2ms, 0.5ms, and 0.1ms respectively using electronic shutter (camera shutter)

Chapter 6 Discussion of Results

The results generally indicate that the reduction in exposure time made it easier to perform ESPI successfully on an object when it was subjected to vibration. This was true of all the pulsing methods investigated. This would normally have been either difficult or impossible to do. Although a shorter exposure time did not guarantee that a successful image would be obtained on every attempt, it increased the likelihood of capturing a satisfactory image considerably.

On six out of ten occasions, it was possible to successfully capture ESPI images of the test specimen under environmental vibration in the laboratory with no shuttering. (i.e. at the full 20ms exposure period.). There was an increase to eight out of ten and ten out of ten through the use of exposure periods of 2ms and 0.5ms respectively. Only eight out of ten were however found to be acceptable for an exposure period of 0.1ms.

At the larger vibration levels produced by the compressor and loudspeaker, the effect of a shorter exposure time became particularly apparent. In these cases, few or no images could be obtained when using the full exposure period.

In the case of the compressor vibration, all the images captured at the full exposure period were generally smudged partly or completely. As the exposure period decreased, the fringe quality of the images obtained improved markedly. Obtaining a good fringe pattern at a reduced exposure time was not a certainty, but the likelihood definitely was increased.

In the case of the loudspeaker vibration, all the ESPI images exhibited nodal and anti-nodal regions when no vibration isolation techniques were employed. Fringes were only visible in the nodal regions and were often smudged, whilst nothing was visible in the anti-nodal areas. As the shuttering time decreased to approximately 2ms, the fringe lines became much clearer, and the distinction between the nodal and anti-nodal areas became less obvious. This improvement continued further for exposure periods of 0.5ms and 0.1ms, although some of the images at low exposure periods were smudged. Again, although a good image was not always achieved, there was a definite benefit to reducing the exposure time.

Table 6.1 below gives a summary of the number of successful images obtained out of ten under the various vibrational conditions and shuttering times for the camera shutter.

Excitation	20ms	2ms	0.5ms	0.1ms
Environmental	6	8	10	8
Compressor	0	8	7	4
Loudspeaker	0	2	7	7

Table 6.1 Summary of acceptability of ESPI images at reduced exposure times

6.1 Findings of ESPI inspection with large disc

The large disc and motor system worked quite well considering its crudeness, and was able to produce pulses as low as 0.4ms. Due to its large size, however, a compact system could not accommodate it as was intended. It vibrated excessively, which would have added to the vibration experienced by the system. The inaccurate pulse frequency control and consequent beating was also problematic. When dynamic stressing (e.g. thermal stressing) is applied, the fringe pattern needs to be observed on the monitor and captured when it reaches the desired state. The beating made this process very difficult on occasion, as the best images often appeared at the same time as the beating occurred.

Both of the discs have the advantage that they do not suffer from light transmission losses, which may be important in the case of low laser power.

6.2 Findings of ESPI inspection with stepper motor

The stepper motor was more compact and vibrated substantially less than the previous system. It was able to maintain the pulse frequency to a higher degree of accuracy, and was capable of producing pulses in the order of 1ms. This was the shortest pulse that was obtainable with this arrangement, although this was limited because the stepper motor could not rotate any faster. Using a different stepper motor could obviously decrease this period. It also did not suffer any of the light transmission losses that the LC or LN shutters did. While being an improvement on the large disc, it was still too large to be incorporated into a compact ESPI system. The electronic circuit to drive the motor was also complicated to construct.

6.3 Findings of ESPI inspection with LC Shutter

The LC shutter was able to provide useful pulses as low as 2ms, although this was very much a function of the laser power utilised and the size of the object being inspected. It provided a vibration-free shuttering mechanism, which was compact and easily controlled, as well as being capable of producing customised pulsing. A single signal generator easily provided the 12V-control voltage.

The minimum shuttering time, however, ruled out this shuttering method because it was too long. At shuttering times of around 2ms, the light levels had already been reduced dramatically due to the slow shutter response. This made it difficult to

perform ESPI properly, and meant that post-capture editing was required in order to obtain satisfactory images.

6.4 Finding of ESPI inspection with Lithium Niobate Shutter

The Lithium Niobate shutter showed good potential, and was able to pulse the laser effectively to below 0.1ms. The shutter is very compact and vibration free and the only disadvantages are the high operating voltages and low light transmission. The high voltage that was required to control the crystal was an initial impediment as suitable components were difficult to locate. Information on circuit construction was also limited.

The benefit of using an external shutter such as the Lithium Niobate crystal is that specialised ESPI such as Double pulse addition ESPI is made possible. In this method, both ESPI pulses are fired in a single TV frame. The technique is particularly suited to vibration analysis. This is possible with the use of disc shutters and the I.C shutter as well, but obviously easier to perform with the I.C and LN shutters.

ESPI inspection was only really possible for pulse durations as short as 0.25ms. Beyond this limit, the images obtained were badly defined due to the diminished laser intensity reaching the camera as a result of the poor light transmission of the shutter's polariser. An obvious solution to this problem would be the replacement the polariser with one that has a higher transmission or increasing the power of the laser. Due to

incorrect calibration, the laser used had an effective power output of approximately 8mW, while suitable diode lasers are readily available with outputs of 300mW.

6.5 Findings of ESPI inspection using Built-in Shutter

The camera shutter proved to be the most successful of the methods that were investigated. It was able to capture ESPI images for shutter periods of as low as 0.1ms and these were well defined after suitable enhancement. The use of the camera's built in shutter is clearly preferable to the use of an external shutter because it does not suffer transmission losses. It also does not require extra equipment like the shutter itself, signal generators etc and is therefore simpler to use.

This feature is not, however standard on all cameras, in which case the use of external shuttering becomes necessary. With the use of the camera shutter it is also not possible to make use of customised pulsing or to perform Double Pulsed Addition ESPI. There are also only eight shuttering speeds, and therefore if the inspection required intermediate speeds, this would not be possible.

Table 6.2 gives a summary of the various techniques investigated and their characteristics.

Device	Min Shuttering time	Negative effect	Positive effect
Large Disc	0.4ms	• Introduces vibration • Too large	• Shutter time good • Simple
Stepper motor and disc	1ms	• Introduces vibration • Shutter time too long • Too large • Complicated electronics	• Simple concept • Good control of pulse frequency and duration
LCD shutter	2-3ms	• Shuttering time too long • Poor light transmission at low pulse durations	• Vibration free • Compact • Simple to operate and control
$LiNbO_3$ shutter	Less than 0.1ms	• Complicated electronics and operation • Poor light transmission	• Vibration free • Very compact • Shutter time good
Camera shutter	0.1ms	• Only eight shuttering speeds	• No light transmission losses • Good shuttering time • Very simple • Pulses synchronised to imaging rate

Table 6.2 Comparison of shuttering techniques

Chapter 7 Conclusions

The "pulsing" of the laser has proved to be a successful method in the elimination of the effects of environmental vibration. Generally there was a distinct improvement in the ability to capture images using "pulsed" ESPI, provided that the pulses were of a sufficiently short duration. This was most apparent for large vibration amplitudes.

The LN shutter and camera shutter were the only successful methods among those that were investigated, and were both able to provide pulses as low as 0.1ms. The choice of one over the other will depend on the circumstances and requirements of the investigation. The only problem of consequence encountered with the LN shutter was its poor light transmission. The camera shutter on the other hand was simple to operate, and does not suffer light transmission losses.

A compromise must be reached for shuttering time so that it is short enough to eliminate vibrational effects, while at the same time ensuring that there are sufficient light levels reaching the camera CCD. This obviously depends on the frequency and amplitude of the environmental vibration, as well as the stability of the object. If high frequency and high amplitude vibration is expected, the shuttering time needs to be reduced further. If the object is securely clamped, this will reduce the vibration amplitude it is exposed to, and hence the shuttering time can be increased.

Chapter 8 Recommendations

The use of the camera shutter should be further investigated. It is capable of subtraction ESPI, which is preferable to addition ESPI for the majority of cases where ESPI is performed.

The Lithium Niobate shutter was also found to have potential for shuttering. If it is to be used, a polariser with higher light transmission should be investigated.

The use of FLC shutters should be considered as an alternative to the Lithium Niobate shutter. These function in much the same way as LC shutters, but are capable of shuttering speeds in the region of 50μs. The FLC cells also require lower voltages. (10 to 12 volts as opposed to 1400V for the LN shutter.) The shutter could thus be driven off a signal generator alone, without the complication of the high voltage switching circuit.

A more powerful laser should be used in order to provide adequate laser light at short shuttering speeds. The ESPI investigation was performed with a 60mW laser that only output approximately 8mW due to poor calibration. Modern diode lasers are able to provide 300mW of power with ease. They are also considerably smaller, and would be easily incorporated into a compact ESPI system.

References

1. Jones R., Wykes C., *Holographic and Speckle Interferometry,* 1st Ed. Cambridge University Press 1983
2. Daniel Albrecht, Marco Franchi, Alfredo C. Lucia, Paolo M. Zanetta, Alfredo Aldrovandi, Teresa Cianfanelli, Patrizia Riitano, Oriana Sartiani, David C. Emmony *Diagnostic of the conservation state of antique Italian paintings on panel carried out at the Laboratorio di Restauro dell'Opificio delle Pietre Dure on Florence, Italy with ESPI-based portable instrumentation.* Journal Cult. Heritage Vol. 1 2000
3. Fricke-Begemann T., Gülker G., Hinsch K.D., Joost H. *Mural inspection by vibration measurements with TV holography* Optics and Lasers in Engineering Vol. 32 2000 pp 537 – 548
4. G. Gülker, K. D. Hinsch, A. Kraft *Deformation monitoring on ancient terracotta warriors by microscopic TV-holography* Optics and Lasers in Engineering 36 (2001) 501–513
5. Various *Non Destructive Testing ASM Handbook Series No.17*
6. D. Findeis, J Gryzagoridis *The Feasibility of Optical Interference-based NDE Methods to Inspect Helicopter Rotor Blades* SPIE Vol. 3994 (2000) pp 59 – 67
7. O. Petilon *New developments of pulsed holography for industrial applications* NDT Net Sept 1998 Vol. 3 No. 9
8. M. Whelan, A. Langhoff, A Lucia *Mechanical testing of biomaterials using speckle interferometry* 11th conference of the ESB July 8 – 11 1998 Toulouse, France
9. R. Ritter, K. Galanulis, D. Winter, E Müller, B Breuckmann *Notes on the application of Electronic Speckle Pattern Interferometry* Optics and Lasers in Engineering Vol. 26 (1997) pp 283 – 299
10. J.R. Tyrer, C. Heras-Palou, T. Slater *Three-Dimensional Femoral Strain Analysis using ESPI* Optics and Lasers in Engineering Vol. 23 (1995) 291 – 303
11. Shuhai J., Kaiduan Y., Yushan T. *The system of double optical path ESPI for the vibration measurement.* Optics and Lasers in Engineering Vol. 34 2000 pp 67 – 74
12. Ettemeyer A. *car body vibration analysis with pulsed ESPI* 1999
13. G. Graham J.N. Petzing, M. Lucas *Modal analysis of ultrasonic block horns by ESPI* Ultrasonics Journal Vol. 37 (1999) 149–157

14. Halliday D. Resnick, R. Walker, J *Fundamentals of Physics Extended*, 4th Ed. New York. John Wiley & Sons 1993

15. R. Spooren *Standard charge-coupled device cameras for video speckle interferometry* Optical Engineering March 1994 Vol. 33 No 3 pp 889 – 896

16. J. Gryzagoridis *Holographic and Electronic Speckle Pattern Interferometry and Shearography*

17. J. Gryzagoridis, D. Findeis, D.F. van Zyl, J.R. Myles *ESPI – a viable NDE tool for plant extension*

18. J.R. Myles *Electronic Speckle Pattern Interferometry (ESPI) NDE of cracks in pressure vessels with FEA modelling* (1997)

19. A.Fémandez, A.J. Moore, C. Pérez-Lopéz, A.F. Doval, J. Blanco-Garcia *Study of Transient Deformations with Pulsed Holography: Application to Crack Detection* Applied Optics Vol. 36 No 10 (1997) pp2058 – 2065

20. G.Pedrini, P.H. Froning, H. Fessler, H.J. Tiziani *Transient vibration measurements using multi-pulse digital holography* Optics and Laser Technology Vol. 29. No 8 pp505 – 511, 1997

21. H Steinbichler, G, Gehring *TV Holography and Holographic Interferometry: Industrial applications* Optics and Lasers in Engineering Vol. 24 (1996) pp 111 – 127

22. P.D. Ruiz, G.H. Kaufmann, O.MoKller, G.E. Galizzi *Evaluation of impact-induced transient deformations using double-pulsed electronic speckle pattern Interferometry and finite elements* Optics and Lasers in Engineering 32 (2000) 473}484

23. Anderson D.J., Valera J.D., Jones J.D.C. *Electronic Speckle Pattern Interferometry using Diode Laser Stroboscopic Illumination* Measurement Science Technology Vol. 4 (1993) 982 – 987

24. C. Buckberry, M. Reeves, A.J. Moore, D.P. Hand, J.S. Barton, J.D.C. Jones *The application of high-speed TV-holography to time-resolved vibration measurements* Optics and Lasers in Engineering 32 (2000) 387}394

25. A.J. Moore C, D.P. Hand. J.S. Barton, J.D.C. Jones *Transient Deformation Measurement with Electronic Speckle Pattern Interferometry and a High-Speed Camera* Applied Optics Vol 38 No 7 1999

26. Information from internet *An Introduction to CCD operation* www.mssl.ac.uk/www_detector/ccdgroup/optheory/ccdoperation.html

27. Information from internet http://www.sharp.ca/lcd_principles.html

28. Information from internet http://www.displaytech.com/index.html

29. Information from internet http://www.scitec.uk.com/

30. Hecht E. *Optics*, 2nd Edition Addison - Wesley Publishing Company, 1987

31. Specification sheet of Toshiba Insulated Gate Bipolar Transistor (IGBT) GT 8 Q101

32. Gerster C. *Fast high-power/high voltage switch using series connected IGBTs with active gate-controlled voltage balancing* 1994

33. Bruel & Kjaer *Measuring Vibration* 1982

34. *Operating Instructions for OPT-110 Optical Power meter*

35. C.A. Sciammarella, G.Bhat, P. Bayeux *The Holostrain system - A portable interferometer* Proceedings of the 1993 SEM 50th Anniversary Spring Conference in Experimental Mechanics 1993 99 45 - 54

36. A. Yariv, P.Yeh *Optical Waves in Crystals – Propagation and Control of Laser Radiation* J Wiley & Sons 1984

Appendices

Appendix 1 Derivation of Out-of Plane Displacement formulae

This derivation provided is based on the path geometry of a single ray of laser light, and is given by Gryzagoridis [16]. This analysis simplifies the derivation considerably. A more thorough derivation is given by Jones [1]. In this case, the ESPI set-up is arranged to measure out-of-plane displacement.

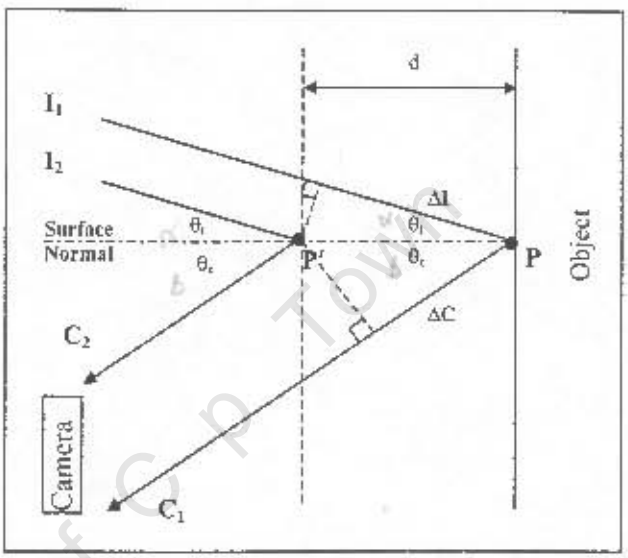

Figure A-1 Derivation of out-of-plane displacement

The surface of an object is assumed to be illuminated with a single ray of laser light I_1 at an angle of θ_i to the object's surface normal. The laser reflects off the surface to the camera along C_1 at an angle of θ_c to the surface normal. As a result of the applied stressing, a point on the object surface is displaced from P to P' through a distance d parallel to the object's surface normal. The incident beam and reflected beam are now I_2 and C_2 respectively.

The surface displacement d is assumed to be small compared to the distance from the laser source to the surface, as well as the distance from the object to the camera, so

the rays I_1 and I_2 and C_1 and C_2 can be assumed to be parallel during the displacement.

The change in path length of the ray from the laser to the camera can be given by

$$\Delta P = \Delta I + \Delta C \qquad \textbf{Eqn A-1}$$

Where ΔI is the change in path length of the ray from the laser source to the object surface I and ΔC is the change in path length of the ray from the object to the camera CCD C as a result of the surface displacement.

From geometry

$$\Delta I = d\cos\theta_i \qquad \textbf{Eqn A-2}$$

And $\Delta C = d\cos\theta_c$ **Eqn A-3**

The total change in path length is thus

$$\Delta P = d(\cos\theta_i + \cos\theta_c) \qquad \textbf{Eqn A-4}$$

This results in a phase change of

$$\Delta\phi = \frac{2\pi}{\lambda} d(\cos\theta_i + \cos\theta_c) \qquad \textbf{Eqn A-5}$$

Constructive interference occurs when there is a phase difference of 2π or 360° and thus the number of fringes is given by

$$n = \frac{\Delta\phi}{2\pi} \qquad \textbf{Equ A-6}$$

Substituting into Equation A-5 and solving for the displacement gives

$$d = \frac{n\lambda}{(\cos\theta_i + \cos\theta_c)} \qquad \textbf{Eqn A-7}$$

For small illumination and camera angles, Equation A-7 can be simplified to

$$d = \frac{n\lambda}{2}$$ **Eqn A-8**

Appendix 2 Derivation of In-Plane Displacement formula

This derivation is based on the path geometry of a single ray of laser light, and is given by Gryzagoridis [16]. This method simplifies the derivation considerably, and a more thorough derivation is given by Jones [1]. In this case, the ESPI set-up is arranged to measure in-plane displacement d along a line perpendicular to the object's surface normal.

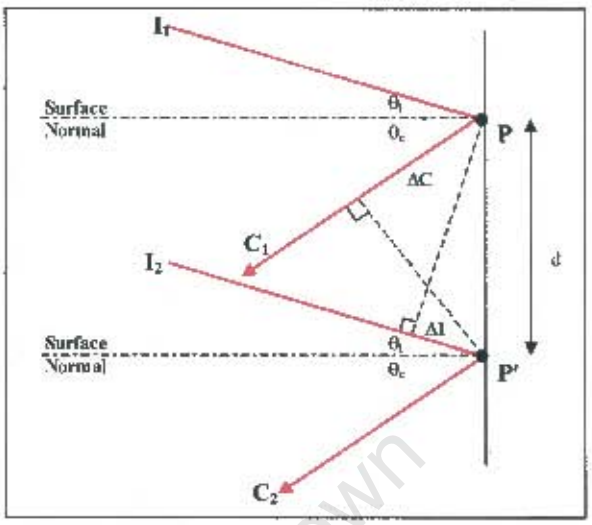

Figure A-2 Derivation of in-plane displacement formula

The surface of an object is again assumed to be illuminated with a single ray of laser light I_1 at an angle of θ_i to the object's surface normal. This reflects off the surface to the camera along C_1 at an angle of θ_c to the surface normal. A point on the object surface is displaced from P to P′ through a distance d perpendicular to the object's surface normal. The incident beam and reflected beam are now I_2 and C_2 respectively.

The change in path length of the ray from the laser to the camera can be given by

$$\Delta P = \Delta I + \Delta C \qquad \textbf{Eqn A-9}$$

Where ΔI is the change in path length of the ray from the laser source to the object surface I and ΔC is the change in path length of the ray from the object to the camera CCD C as a result of the surface displacement.

From geometry

$$\Delta I = d\sin\theta_i \qquad \textbf{Eqn A-10}$$

And $\Delta C = d\sin\theta_c$ **Eqn A-11**

The total change in path length is thus

$$\Delta P = d(\sin\theta_i - \sin\theta_c) \qquad \textbf{Eqn A-12}$$

This results in a phase change of

$$\Delta\phi = \frac{2\pi}{\lambda} d(\sin\theta_i - \sin\theta_c) \qquad \textbf{Eqn A-13}$$

Constructive interference occurs when there is a phase difference of 2π or 360° and thus the number of fringes is given by

$$n = \frac{\Delta\phi}{2\pi} \qquad \textbf{Eqn A-14}$$

Substituting into Equation A-13 and solving for the displacement gives

$$d = \frac{n\lambda}{(\sin\theta_i - \sin\theta_c)} \qquad \textbf{Eqn A-15}$$

For small angles sinθ approaches zero, and the sensitivity decreases. The sensitivity increases as θ increases, but as θ approaches 90°, the surface can no longer be illuminated.

If θ_i is the same as θ_c the change in path length is zero. In-plane displacement sensitivity can be minimised by making the illumination and camera angles similar. The path change due to a vertical component is a similar sine term, and can be ignored if the laser illumination and camera are at the same height.

Appendix 3 Pulse duration calculations

Large Disc

Name	Chopper	Chopper position	Object position	Loading	Rotational speed rpm	Rotational speed metres/sec	Radius mm	Chord length mm	Time of exposure ms	AGC
TLD1	Large disc	Off table	On table	Hair dryer	1500.0	157.10	90	77	5.2	on
TLD2	Large disc	Off table	On table	Hair dryer	1501.5	157.26	134	64	3.2	on
TLD3	Large disc	Off table	On table	Hair dryer	1500.5	157.15	117	32	1.9	on
TLD4	Large disc	Off table	On table	Hair dryer	1500.0	157.10	120	15	0.9	on
*LDS1	Large disc	Off table	On table	Hair dryer	1501.0	157.21	85	70	3.2	on
*LDS2	Large disc	Off table	On table	Hair dryer	1500.0	157.10	139	54	3.2	on
*LDS3	Large disc	Off table	On table	Hair dryer	1500.0	157.10	117	30	1.9	on
*LDS4	Large disc	Off table	On table	Hair dryer	1501.0	157.10	131	10	0.6	on
*LDS5	Large disc	Off table	On table	Hair dryer	1500.0	157.10	141	5	0.3	on
GLD1	Large disc	Off table	Off table	Hair dryer	1500.0	157.10	96	77	5.2	on
GLD2	Large disc	Off table	Off table	Hair dryer	1500.0	157.10	109	54	3.2	on
GLD3	Large disc	Off table	Off table	Hair dryer	1500.0	157.10	117	30	1.9	on
GLD4	Large disc	Off table	Off table	Hair dryer	1500.0	157.10	131	10	0.6	on
GLD5	Large disc	Off table	Off table	Hair dryer	1500.0	157.10	141	5	0.3	on
GLD6.1	Large disc	Off table	Off table	Hair dryer	1500.0	157.10	89	77	5.2	on
GLD6.2	Large disc	Off table	Off table	Hair dryer	1500.0	157.10	108	54	3.2	on
GLD6.3	Large disc	Off table	Off table	Hair dryer	1500.0	157.10	117	30	1.9	on
GLD6.4	Large disc	Off table	Off table	Hair dryer	1500.0	157.10	131	10	0.6	on
GLD6.5	Large disc	Off table	Off table	Hair dryer	1500.0	157.10	141	5	0.3	on
SLD1-EA	Large disc	Off table	Off table	Hair dryer	1500.0	157.10	96	76	5.1	on
SLD1-EU	Large disc				1500.0	157.10	109	54	3.2	
SLD1-EC	Large disc				1500.0	157.10	117	33	1.9	
SLD1-EF	Large disc	Off table	Off table	Hair dryer	1500.0	157.10	131	10	0.6	on
SLD1-EF	Large disc	Off table	Off table	Hair dryer	1500.0	157.10	141	5	0.3	on

Stepper motor and disc

Name	Chopper	Object position	Loading	Rotational speed rpm	Rotational speed metres/sec	Radius mm	Chord length mm	Time of exposure ms	AGC
TS1	Stepper motor	On table	Hair dryer	2500.0	26.18	36	12	0.95	on
TS2	Stepper motor	On table	Hair dryer	2500.0	26.18	53	12	0.65	on
TS3	Stepper motor	On table	Hair dryer	2500.0	26.18	93	4	0.42	on
TSA	Stepper motor	On table	Hair dryer	5000.0	52.37	57	12	0.23	on
TS5	Stepper motor	On table	Hair dryer	5000.0	52.37	77	4	0.08	on
TSS1	Stepper motor	On table	Hair dryer	2500.0	26.18	46	12	0.46	on
TSS2	Stepper motor	On table	Hair dryer	2500.0	26.18	534	12	0.65	on
TSS3	Stepper motor	On table	Hair dryer	2500.0	26.18	81	4	0.42	on
TSS4	Stepper motor	On table	Hair dryer	5000.0	52.37	57	12	0.23	on
TSS5	Stepper motor	On table	Hair dryer	5000.0	52.37	77	4	0.08	on
GS1	Stepper motor	Off table	Hair dryer	2500.0	26.18	46	12	0.46	on
GS2	Stepper motor	Off table	Hair dryer	2500.0	26.18	53	12	0.65	on
GS3	Stepper motor	Off table	Hair dryer	2500.0	26.18	81	4	0.42	on
GS4	Stepper motor	Off table	Hair dryer	5000.0	52.37	57	12	0.23	on
GS5	Stepper motor	Off table	Hair dryer	5000.0	52.37	77	4	0.08	on
GSC1	Stepper motor	Off table	Hair dryer	2500.0	26.18	46	12	0.46	on
GSC2	Stepper motor	Off table	Hair dryer	2500.0	26.18	53	12	0.65	on
GSC3	Stepper motor	Off table	Hair dryer	2500.0	26.18	81	4	0.42	on
GSC4	Stepper motor	Off table	Hair dryer	5000.0	52.37	57	12	0.23	on
GSC5	Stepper motor	Off table	Hair dryer	5000.0	52.37	77	4	0.08	on
SMTeaS1	Stepper motor	Off table	Hair dryer	2500.0	26.18	46	12	0.46	on
SMTeaS2	Stepper motor	Off table	Hair dryer	2500.0	26.18	53	12	0.65	on
SMTeaS3	Stepper motor	Off table	Hair dryer	2500.0	26.18	93	4	0.42	on
SMTeaS4	Stepper motor	Off table	Hair dryer	5000.0	52.37	57	12	0.23	on
SMTeaS5	Stepper motor	Off table	Hair dryer	5000.0	52.37	77	4	0.08	on

Appendix 4 Accelerometer Specification Sheet

Models 732A & 736
High Sensitivity/High Frequency Accelerometer

Features:
- Wide dynamic range
- High sensitivity
- Compact construction to fit in tight spaces
- Wide frequency range
- Standardized sensitivity
- Hermetically sealed

Applications:
- Fans
- Bearings
- Rotating machinery
- Laboratory research
- Predictive maintenance

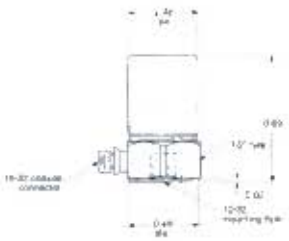

Models 732A & 736

SPECIFICATIONS	732A	736	UNITS
DYNAMIC			
Sensitivity, ±5 %, 25 °C	10	100	mV/g
Acceleration Range[1]	250	50	g peak
Amplitude Nonlinearity	1		%
Frequency Response:			
±5 %	3 - 15,000	8 - 15,000	Hz
±3 dB	1 - 25,000	2 - 25,000	Hz
Resonance Frequency, mounted, nom.			kHz
Transverse Sensitivity, max.	5		% of axial
Temperature Response	see graph		
ELECTRICAL			
Power Requirement, voltage source	18 - 30		VDC
current regulating diode[2]	2 - 10		mA
Electrical noise, equiv. g, nom.,			
Broadband 2.5 Hz to 25 kHz	2000	150	µg
Spectral 10 Hz	100	10	µg/√Hz
100 Hz	30	2	µg/√Hz
1,000 Hz	10	1	µg/√Hz
10,000 Hz	5	0.8	µg/√Hz
Output Impedance, max.	100	150	Ω
Bias Output Voltage, nom.	10		VDC
Grounding	case grounded		
ENVIRONMENTAL			
Temperature Range	-50 to 120		°C
Vibration Limit	500		g peak
Shock Limit	5000		g peak
Electromagnetic Sensitivity, equiv. g	100		ug/gauss
Base Strain Sensitivity	0.005		g/µstrain
PHYSICAL			
Weight	15		grams
Case Material	stainless steel		
Mounting	10-32 tapped hole		
Output Connector	10-32 coaxial		
Cabling Mating Connector	Microdot 10-32 (R1)		
Standard Cable	J93 coaxial, Teflon jacket, 30 pF/ft		

NOTES [1] Signal distortion can occur when measuring high vibration levels, especially with long cables. A 24-30 VDC powering source is recommended for minimizing distortion. Current regulating diode must be at least 2 mA plus 1 mA per 1000 pF of cable capacitance. [2] A maximum current of 6 mA is recommended for operating temperatures in excess of 100 °C.

OPTIONS: Customer specified sensitivity, filtering, top connector (BNC), PVC jacketed cable

ACCESSORIES SUPPLIED: SF1 mounting stud, R12-J93 10 cable assembly

ACCESSORIES AVAILABLE: Power supplies, amplifiers, signal conditioners, cementing studs, magnetic mounting bases, isolating studs

TYPICAL TEMPERATURE RESPONSE

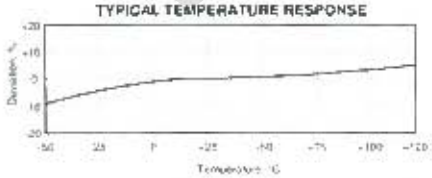

TYPICAL FREQUENCY RESPONSE

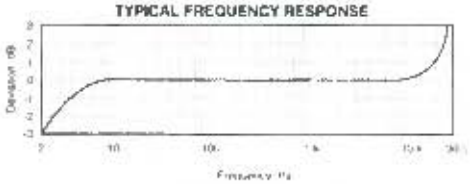

Due to continued research and product development, Wilcoxon Research reserves the right to amend this specification without notice.

Wilcoxon Research, 2096 Gaither Road, Rockville, Maryland 20850 USA • 1-800-WILCOXON or (301) 330-8811 • Fax (301) 330-8873

Figure A-3 Accelerometer specification sheet

Appendix 5 Stepper Disc drawing

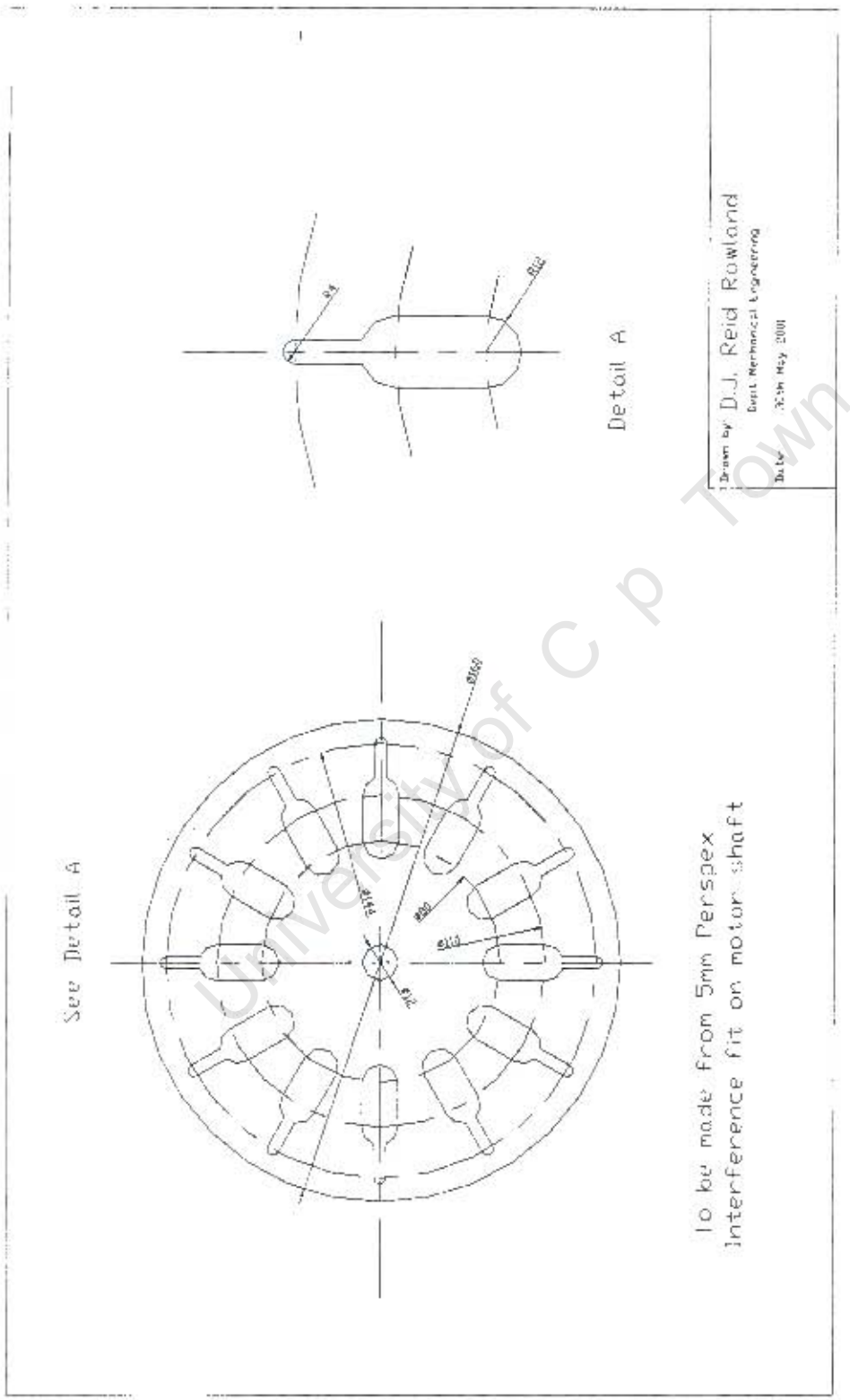

Figure A-4 Drawing of stepper motor disc